The Novel Role of Macrophage Migration Inhibitory Factor (MIF) in Mediating Adiposity and Non-Alcoholic Fatty Liver Disease (NAFLD)

by

Liujun Chen

A Thesis Submitted to the Faculty of Graduate Studies of

The University of Manitoba

In partial fulfillment of the requirements of the degree of

DOCTOR OF PHILOSOPY

College of Pharmacy

University of Manitoba

Winnipeg

ABSTRACT

Metabolic syndrome, marked by obesity, insulin resistance, hypertension, and hyperlipidemia, poses significant health challenges, with obesity being its core symptom. The pathogenesis of obesity is intricately linked with cardiovascular, and hepatic complications, including heart disease, stroke, non-alcoholic fatty liver disease (NAFLD), and type 2 diabetes (T2D). Despite its prevalence, the mechanisms underpinning obesity remain elusive. This dissertation delves into the role of macrophage migration inhibitory factor (MIF), a pro-inflammatory cytokine in regulating obesity and NAFLD. Our research unveils two key findings: **(1) The Roles of MIF in Adipose Tissue during Obesity Development**: Hormone-sensitive lipase (HSL) plays a fundamental role in mediating the free fatty acids release (FFAs) from adipose tissue by catalyzing triglycerides and diacylglycerides. Inhibition of adipose HSL significantly exacerbates the progression of obesity. Our work unveiled that extracellular MIF downregulates HSL levels by activating the 5' AMP-activated protein kinase (AMPK)/c-Jun N-terminal kinases (JNK) signaling pathway via its membrane receptor, cluster of differentiation 74 (CD74). Evidently, blocking extracellular MIF action with a neutralizing antibody mitigates obesity in mice fed a high-fat diet (HFD), underscoring the dominant role of extracellular MIF in HSL downregulation in obesity development under physiological context. Conversely, intracellular MIF exhibited an opposing effect by inhibiting JNK phosphorylation. Intracellular MIF deficiency significantly downregulated the HSL expression and activation shown as in *Mif*$^{-/-}$ mice, thereby exacerbating obesity during HFD. Thus, extracellular and intracellular MIF exert contrasting influences over HSL regulation during the development of obesity.

(2) MIF's Role in Exacerbating NAFLD: We explored the role of MIF in the pathogenesis of one obesity complication, NAFLD. Our findings revealed that elevated MIF levels increased

hepatic CD74 protein levels without altering gene expression, independently of liver inflammation both *in vitro* and *in vivo*. The escalated hepatic CD74 levels were associated with the progression of hepatic steatosis and fibrosis. These high MIF levels mediated the CD74 protein the accumulation, and related pathological phenotype in the liver could be ameliorated through MIF neutralization or MIF knockout. We observed that the increase of MIF-induced CD74 accumulation didn't rely on a direct physical binding interaction between MIF and CD74. Caspase-4 recognized as a significant contributor to CD74 degradation. Our study elucidates a novel mechanism wherein endocytic MIF hinders caspase-4 cleavage and its subsequent activation, consequently stabilizing CD74 levels and promoting hepatic CD74 accumulation, ultimately contributing to the onset of NAFLD.

In summary, our research illuminated the intricate mechanisms by which MIF impacts obesity and NAFLD. Activation of MIF engaged the AMPK/JNK axis, resulting in the downregulation of HSL-mediated lipolysis, leading to adipocyte hypertrophy and contributing to obesity development. Furthermore, hepatic MIF sustained CD74 protein through caspase-4 inhibition, playing a pivotal role in mediating obesity-related complications in the liver. These findings offered valuable insights into potential therapeutic avenues for addressing metabolic dysfunctions associated with obesity and NAFLD.

LAY SUMMARY

Unlocking the Puzzle of MIF in Metabolic Syndromes

Obesity is on the rise, and with it, a cluster of health issues known as metabolic syndrome. This syndrome involves problems like insulin resistance and too many fatty acids in the blood, which can lead to serious conditions like heart disease, fatty liver disease, and diabetes. In this dissertation, we dive deep into the molecular mysteries that link a specific protein, macrophage migration inhibitory factor (MIF), to metabolic syndrome, particularly focusing on obesity, insulin resistance, and fatty liver disease. Our research has unveiled some key insights: (1) MIF's Double-Edged Sword: MIF can be a friend or foe. First, it stops a crucial enzyme called Hormone-Sensitive Lipase (HSL) in its tracks, making fat cells swell and leading to obesity. Second, when MIF is inside cells, it plays a different tune. It teams up with other proteins to put a brake on HSL, and when this brake fails, it can trigger even more obesity. (2) MIF's Role in Fatty Liver Disease: MIF doesn't stop at obesity. It's also a major player in non-alcoholic fatty liver disease (NAFLD). It does this by protecting its membrane receptor, a protein called CD74, which is a key player in liver health. Even without liver inflammation, high levels of MIF can mess with CD74 leading to NAFLD. Briefly, this research helps us better understand how MIF fits into the complex puzzle of metabolic syndromes. This knowledge opens doors to potential treatments that could tackle the connections between inflammation and metabolic issues, offering hope for people dealing with these health challenges.

ACKNOWLEDGEMENTS

I'm grateful to my mentor, Dr. Dake Qi for his lasting guidance, effort, patience, constructive feedback, willingness, and cooperation leading to the completion of my Ph.D. study. I also want to express my gratitude to NSERC and CIHR for supporting my research, and China Scholarship Council (CSC) to provide me with a fellowship.

I would like to sincerely thank my committee members, Dr. Lucy Marzban and Dr. Xi Yang, and my former committee member, Dr. Mohammed Moghadasian for valuable advice and guidance. They are always my powerful brain trust, providing professional guidance for me at every step of my studies. I also thank many past and current lab members in Dr. Qi's laboratory, including Yiheng Huang, Xi Chen, Yadan Qi, Lisha Li, Hongbo Chang, Shunyu Liu, Yaqi Fan, Qiaozhi Li, Songjie Bai, Summer Li, Haleh Zabihi, for their support during my study.

I also appreciate the courses and training organized by the College of Pharmacy at the University of Manitoba. Especially, I am grateful to the Dean of Pharmacy, Dr. Lalitha Raman-Wilms, and the vice Dean of Pharmacy in research, Dr. Xiaocheng Gu for their support in administration and all the professors, technicians, and pharmacy coworkers for their incredible guidance whenever I required. Furthermore, heartfelt thanks to my classmates for contributing to the creation of a positive and supportive environment within the College of Pharmacy.

I would like to thank the metal supports from my family and my friends in China and Canada, and the funding from the CIHR, NSERC and CSC. At the end, I am asking forgiveness for sacrificing experimental animals for my study, and their participation is acknowledged with a heavy heart.

PUBLICATION LIST

First author publications

1. **Liujun Chen**, Lisha Li, Donghong Cui, Yiheng Huang, Haibin Tong, Haleh Zabihi, Shuxia Wang, Yadan Qi, Ted Lakowski, Lin Leng, Suixin Liu, Hong Wu, Lawrence H Young, Richard Bucala, Dake Qi (2023) Extracellular MIF Downregulates Adipose Hormone Sensitive Lipase and Contributes to Obesity. ***Molecular Metabolism*** 79:101834.

Author contributions

I (Liujun Chen) performed the major experiments. I, Lisha, Yiheng and Yadan, Haleh participated in animal studies. Donghong, Haibin, Shuxia, Lin and Richard contributed intellectually to data analysis and manuscript editing. Ted was involved in the preparation of recombinant MIF proteins. Lawrence and Richard provided overall scientific support for the research project and Dake Qi designed and managed the research. All authors read and approved the final manuscript. D. Q. is the guarantor of this work and, as such, had full access to all the data in the study and takes responsibility for the integrity of the data and the accuracy of the data analysis.

Co-author publications

1. Yiheng Huang, **Liujun Chen**, Lisha Li, Yadan Qi, Haibin Tong, Hong Wu, Jinjie Xu, Lin Leng, Sukhinder Cheema, Guang Sun, Zhengyuan Xia, John McGuire, Brian Rodrigues, Lawrence Young, Richard Bucala, Dake Qi (2023) Downregulation of adipose LPL by PAR2 contributes to the development of hypertriglyceridemia. ***JCI Insight*** (*Under revision*)

2. Yiheng Huang, Donghong Cui**, Liujun Chen**, Haibin Tong, Hong Wu, Yadan Qi, Kangxing Song, Grace Muller, Jinjie Xu, Xiang Gao, Kathleen E. Fifield, Lingyan Wang, Sukhinder Cheema, Zhengyuan Xia, Lin Leng, Jackie Vanderluit, Guang Sun, Lawrence H. Young, Richard Bucala, John McGuire, Dake Qi (2023) A pref-1-controlled non-inflammatory mechanism of insulin resistance. ***iScience*** 26: 106923.

3. Ming Liu, Zikun Xie, Guang Sun, **Liujun Chen**, Dake Qi, Hongwei Zhang, Jieying Xiong, Andrew Furey, Proton Rahman, Guanghua Lei, Guangju Zhai (2021) Macrophage migration inhibitory factor may play a protective role in osteoarthritis. ***Arthritis Research & Therapy*** 23(1): 59.

4. Ming Liu, Zikun Xie, Christie A. Costello, Weidong Zhang, **Liujun Chen**, Dake Qi, Andrew Furey, Edward W. Randell, Proton Rahman, Guangju Zhai (2021) Metabolomic Analysis Coupled with Extreme Phenotype Sampling Identified That Lysophosphatidylcholines are Associated with Multisite Musculoskeletal Pain. ***Pain*** 162(2): 600-608.

TABLE OF CONTENTS

ABSTRACT **2**

LAY SUMMARY **4**

ACKNOWLEDGEMENTS **5**

PUBLICATION LIST **6**

LIST OF FIGURES **13**

LIST OF TABLES **16**

ABBREVIATION **17**

CHAPTER 1: INTRODUCTION **21**

1.1 Metabolic Syndrome **21**

1.2 Obesity **21**

1.2.1 Definition of Obesity 21

1.2.2 Pathophysiology/Mechanisms of Obesity 22

1.2.2.1 The genetic factors *22*

1.2.2.2 The lifestyle *22*

1.2.2.3 Cellular mechanisms of obesity *23*

1.2.2.3.1 Adipocyte hyperplasia 24

1.2.2.3.2 Adipocyte hypertrophy 28

1.2.2.3.3 Adipokines and obesity 30

1.3 Obesity-related Complications **31**

1.3.1 Insulin Resistance 31

1.3.1.1 Definition of insulin resistance *31*

1.3.1.2 Molecular mechanisms of insulin resistance *31*

1.3.2 NAFLD 34

1.3.2.1 Definition and prevalence of NAFLD *34*

1.3.2.2 Cellular molecular mechanisms of NAFLD *36*

1.4 Current Therapies for Obesity and Obesity-associated Complications **38**

1.4.1 Pharmacological Therapies for Obesity 38

1.4.2 Pharmacological Therapies for Hyperlipidemia 40

1.4.3 Pharmacological Therapies for Hyperglycemia 42

1.5 Macrophage Migration Inhibitory Factor (MIF) **45**

1.5.1 The Basic Structure and Function of MIF 45

1.5.2 The Cellular Signaling Transduction of MIF 46

1.5.2.1 Cluster of differentiation 74 (CD74)/ cluster of differentiation 44 (CD44) receptors *47*

1.5.2.2 C-X-C chemokine receptors (CXCRs) *47*

1.5.2.3 Intracellular effects of MIF *48*

1.5.3 MIF Polymorphisms and Metabolic Dysfunction 49

1.6 The Gap of Knowledge **51**

1.7 Overarching Hypotheses, Research Goals and Specific Aims **52**

1.7.1 Research Hypotheses 52

1.7.2 Overarching Research Goals and Specific Aims 52

CHAPTER 2: MATERIALS AND METHODS **54**

2.1 Antibodies and Reagents **54**

2.2 Experimental Animals 54

2.3 Cell Culture **55**

2.3.1 3T3-L1 Cell Culture 55

2.3.2 HepG2 Cell Culture 56

2.4 MIF Neutralization with Anti-MIF Antibody **56**

2.5 Histology **57**

2.5.1 Oil red O Staining 57

2.5.1.1 Oil red O staining of 3T3-L1 adipocytes *57*

2.5.1.2 Oil red O staining of Tissues *58*

2.5.2 Hematoxylin-eosin (H&E) Staining 58

2.5.3 Trichrome Staining 59

2.6 The Lipid Profiles Quantification **60**

2.7 Enzyme-Linked Immunosorbent Assay (ELISA) **60**

2.8 siRNA Transfection **60**

2.9 Samples Preparation and Assessment **61**

2.9.1 RNA Extraction 61

2.9.2 Reverse Transcription (RT) of RNA to Obtain cDNA 62

2.9.3 Quantitative qPCR 65

2.9.4 Protein Extraction 65

2.9.5 Co-immunoprecipitation 66

2.9.6 Western Blot Analysis 67

2.10 Statistical Analysis **67**

CHAPTER 3: Different Roles of Extracellular and Intracellular MIF in Mediating Adipose Hormone-sensitive Lipase During the Development of Obesity **69**

3.1 ABSTRACT **69**

3.2 INTRODUCTION **70**

3.3 RESULTS **72**

3.3.1 The Activation of AMPK Inhibits HSL and Lipolysis through JNK in Adipocytes ... 72

..... 74

3.3.2 Extracellular MIF Downregulates Lipolysis through the AMPK/HSL Pathway Which Facilitates Lipid Storage in Adipocytes following High Palmitic Acid Treatment..... 76

3.3.3 High Plasma MIF Induces Adipocyte Hypertrophy and Obesity through Activating the AMPK/JNK Signaling and Inhibiting HSL 81

3.3.4 High Caloric Diet Upregulates Plasma MIF that Activates Adipose AMPK/HSL Signaling and Adipocyte Hypertrophy 84

3.3.5 MIF Receptor, CD74 is Involved in the MIF/AMPK/JNK/HSL Signaling Pathway and Obesity 93

3.3.6 Deficiency of Intracellular MIF Inhibits HSL Expression through JNK but Independent of AMPK..... 96

3.4 DISCUSSION..... 103

CHAPTER 4: The Role of MIF in Stabilizing CD74: A Novel Mechanism Contributes to the Development of NAFLD..... 110

4.1 ABSTRACT..... 110

4.2 INTRODUCTION 111

4.3 RESULTS 113

4.3.1 MIF Upregulates Non-Transcriptional Hepatic CD74 Levels in the Absence of Inflammation..... 113

4.3.2 Transgenic Upregulation of Circulating MIF Levels Increases Lipid Accumulation and Fibrosis in Liver..... 116

4.3.3 High Circulating MIF Levels following High Fat Diet (HFD) Upregulate Non-Inflammatory and Non-Transcriptional Hepatic CD74 Levels that Contribute to the Development of Liver Steatosis and Fibrosis 118

4.3.4. Neutralization of MIF Reverses HFD-Induced Upregulation of Non-Transcriptional CD74 Levels and Attenuates NAFLD Development 120

4.3.5 Genetic Deficiency of MIF Reduces Hepatic CD74 Levels and NAFLD following HFD Feeding..... 122

4.3.6 MIF Inhibits Cleavage of Caspase-4 that Facilitates the Degradation of CD74 in Liver 124

4.4 DISCUSSION 127

CHAPTER 5: DISCUSSION AND CONCLUSION 131

5.1 General Discussion and Conclusion 131

5.2 Strengths and Limitations 136

5.2.1 Strengths: 136

5.2.2 Limitations: 136

5.3 Therapeutic Implications 137

5.4 Future Work 138

BIBLIOGRAPHY: 140

LIST OF FIGURES

1-Figure 1.1 Altered adipose tissue and adipocyte function in the pathogenesis of metabolic disorders 26

2-Figure. 1.2. Adipocyte differentiation is a complex and tightly regulated process 27

3-Figure 1.3. Regulation of lipogenesis and lipolysis in adipocytes. 29

4-Figure 1.4. Insulin signal pathways 33

5-Figure 1.5 Natural history of NAFLD. 35

6-Figure 1.6 Metabolic causes of NAFLD. 37

7-Figure 1.7 Schematic representation of the human *Mif* gene: exons, predicted transcription factor-binding sites, and polymorphisms (-173 SNP and -794 CATT). 50

8-Figure 3.3.1. AMPK activation inhibits HSL and lipolysis through JNK in adipocytes..... 74

9-Figure 3.3.2. The effects of AICAR on AMPK and PKA/CREB. 75

10-Figure 3.3.3. Extracellular MIF downregulates lipolysis through the AMPK/HSL pathway which facilitates lipid storage in adipocytes following high palmitic acid treatment..... 79

11-Figure 3.3.4. The effects of MIF on phosphorylation of Akt and PKA. 80

12-Figure 3.3.5. High plasma MIF induces adipocyte hypertrophy and obesity through activating the AMPK/JNK/HSL signaling pathway. 83

13-Figure 3.3.6. High caloric diet induces insulin resistance and hyperlipidemia. 86

14-Figure 3.3.7. High caloric diet upregulates plasma MIF that activates adipose AMPK/HSL signaling pathway and augments adipocyte hypertrophy. 88

15-Figure 3.3.8. Neutralization of MIF reverses HFD induced metabolic dysfunction. 91

16-Figure 3.3.9. Neutralization of MIF did not affect HFD induced inflammatory gene expression. 92

17-Figure 3.3.10. The MIF receptor, CD74 is involved in the MIF/AMPK/JNK/HSL signaling pathway. 95
18-Figure 3.3.11. Deficiency of intracellular MIF inhibits HSL expression through JNK but independent of AMPK. 99
19-Figure 3.3.12. *Mif*$^{-/-}$ mice have unchanged HSL phosphorylation at the site of Ser^{565} following HFD compared to WT. 100
20-Figure 3.3.13. *Mif*$^{-/-}$ mice have exacerbated hyperlipidemia and tissue specific insulin resistance in liver and skeletal muscle. 101
21-Figure 3.3.14. *Mif*$^{-/-}$ mice have more severe whole-body insulin resistance compared to WT following HFD. 102
22-Figure 3.3.15. The schematic diagram regarding the effects of extracellular and intracellular MIF on regulating HSL. 109
23-Figure 4.3.1. MIF increases non-transcriptional CD74 protein levels *in vitro* and *in vivo*. .. 114
24-Figure 4.3.2. Hepatic MIF expression in WT and *Mif* lung Tg mice. 115
25-Figure 4.3.3. Transgenic upregulation of circulating MIF levels increases lipid accumulation and fibrosis in the liver. 117
26-Figure 4.3.4. High circulating MIF levels following a HFD upregulate non-inflammatory and non-transcriptional hepatic CD74 levels, leading to the development of hepatic steatosis and fibrosis. 119
27-Figure 4.3.5. The neutralization of MIF reverses HFD-induced upregulation of non-transcribed CD74 levels and attenuates NAFLD development. 121
28-Figure 4.3.6. Transgenic deficiency of MIF downregulates hepatic CD74 levels and NAFLD following HFD feeding. 123

29-Figure 4.3.7. MIF inhibits cleavage of caspase-4 that promotes the stability of CD74 in liver. 126

30-Figure 4.3.8 Graphical abstract summarizing the role of MIF in NAFLD and proposed underlying mechanism 130

LIST OF TABLES

1-Table 1.1 Medications approved for long-term weight managements 39

2-Table 1.2 Medication categories for lipid disorders 41

3-Table 1.3 Medication categories for glucose-lowering treatment 43

4-Table 2.1. List of PCR primer sequences 62

ABBREVIATION

MS: Metabolic Syndrome

T2D: Type 2 diabetes

MIF: Macrophage migration inhibitory factor

CVD: Cardiovascular disease

NAFLD: Non-alcoholic fatty liver

BMI: Body mass index

MC4R: Melanocortin-4 receptor

POMC: Pro-opiomelanocortin

CI: Confidence interval

COVID-19: Coronavirus disease-19

WAT: White adipose tissue

SVF: Stromal vascular fraction

HFD: High fat diet

PPARγ or PPAR-γ: Peroxisome proliferator-activated receptor γ

FASN or *FAS*: fatty acid synthase

C/EBPα: CCAAT/enhancer binding protein α

C/EBPδ: CCAAT/enhancer binding protein δ

GLUT-4: Glucose transporter type 4

FABP4: Fatty Acid-Binding Protein 4

TNF-α or TNFα,*Tnfα:* Tumor necrosis factor α

LPL: Lipoprotein lipase

HSL: Hormone-sensitive lipase

CD36: Cluster of differentiation 36

ATGL: Adipose triglyceride lipase

MGL: Monoglyceride lipase

IL-6 or *Il6*: Interleukin 6

IL-1β or *Il1b*: Interleukin 1 β

MCP1: Monocyte chemoattractant protein 1

IL-1ra: Interleukin 1 receptor antagonist protein

IL-10: Interleukin 10

SAT: Subcutaneous adipose tissue

VAT: Visceral adipose tissue

IP-10: Interferon γ-induced protein 10

LEPR/LepR: Leptin receptors

IRSs: Insulin receptor substrates

JNK: c-Jun N-terminal kinases

IKK: IκB kinase

PKR: Protein kinase RNA-activated, or protein kinase R

S6K: Ribosomal protein S6 kinase

PKC: Protein kinase C

ERK: Extracellular signal-regulated kinase

mTOR: Mammalian target of rapamycin, or FK506-binding protein 12-rapamycin-associated protein 1 (FRAP1)

NASH: Non-alcoholic steatohepatitis

HCC: Hepatocellular carcinoma

FFAs or FA: Free fatty acids

TG: Triglyceride

HDL: High-density lipoprotein

LDL: Low-density lipoprotein

HMG-CoA reductase: 3-hydroxy-3-methyl-glutaryl-coenzyme A reductase

PPARα: Peroxisome proliferator-activated receptor α

SREBP: Sterol regulatory element-binding protein

PCSK9: Proprotein convertase subtilisin/kexin type 9

PUFAs: Polyunsaturated fatty acids

DPP-4: Dipeptidyl peptidase-4

GLP-1: Glucagon-like peptide-1

TZDs: Thiazolidinediones

Cpt1a: Carnitine palmitoyltransferase I, or carnitine acyltransferase I

CRP: C-reactive protein

MMP-9: Matrix metalloproteinase-9

CD74: Cluster of differentiation 74, or HLA class II histocompatibility antigen gamma chain also known as HLA-DR antigens-associated invariant chain

IL-2: Interleukin 2

TLR4: Toll-like receptor 4

CXCRs: C-X-C chemokine receptors

CXCR2: Interleukin 8 receptor beta is a chemokine receptor

CXCR4: C-X-C chemokine receptors 4, also known as fusin or CD184 (cluster of differentiation 184)

CXCR7: C-X-C chemokine receptors 7

CXCL8: C-X-C motif chemokine ligand 8

CD44: Cluster of differentiation 44

MHC: Major histocompatibility complex

NF-κB: Nuclear factor kappa-light-chain-enhancer of activated B cells

CD74-ICD: Intracellular domain of CD74

RUNX: Runt related transcription factors

Akt: Protein kinase B

P53: Tumor protein P53

HSP90: Heat-shock protein 90

SOD1: Superoxide dismutase 1

ALS: Amyotrophic lateral sclerosis

SNPs: Single-nucleotide polymorphisms

AMPK: 5' AMP-activated protein kinase

Acta2: Actin alpha 2, or Alpha-smooth muscle actin or α-Sma

Col1A1: Collagen, type I, alpha 1, also known as alpha-1 type I collagen

Tgfb: Transforming growth factor beta (TGF-β)

CHAPTER 1: INTRODUCTION

1.1 Metabolic Syndrome

Metabolic Syndrome (MS) is characterized by a cluster of metabolic abnormalities, including dyslipidemia, hypertension, hyperglycemia, insulin resistance, and central obesity. Among these symptoms, obesity has been considered the core symptom that may initiate and exacerbate other symptoms. Obesity also increases the risk of cardiovascular disease (CVD), stroke, type 2 diabetes (T2D), and non-alcoholic fatty liver (NAFLD) [1] [2] [3] [4]. NAFLD is due to overwhelming lipid accumulation in the liver, and it is a common disease associated with obesity. However, to date, the mechanism regulating obesity and NAFLD is not fully elucidated. Thus, our current research investigated the molecular mechanisms of obesity and NAFLD.

1.2 Obesity

1.2.1 Definition of Obesity

Obesity is a key global health issue, and its morbidity has significantly increased over the past decades in both developed and developing countries [5] [6]. In general, obesity is defined as a chronic abnormal or excessive fat accumulation, often physiologically evidenced by enlarged adipocyte size or "adipocyte hypertrophy." It also leads to metabolic changes in other crucial organ systems, including liver, skeletal muscle, and heart. The body mass index (BMI) is the common indicator of obesity or overweight (BMI > 25 is overweight and BMI >30 is obese). Obesity is caused by various factors including genetic disorders, excess caloric consumption (Western diet), sedentary lifestyle, and certain medications [7] [8] [9].

1.2.2 Pathophysiology/Mechanisms of Obesity

1.2.2.1 The genetic factors

Genetic induced obesity is attributed to chromosomal deletions, large-scale genetic abnormalities, or single-gene defects. Genetic-induced obesity can be broadly categorized into monogenic and polygenic obesity, both linked to abnormal neural regulation of food intake and thermogenesis [10]. Monogenic obesity is typically stems from gene mutations or deletions, such as melanocortin-4 receptor (MC4R, the most frequent mutation), leptin, or pro-opiomelanocortin (POMC) [11]. Of them, the mutations of the MC4R gene account for almost 4% of monogenic obesity [12]. These genes play crucial roles in the regulation of food intake, energy expenditure [13], and hormone secretion [7 8 9]. For example, leptin deficiency, leptin receptor mutations, and rare defects of the POMC gene contribute to severe hyperphagia in humans and animal models [14 15 16]. Common polygenic variants related to fat mass, also increase susceptibility to obesity both in children and adults. For instance, the rs9939609 variant has been identified as an obesity susceptibility locus, heightening the risk of obesity [17].

1.2.2.2 The lifestyle

Compared to genetic factors (≤ 5%), dietary habits play a more significant role in the pandemic of obesity [18 19]. The Western diet, characterized by its high fat and sodium content,[20] increases the risk of obesity [21 20], cardiovascular disease, and cancer [22]. In contrast, diets rich in vegetables, fruits, whole grains, nuts, and yogurt demonstrate a negative correlation with body weight gain and a reduced risk of fatal diseases [23].

A sedentary lifestyle is another significant factor exacerbating obesity [17 24]. The unprecedented period of mandatory isolation during the COVID-19 pandemic has provided a

unique opportunity to investigate the association between body weight gain and changes in physical activities. The reduction of physical activities was significantly associated with increased body weight gain [25], particularly in children and adolescents [26]. As a result, the global obesity pandemic worsened due to COVID-19 [27] [28] [29]. Conversely, numerous prior studies have highlighted that increased physical activity could ameliorate and even reverse obesity. Engaging in regular physical activity for 250 minutes per week increases energy expenditure, thereby contributing to a reduction in body weight [30].

Many medications, including atypical antipsychotics (e.g., clozapine, olanzapine, risperidone) [31] [32], antihyperglycemics (e.g., thiazolidinediones), and steroid hormones (e.g., corticosteroids, glucocorticoids) [33] [34], as well as antihypertensive drugs (e.g., nitrendipine, atenolol) [35] are known to induce obesity [31] [36] [37]. Approximately 70% of patients with mental disorders are overweight or obese [38] [39]. The overweight or obese condition in these patients is further exacerbated following antipsychotic therapies [40], especially, clozapine and olanzapine, which may increase body weight gain by an average of 4.5-16.2 kg and 3.6-10.2 kg, respectively [41]. Antihyperglycemic medications, such as pioglitazone and rosiglitazone also contribute to increased body weight due to their effects on lipogenesis [41]. Long-term treatment of glucocorticoids increases body weight (e.g., cortisone,1.5-8.4 kg) [42] [43] [44] and triggers metabolic dysfunction. Beta-blockers as a typical antihypertensive drug also enhance body weight gain [45] to different extents. Notably, among beta-blockers, atenolol (-0.5+3.4 kg [46] [47]), propranolol (-0.5+2.3 kg [48] [49]), and metoprolol (1.2-2.0 kg [50] [51]) are associated with the highest body weight gain [41].

1.2.2.3 Cellular mechanisms of obesity

White adipose tissue (WAT) is a primary contributor to obesity [52], consisting of adipocytes and non-adipocytes cells. The non-adipocytes cells collectively known as the stromal vascular

fraction (SVF), comprising preadipocytes, macrophages, fibroblasts, and vascular endothelial cells [8]. Although the total number of adipocytes is solidified in childhood and remains steady throughout the whole of adulthood [53], approximately 10% of these cells undergo renewal annually under physiological conditions. Nevertheless, any aberration or malfunction within these cellular components has the potential to instigate the development of obesity.

1.2.2.3.1 Adipocyte hyperplasia

Hyperplasia refers to “increased cell number”, which is a process that expands adipose tissue and provides a beneficial effect against insulin resistance and metabolic dysfunction [54 55]. In the initial phase, known as "healthy adipose expansion," smaller adipocytes, derived from preadipocytes, undergo increased differentiation [20 21 56 57] (Figure 1.1). HFD rich in saturated fatty acids triggers the proliferation of adipocyte precursor cells [58] and subsequent adipocyte hyperplasia [59], whereas n-3 polyunsaturated fatty acids suppress adipocyte differentiation [60]. Transcriptional factors such as peroxisome proliferator-activated receptor γ (PPAR-γ) and CCAAT/enhancer binding protein α/β (C/EBP α/β) play vital roles in adipocyte maturation following hyperplasia [61 62]. The early differentiation stage of preadipocytes involves the expression of C/EBPβ, which subsequently triggers the expression of PPAR-γ and C/EBP α [63]. These transcription factors, in turn, prompt the expression of pivotal adipogenic genes such as glucose transporter type 4 (GLUT4), fatty acid-Binding protein 4 (FABP4), and adiponectin (Figure 1.2) [64]. Notably, inflammation and proinflammatory cytokines downregulate adipocyte hyperplasia. For example, tumor necrosis factor alpha (TNF-α) disrupts the differentiation of preadipocytes in adipose inflammatory cell milieu. Moreover, studies indicate that overexpression of GLUT4 facilitates adipocyte hyperplasia in mice [65], while TNF-α exhibits an inverse effect by reducing GLUT4 expression and subsequently impeding hyperplasia [7 15]. Additionally, in the late stage of obesity

(metabolically unhealthy obesity), dysfunctional preadipocytes display a macrophage-like phenotype [22]. Consequently, the number of preadipocytes is negatively correlated with BMI and adipocyte cell size during the metabolically unhealthy obese state [22].

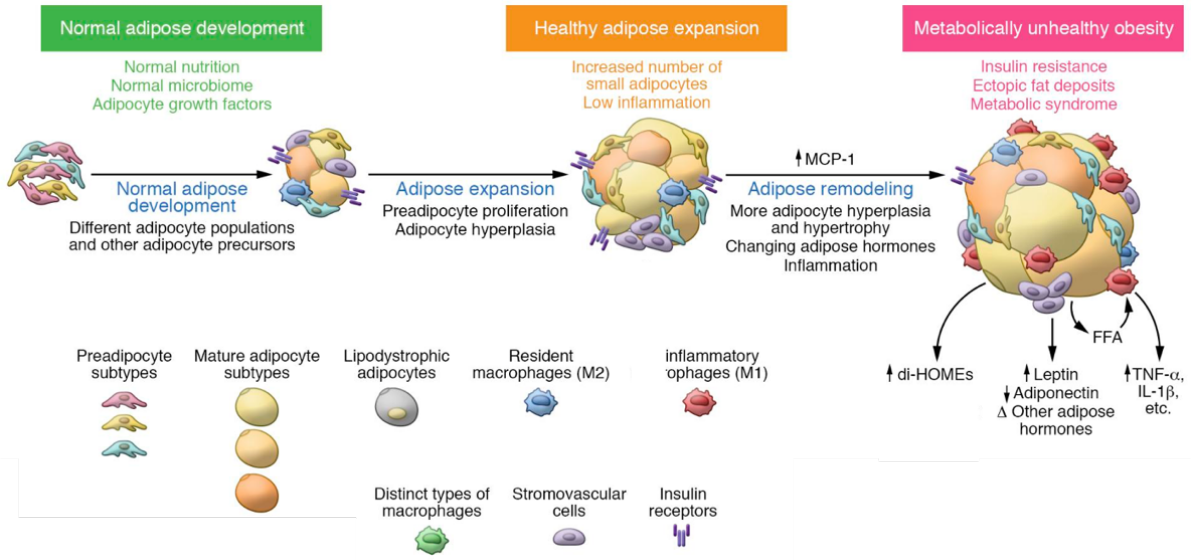

1-Figure 1.1 Altered adipose tissue and adipocyte function in the pathogenesis of metabolic disorders [53]

The figure delineates a chronological progression from left to right, showcasing the transformation of preadipocytes into mature adipocytes. This transition is succeeded by adipose tissue expansion attributed to preadipocyte proliferation and adipocyte hyperplasia, followed by adipocyte hypertrophy, inflammation within the adipose tissue, and alterations in adipocyte hormone profiles ultimately resulting in metabolic syndrome.

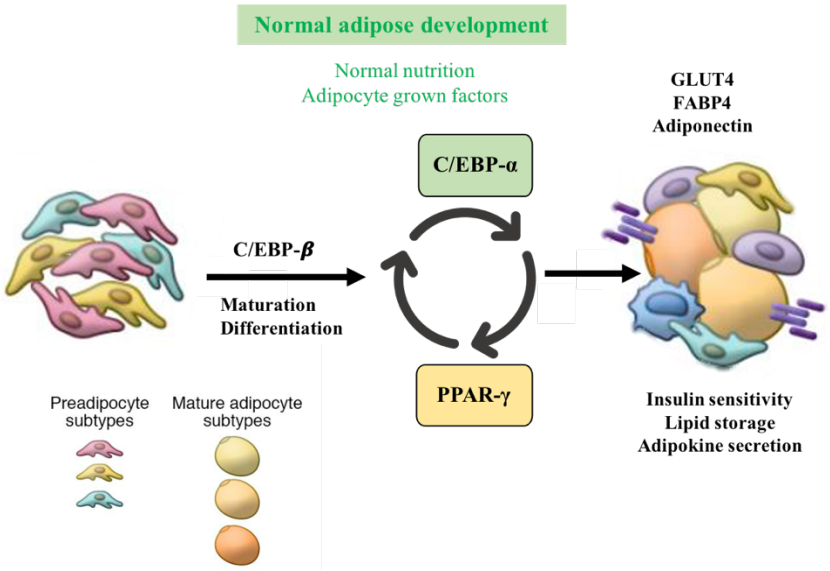

2-Figure. 1.2. Adipocyte differentiation is a complex and tightly regulated process

The differentiation of adipocytes is a multifaceted process governed by diverse signaling pathways, culminating in the activation of C/EBP-α and PPAR-γ *in vitro*. These transcription factors play a pivotal role in initiating and sustaining the expression of crucial adipogenic genes including GLUT4, fatty acid binding protein (FABP)-4, and adiponectin, which are vital for the optimal functioning of adipocytes [64].

1.2.2.3.2 Adipocyte hypertrophy

Within the realm of obesity pathophysiology, in addition to hyperplasia, adipocyte enlargement, referred to as "adipocyte hypertrophy" (Figure 1.1), is a notable phenomenon. Adipocyte hypertrophy manifests as an excessive accumulation of lipids within adipocytes [16], precipitated by heightened lipogenesis and lipolysis processes (Figure 1.3). Various enzymes and proteins govern lipid storage and mobilization in adipocytes, such as lipoprotein lipase (LPL), cluster of differentiation 36 (CD36), HSL. LPL plays a critical role in promoting the cellular uptake of chylomicron remnants, cholesterol-rich lipoproteins, and free fatty acids, which facilities lipid storage in adipocytes [66 67]. In the context of human and rodent obesity, adipose LPL is upregulated, implying its potential contribution to adipocyte hypertrophy [68]. CD36 is a fatty acid transporter, and its deficiency partially protects mice from adipocyte hypertrophy and obesity induced by high-fat diets [69]. In contrast to the process of lipogenesis, lipolysis regulates fatty release from adipocytes and it is mainly catalyzed by three lipases in consecutive steps, including adipose triglyceride lipase (ATGL), HSL, monoglyceride lipase (MGL) [70 71 72]. HSL, recognized as the rate-limiting enzyme in lipolysis within adipocytes [73], exhibits reduced gene expression in obese subjects [74]. The deletion of HSL in adipocytes diminishes lipolysis and then enlarges the adipocytes in WAT [75 76]. In summation, both increased lipid storage and decreased lipolysis within the adipocytes may contribute to the development of adipocyte hypertrophy in obesity.

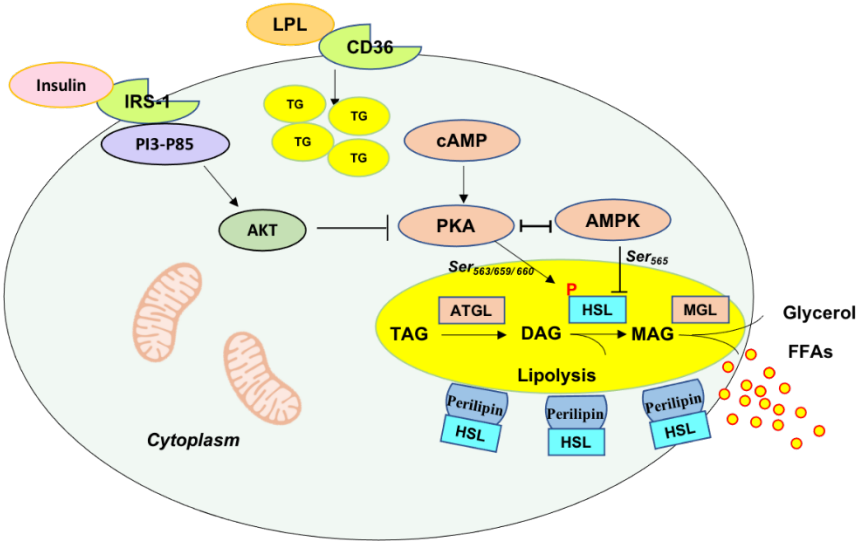

3-Figure 1.3. Regulation of lipogenesis and lipolysis in adipocytes.

Lipogenesis: LPL facilities chylomicron remnants, cholesterol-rich lipoproteins, and free fatty acids uptake through CD36 in adipocytes [66] [67]. *Lipolysis*: Desnutrin/ATGL serves as the catalyst for the onset of lipolysis by breaking down TG into DAG. HSL further metabolizes DAG into monoacylglycerol (MAG), which is then enzymatically cleaved by MAG lipase, resulting in the production of glycerol and three FFAs. Hormonal regulation involves increased cAMP levels and activation of PKA. However, insulin activates AKT, counteracting this effect. PKA phosphorylates HSL at specific sites (Ser [563, 659, 660]), while also disrupting AMPK activation at the inactive site Ser [565] on HSL. This promotes HSL translocation to lipid droplets for DAG hydrolysis and also affects perilipin, enhancing access for lipases [295] [309] [310].

1.2.2.3.3 Adipokines and obesity

WAT is not only a reservoir for energy storage, but also functions as an endocrine organ system to secrete active proteins, "adipokines" to maintain metabolic homeostasis [77]. Adipokines encompass a spectrum of hormones and cytokines, including prominent examples like adiponectin, leptin, TNF-α, interleukin 6 (IL-6), interleukin 1 beta (IL-1β), monocyte chemoattractant protein-1(MCP1), MIF, interleukin 1 receptor antagonist protein (IL-1ra), and interleukin 10 (IL-10) [78] [79] [80] [81] [82]. Notably, IL-6, interleukin-8 (IL-8), and TNF-α exhibit a positive correlation with adipocyte size, while anti-inflammatory cytokines like interleukin 10 (IL-10), interleukin 1 receptor antagonist protein (IL-1ra), and adiponectin demonstrate an inverse correlation with adipocyte size [78] [83]. In different adipose tissue depots, subcutaneous adipose tissue (SAT) and visceral adipose tissue (VAT) exhibit distinct adipokine expression profiles. Generally, proinflammatory cytokines are highly expressed in VAT, whereas leptin and interferon γ-induced protein 10 (IP-10) dominate in SAT [83] [84]. The secreted adipokines eventually exert regulatory effects on food intake, insulin sensitivity, and glucose/fatty acid metabolism, collectively contributing to the development and progression of obesity.

Adiponectin promotes lipid storage in adipocytes by increasing the expression of lipogenic genes, such as *PPAR-γ* target genes and *LPL*. In addition, it may also elevate heparin-releasable LPL in plasma [85] [86]. Leptin acts on leptin receptors (LEPR/LepR) in the hypothalamus, suppressing appetite and increasing energy expenditure [87]. However, elevated circulating leptin levels are often associated with leptin resistance in obese subjects, mitigating its inhibitory effects on appetite [88] [89] [90]. Thus, *leptin*-deficient *ob/ob* mice and *leptin* receptor-deficient *db/db* mice exhibit hyperphagia, obesity, and metabolic dysfunction [91] [92]. The proinflammatory cytokine, TNF-α stimulates lipolysis in adipose tissue through increasing HSL phosphorylation [93]. TNF-α also disrupts the

insulin signaling transduction by downregulating insulin receptor substrate-1 and GLUT-4 expression in 3T3-L1 adipocytes [7] [15]. Neutralization of TNF-α or transgenic deletion of TNF-α receptor has been shown to restore glucose uptake in adipocytes isolated from obese *fa/fa* rats [4] [80] [94]. These collectively underscore the intricate involvement of adipokines in obesity and metabolic dysregulation.

1.3 Obesity-related Complications

Obesity significantly escalates the risk of various serious health conditions and symptoms, including insulin resistance, T2D, cardiovascular disease, hypertension, hyperlipidemia, NAFLD [95], etc.

1.3.1 Insulin Resistance

1.3.1.1 Definition of insulin resistance

Insulin resistance is characterized by a pathological state wherein systemic cells, particularly those in muscle, liver, and adipose tissue, exhibit reduced responsiveness to normal endogenous insulin concentrations. This diminished responsiveness necessitates elevated insulin levels in circulation to facilitate the storage of glucose and lipids in the cells [96]. The development of obesity is often intricately linked with insulin resistance, with obesity exacerbating this condition. Weight loss interventions have been observed to mitigate inflammation, improve insulin sensitivity in peripheral tissues, and enhance β-cell function [97] [98] [99] [100].

1.3.1.2 Molecular mechanisms of insulin resistance

Insulin plays a crucial role in regulating metabolic homeostasis (Figure 1.4), including mediating general glucose uptake and glycogen synthesis [101], hepatic gluconeogenesis and glycogenolysis [102], etc. Insulin binds with the α subunits of insulin receptors to initiate tyrosine

phosphorylation of insulin receptors and insulin receptor substrates (IRSs). The downstream protein, Akt (RAC (Rho family)-alpha serine/threonine-protein kinase also called protein kinase B, PKB) promotes the translocation of GLUT4 to the plasma membrane, resulting in glucose uptake [103] [104]. However, under the influence of nutrients or inflammatory factors [103] [105] [106], such as c-Jun N-terminal kinases (JNK), IkappaB kinase (IKK), protein kinase R (PKR), ribosomal protein S6 kinase (S6K), protein kinase C (PKC), extracellular signal-regulated kinase (ERK) and mammalian target of rapamycin (mTOR) are activated. These activations together or individually lead to serine phosphorylation rather than tyrosine phosphorylation of IRS-1, eventually blunting the insulin signaling pathway [107] [108] [109].

In the context of obesity, elevated levels of circulating fatty acids can initiate signaling pathways that lead to insulin resistance in adipose tissue. Furthermore, obesity enhances the release of adipokines, including TNF-α, which exacerbates this insulin resistance. Additionally, lipid or lipid metabolites present in the circulation, such as diacylglycerol and ceramides, activate proteins like PKC, IKK, and JNK. These activated proteins subsequently promote the serine phosphorylation of IRS-1, further contributing to insulin resistance [110].

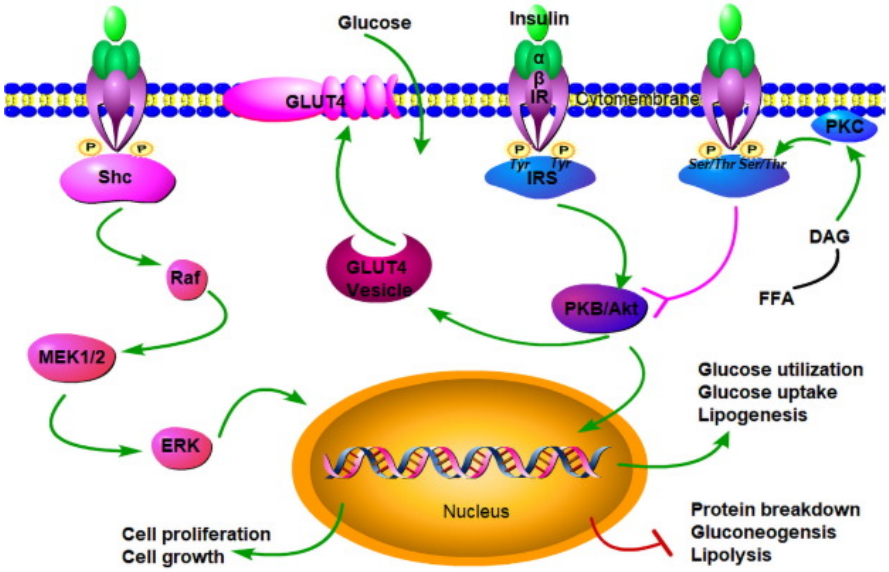

4-Figure 1.4. Insulin signal pathways

Insulin promotes glucose uptake and utilization, and adipogenesis; inhibits gluconeogenesis and glycolysis; and prevents protein decomposition and lipolysis through the IRS/ PI3K/Akt pathway. The change in Ser/Thr phosphorylation on IRS-1 is involved in insulin resistance induced by FFAs. PKC, protein kinase C [103].

1.3.2 NAFLD

1.3.2.1 Definition and prevalence of NAFLD

Liver steatosis is an important disease commonly associated with obesity [111]. NAFLD characterized by an excessive accumulation of lipids within the liver [112], presenting a diverse spectrum of histological alterations ranging from simple macrovascular steatosis to the more severe non-alcoholic steatohepatitis (NASH) and fibrosis. The prevalence of NASH ranges from 3-15% in the general NAFLD population. Without treatment, NASH can progress to advanced liver conditions such as cirrhosis and hepatocellular carcinoma (HCC) (Figure 1.5). Over the past decades, the epidemic of NAFLD continued unabated in parallel with ongoing rise in obesity [113]. Thus, early diagnosis and timely interventions are crucial in preventing the onset of NAFLD and its progression to cirrhosis and HCC. However, so far, none of pharmacological interventions specifically targeting in the liver have been found to effectively counteract NAFLD [114 115].

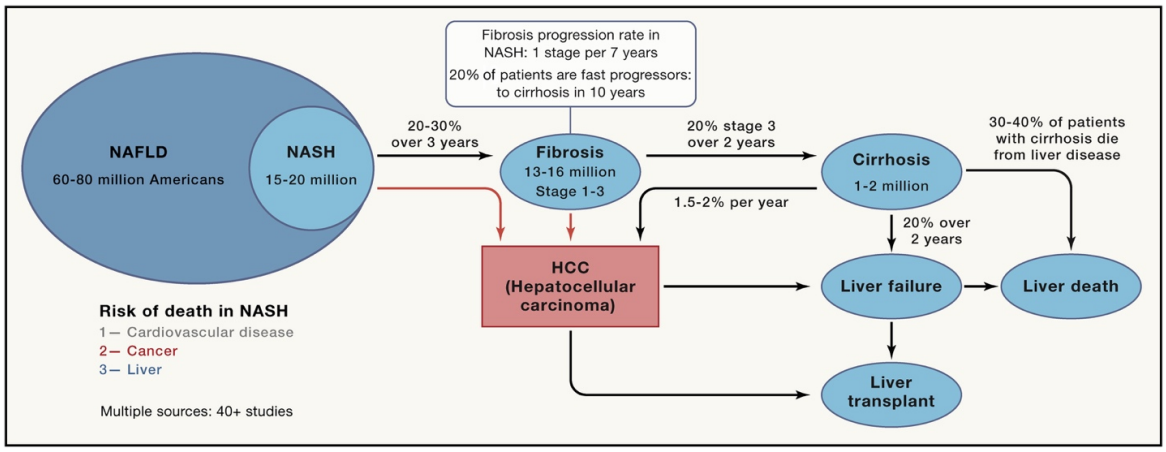

5-Figure 1.5 Natural history of NAFLD.

NAFLD affects a substantial portion of the American population, estimated at up to 80 million individuals. Its progressive manifestation, known as NASH, is observed in around 20% of those afflicted with NAFLD. NASH poses a significant risk of progressing to liver fibrosis, with approximately 15% of individuals ultimately developing cirrhosis. This subgroup of NASH cirrhosis patients faces an elevated risk of HCC and necessitates rigorous screening and surveillance for HCC. Moreover, they face an increased risk of liver decompensation, often requiring liver transplantation. Notably, individuals with cirrhosis experience a significantly elevated risk of liver-related mortality. In the broader context, within the NAFLD population, cardiovascular disease stands as the foremost cause of mortality, followed by cancer and liver-related fatalities [311].

1.3.2.2 Cellular molecular mechanisms of NAFLD

Hepatocytes constitute a significant portion of the liver mass, approximately 55-65%, and play a critical role in regulating lipid and glucose metabolism. Hepatocytes, typically engaged in lipoprotein synthesis [116], experience lipid accumulation in response to a HFD when peripheral tissues, like adipose tissue and skeletal muscle, fail to adequately deposit excess lipids in circulation (Figure 1.6). Hepatic lipid accumulation results in oxidative stress, endoplasmic reticulum (ER) stress, and mitochondrial dysfunction that further induce cell death. Elevated levels of circulating FFAs and proinflammatory cytokines induced by obesity, activate hepatic resident immune cells, Kupffer cells and hepatic stellate cells. These activated Kupffer cells boost the production of inflammatory factors, including TNF-α and MIF [7] [117], instigating more immune cell infiltration and subsequent liver inflammation [118]. Concurrently, the activated stellate cells increase the production of extracellular matrix and collagen in response to hepatic lipid-induced liver damage [119], contributing to fibrosis and exacerbating the progression of NAFLD. In severe cases, this progression may culminate in the development of cirrhosis and hepatocellular carcinoma [120].

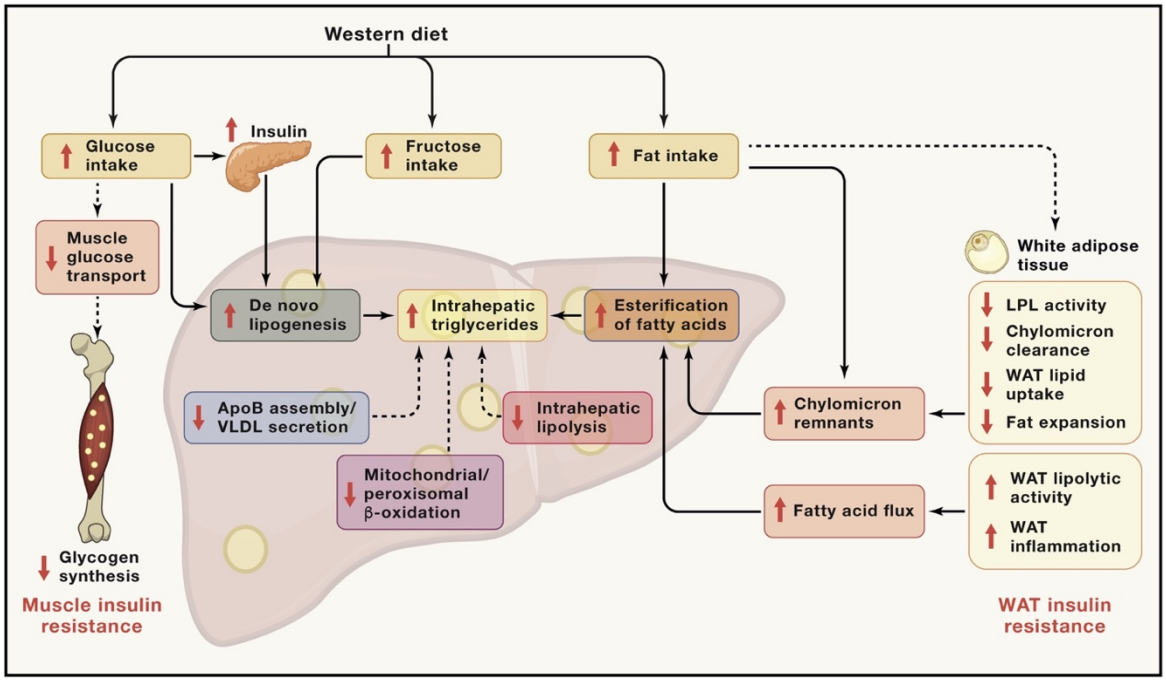

6-Figure 1.6 Metabolic causes of NAFLD.

An escalated caloric intake, particularly through a Western diet abundant in sucrose, high-fructose corn syrup, and saturated fats, is linked to the development of NAFLD and increased deposition of lipids in non-adipose tissues, notably skeletal muscles. The augmented intramyocellular lipid content, often preceding the onset of NAFLD, induces insulin resistance within the muscles, leading to the hindrance of insulin signaling. Consequently, insulin-stimulated glucose transportation and muscle glycogen synthesis are reduced. This impaired glycogen storage in muscle necessitates the redirection of ingested glucose to the liver. Concurrently, compensatory hyperinsulinemia in the portal vein due to muscle insulin resistance activates SREBP1c, thereby enhancing the expression of crucial hepatic enzymes regulating de novo lipogenesis (DNL). This cascade ultimately results in heightened VLDL production, hypertriglyceridemia, and the onset of NAFLD. Monosaccharides can further aggravate NAFLD development by activating other transcription factors like ChREBP, PPARγ coactivator 1-β, and LXR, consequently stimulating hepatic lipogenesis. Additionally, insulin resistance or inflammation in white adipose tissue (WAT) elevates lipolysis rates, leading to an increased supply of fatty acids to the liver. This surplus promotes the esterification of fatty acids into hepatic triglycerides, contributing to NAFLD in a substrate-dependent, largely insulin-independent manner. Triglyceride-rich lipoproteins (TRLs) are normally cleared from the bloodstream via peripheral LPL activity. However, endogenous inhibitors of LPL (e.g., ApoC3, ANGPTL3/8 complex, and ANGPTL4) attenuate peripheral triglyceride clearance, thereby augmenting hepatic triglyceride uptake from TRLs like chylomicron remnants [311].

1.4 Current Therapies for Obesity and Obesity-associated Complications

The management of obesity and its related complications primarily emphasizes lifestyle modifications and enhanced physical activity. However, there are also pharmaceutical interventions aimed at weight loss and lowering the plasma lipid and glucose levels, which have demonstrated effectiveness in addressing obesity-related complications, including diabetes and cardiovascular diseases [1].

1.4.1 Pharmacological Therapies for Obesity

Weight loss plays a pivotal role in managing metabolic syndrome, with studies demonstrating notable improvements in metabolic syndrome [100] with even a modest reduction (5% to 10%) in initial body weight, often accompanied by decreased inflammatory biomarkers [99]. Currently, there are four categories of medications approved for chronic weight management, including (1) Sympathomimetic amine anorectic with or without antiepileptic (e.g., Phentermine); (2) Lipase inhibitor (e.g., Orlistat); (3) Opioid antagonist-aminoketone antidepressant combination (e.g., Naltrexone-bupropion); (4) Glucagon Like peptide 1 receptor agonist (e.g., Liraglutide and Semaglutide) [97] (Table 1.1). Orlistat is the only medication that targets non-appetite mechanisms [121]. Phentermine, an amphetamine analogue, functions by elevating hypothalamic noradrenaline concentration. Its usage is typically restricted to short-term therapeutic interventions. However, the use of phentermine is always accompanied by the risk of severe primary pulmonary hypertension and other side effects[121]. Semaglutide demonstrates significant reductions in body weight [122 123], improves metabolic homeostasis, and diminishes cardiovascular risk in patients with type 2 diabetes [124]. While these existing pharmacological therapies for obesity are effective but their side effects hamper their prevalent use in obesity and type 2 diabetes. Therefore, ongoing research is exploring new pharmacological targets.

1-Table 1.1 Medications approved for long-term weight managements [97] [125] [126]

Drug (Approved)	Mode of action	Route and Dose [97]	Study Duration Week	Mean Weight loss kg (%)	Common Side Effects	Contraindication
Phentermine-Topiramate (1959)	•Phentermine acts on hypothalamus to stimulate norepinephrine release from adrenal. •Topiramate acts on multiple cellular targets as an antiepileptic agent gland. •Promotes feeling of satiety and decreases appetite to reduce food intake [125] •Decrease lipogenesis	Oral; 7.5 mg phentermine and 46 mg topiramate once a day	56	~7% [97]	•Insomnia/dry mouth •Constipation •Paresthesia/Dizziness •Dysgeusia	•Pregnancy (No data) •Hyperthyroidism •Coadministration with MAO inhibitors •Glaucoma •Drug abuse
Orlistat (1999)	•Preventing hydrolysis of dietary fat (triglycerides) into absorbable free fatty acids and monoacylglycerols [127]	Oral, 120mg 3 times a day [125]	52	5.8%-8.8%[11]	•Gastrointestinal side effects •Reduced absorption of fat-soluble vitamins, VD [128]	•Pregnancy •Chronic malabsorption syndrome, cholestasis
Naltrexone-bupropion (2014)	•Increases levels of dopamine and POMC neuronal activity •Blocks opioid receptors on POMC neurons, preventing feedback inhibition of these neurons and further increasing POMC activity	Oral; 16 mg naltrexone and 180 mg bupropion twice a day	56	3·2% [97]	•Nausea/Vomiting •Constipation/diarrhea •Headache/dizziness •Insomnia/dry mouth •Hypertension •Anxiety	•Pregnancy •Uncontrol hypertension •Seizure disorders •Anorexia nervosa or bulimia Drug or alcohol withdrawal • Long-term opioid use • Use of monoamine oxidase inhibitor
Liraglutide (2014)	**GLP1R agonist** [126] [129]**:** •Increases satiety •inhibits gastric emptying •Decreases calorie ingestion through CNS •Reduces acid secretion •Inhibit adipogenesis [130] and increasing thermogenesis[131]	Subcutaneously; 3 mg once a day	56 [132]	4% [97]	•Increased heart rate, •Headache •Nausea/vomiting •Diarrhea/constipation •Hypoglycaemia	•Pregnancy •Person with family history of medullary thyroid cancer or multiple endocrine neoplasia type 2
Semaglutide (2021)	**GLP1R agonist** [126] [133] •Inhibits glucagon, which is a hormone that increases blood sugar •Reduces appetite and slows down digestion in the stomach to reduce food intake	Subcutaneously; 2·4 mg once per week, or oral, 10 mg, one a day [134]	68-104	10%-20% [122] [123]	•Nausea and diarrhea [135] •Kidney problems •Diabetic retinopathy •Allergic reactions •Low blood sugar •Pancreatitis[136] •Hypoglycaemia	•People with heart problems

1.4.2 Pharmacological Therapies for Hyperlipidemia

Dyslipidemia refers to a cluster of lipid disorders, including high plasma TG (hypertriglyceridemia), low plasma high-density lipoprotein (HDL), and high plasma Low-density lipoprotein (LDL) concentrations [130]. Obesity is commonly associated with dyslipidemia. The medications addressing dyslipidemia primarily target adipogenesis, free fatty acid oxidation, and inflammation (Table 1.2).

Statins represent the frontline pharmaceuticals for addressing dyslipidemia, functioning through the inhibition of 3-Hydroxy-3-methylglutaryl-coenzyme A reductase (HMG-CoA reductase), a pivotal enzyme in the conversion of HMG-CoA to mevalonic acid. Moreover, statins elevate the expression of LDL receptors, promoting LDL catabolism within the liver, consequently leading to a decrease in plasma LDL and triglycerides (TG), and an increase in plasma HDL levels [137]. Fibrates act by enhancing fatty acid β-oxidation through peroxisome proliferator-activated receptor alpha (PPARα), thereby reducing hepatic TG secretion [138]. Notably, both statins and fibrates upregulate genes related to adipogenesis (e.g., *LPL*, *PPARγ*, sterol regulatory element-binding protein, *SREBP*) and dampen the gene expression of inflammatory cytokines [139]. Niacin is an effective drug to increase HDL levels [140], but a high dose of nicotinic acid is hepatotoxic. Proprotein convertase subtilisin/kexin type 9 (PCSK9) inhibitors and polyunsaturated fatty acids (PUFAs) facilitate lipid uptake and storage [141], reducing free fatty acid efflux [138] from adipocytes. These actions collectively ameliorate hyperlipidemia and contribute to a relative reduction in the risk of cardiovascular diseases.

2-Table 1.2 Medication categories for lipid disorders[130 142 143]

Drugs category (e.g.)	Mode of action	Target Lipids	FA oxidation	Anti-inflammation	Common Side Effects
Statins (1987) **•Atorvastatin** **•Fluvastatin** **•Pravastatin** **•Rosuvastatin** **•Simvastatin**	•HMG-CoA reductase inhibitors •competitively inhibit the HMG-CoA that catalyses the rate-limiting step in the synthesis of cholesterol •Stimulate lipoprotein lipase	LDL↓ VLDL↓ TG↓ HDL↑	↓[144], increase lipid accumulation liver[139]	↑	•Gastrointestinal upset •Dizziness/ headache •Myalgia •Transient disturbance of liver function tests
Fibrates (1975) **•Fenofibrate** **•Bezafibrate** **•Gemfibrozil** **•Ciprofibrate**	•PPARa agonists[138], increase caloric intake to FA oxidation •Increase FA hepatic uptake and reduce hepatic TG production •Increase LPL activity •Reduce plasma leptin concentration	TG↓ VLDL↓ HDL↑	↑	↑	•Gastrointestinal upset •Rash or pruritus •Dizziness, headache
Bile Acid-Binding (Anion-Exchange) Resins（1988） **•Colesevelam** **•Colestipol** **•Colestyramine**	•Bile acid-binding resins are insoluble, nonabsorbable polymers that bind bile salts in the gut and prevent enterohepatic circulation of bile acids •As a feedback effect, increases the conversion of cholesterol to bile acids in liver •Then increase the hepatic LDL receptor to transport for LDL	LDL↓ TC↓ HDL↑	—	↑[145]	•Headache •Constipation or, occasionally, diarrhoea •Interference with the absorption of certain acidic drugs
Nicotinic Acid and Derivatives (1957) **•Nicotinic acid (niacin)** **•Acipimox**	•Inhibits hormone-sensitive lipase and decreases lipolysis •Inhibits VLDL and LDL secretions and productions from Liver •Inhibits HDL-C hepatic uptake	TG↓ VLDL↓ TC↓ HDL↑	↑[146]	↑[147 148]	•Flushing •Liver damage •Headache •Abdominal pain, dyspepsia, and diarrhoea
Specific Cholesterol Absorption Inhibitor (2002) **•Ezetimibe**	•Acts at the brush border of the small intestinal mucosa to inhibit the NPC1L1 transporter and reduce cholesterol absorption from the gut by about 50%, but no effects on TG •A generic medication (Homozygous familial hypercholesterolemia)	LDL↓ TC↓	↑[149]	↑[150]	•Diarrhoea, abdominal pain. •Headache •Angioedema
PCSK9 Inhibitors (2015) **•Evolocumab** **•Alirocumab** **• Monoclonal antibodies**	•Inhibit the PCSK9 induced LDL receptors degradation in liver cells surface, which in turn increases LDL receptor expression reduces circulating LDL cholesterol by 45-70% •Lowers mean lipoprotein(a)[151]	LDL↓	↑[152 152]	—[153]	•Nasopharyngitis •Arthralgia, back pain •Injection site pain •Rash
Polyenoic Free Acid (PUFA) (2012) **•Omega-3 fatty acids (EPA)** **•DHA, α-linolenic acid** **•Omega-6 fatty acids** (evening primrose oil, g-linoleic acid)	•PPAR-α activation[138] •Inhibit lipogenesis but elevates β-oxidation	TG↓ VLDL↓ HDL↑	↑[154]	↑[141]	•Gastrointestinal upset with nausea, belching, diarrhoea, or constipation •Prolonged bleeding time

TC, total cholesterol, HDL, High-density lipid, IDL, intermediate-density lipid, LDL, low-density lipid, VLDL very-low-density lipid, TG, triglyceride, HMG-CoA, 3-Hydroxy-3-Methylglutaryl-Coenzyme a, FA, free fatty acid, LPL, Lipoprotein lipase, which facilitates FA uptake in cells. EPA, eicosapentaenoic acid, DHA, docosahexaenoic acid,
↑, increase, ↓decrease, —, no effects or no data.

1.4.3 Pharmacological Therapies for Hyperglycemia

Hyperglycemia arises from insufficient insulin function or secretion by pancreatic β-cells. Hence, the management of hyperglycemia aims to compensate for these defects in insulin. In the realm of antihyperglycemic medications, the initial category comprises sulfonylureas, meglitinides, dipeptidyl peptidase-4 (DPP-4) inhibitors, and GLP-1 agonists (Table 1.3). These agents primarily operate by stimulating the release of endogenous insulin. The activation of GLP-1 receptors additionally augments post-prandial lipid-buffering capacity and insulin sensitivity within adipose tissue, consequently impeding ectopic fat accumulation in the liver and skeletal muscle. Thiazolidinediones (TZDs) function as selective agonists of PPAR-γ, promoting adipose lipid storage, reducing circulating fatty acid levels, and enhancing insulin sensitivity. TZDs also increase the expression of fatty acid transporters (CD36), fatty acid oxidation factors (carnitine palmitoyltransferase I, CPT1A), and lipid droplet-associated proteins (Plin2) [155], resulting in significant improvements in insulin sensitivity across adipose tissue, muscle, and liver. TZDs also exhibits anti-inflammatory properties by mitigating plasma levels of C-reactive protein (CRP), MCP-1, and matrix metalloproteinase-9 (MMP-9) [99].

It is worth noting that prevailing medications for obesity and its associated complications possess anti-inflammatory properties. Nevertheless, the extent to which targeting inflammatory factors might augment these therapeutic approaches remains predominantly uncertain. Therefore, our primary research focus centers on elucidating the regulatory role of the proinflammatory cytokine MIF, in regulating obesity and its complication, NAFLD.

3-Table 1.3 Medication categories for glucose-lowering treatment [156] [157] [158]

Drugs category (e.g.)	Mode of action	Route	Effects on AD/BW Anti-inflammation	Common Side Effects
Insulins **•Rapid- and short-acting insulins** **•Long-acting insulins** **•Insulin complexes**	•Promote glucose/FA uptake and glycogen/ triglycerides storage •Inhibit protein catabolism but increase protein synthesis •Slow down the basal metabolism and increase in accumulation of fat and cause weight gain in a dose dependent manner [159]	Injectable	Adipogenesis ↑ An-inflammation ↑ Bodyweight ↑↑	•Hypoglycaemia •Local fat hypertrophy at the injection site •Immunogenic reactions
Amylin agonist **Pramlintide**	•Mimics action of hormone amylin; decreases release of glucagon, slows gastric emptying, and suppresses appetite	Injectable	Adipogenesis ↑ An-inflammation ↑ Bodyweight ↓ [160]	•Nausea/vomiting/anorexia •Hypoglycemia
GLP-1 agonists **•Albiglutide** **•Liraglutide** **•Semaglutide** [134] (oral/injectable)	•Mimic actions of GLP hormone •Enhances glucose-dependent pancreatic insulin secretion by the pancreatic b-cell •Increases cAMP leading to insulin release in the presence of elevated glucose concentration [125] •PPARα agonists [138], increase caloric intake to FA oxidation in adipose tissue	Injectable	Adipogenesis — An-inflammation ↑ Bodyweight ↓↓	•Gastrointestinal upset •Dizziness/headache/fatigue/agitation, •Injection-site reactions
Sulfonylureas **•Glyburide** **•Glipizide** **•Glimepiride**	•Enhances glucose-dependent insulin secretion by the pancreatic b-cell by bind to the sulfonylurea receptor SUR1, and close K_{ATP} channel but open voltage-gated Ca^{2+}channels to increase the first and second phases insulin secretions •Increase GLUT4 expression and insulin sensitivity and glycogen storage[161]	Oral	Adipogenesis ↑ An-inflammation ↑ Bodyweight ↑	•Gastrointestinal disturbance •Weight gain •Skin rashes •Hyponatremia (Glipizide and glimepiride) •Might accelerate the rate of pancreatic β-cell loss
Meglitinides **•Repaglinide** **•Nateglinide**	•Similar to sulfonylureas, but has lower affinity to SUR1 than it	Oral	Adipogenesis ↑ An-inflammation ↑ Bodyweight —	•Gastrointestinal upset
Biguanide **•Metformin**	•Inhibition of mitochondrial respiratory chain complex 1, activates AMPK switches cells from an anabolic to a catabolic state and shut down the ways consume ATP •Decreased hepatic glucose production •Increases FA oxidation and reduces TG •Increase insulin sensitivity of peripheral tissues (IR, AKT signaling pathway) •Increased synthesis of GLP-1	Oral	Adipogenesis ↓ An-inflammation ↑ Bodyweight ↓	•Gastrointestinal upset •Decreased vitamin B12 absorption •Inhibition of pyruvate metabolism encourages lactate accumulation, rare lactic acidosis
Thiazolidinediones (TZDs) **•Pioglitazone**	•Acts is an insulin sensitizer in peripheral tissues •Activate PPAR-γ, which is abundant in adipose tissue •Facilitate adipocyte differentiation and increase adipocyte numbers to takes up TG •Supress proinflammatory genes expression	Oral	Adipogenesis ↑ An-inflammation ↑ Bodyweight ↑↑[1]	•Gastrointestinal disturbances •Headache/dizziness/visual disturbances •Anaemia/heart failure •Increased risk of bladder cancer and fractures •Rare liver dysfunction
DPP-4 inhibitors (gliptins) **•Albiglutide** **•Liraglutide** **•Semaglutide**	•Inhibit the enzyme (DPP-4) that breaks down incretins (include GIP, GLP-1), leading to increase in glucose-dependent pancreatic insulin release, decrease in glucagon release	Oral	Adipogenesis ↑ An-inflammation ↑ Bodyweight —	•Nausea/vomiting/ dyspepsia •Oedema •Headache/dizziness/fatigue/nasopharyngitis •Rare pancreatitis/severe joint pains

SGLT2 inhibitors **•Canagliflozin** **•Empagliflozin** **•Dapagliflozin** **•Ertugliflozin**	•Reduce renal glucose reabsorption and hence increase glucose excretion by inhibiting SGLT2 in proximal tubules of kidney	Oral	Adipogenesis ↑ An-inflammation ↑ Bodyweight ↓[162]	•Increased risk of urinary tract and genital infections •Thirst and polyuria with increased risk of hypovolaemia and electrolyte imbalance •Constipation •Increased risk of diabetic ketoacidosis in type 2 diabetes mellitus
Glucosidase inhibitor **•Acarbose**	•Retard intestinal absorption of carbohydrates by preventing alpha-glucosidase action in enterocytes of the brush border of the mucosa, thus impairing carbohydrate digestion and absorption •Cause the release of GLP-1 in systemic circulation	Oral	Adipogenesis ↑ An-inflammation ↑ Bodyweight—	•Flatulence/loose stools •Rare hepatitis
Drug for treatment of hypoglycaemia **•Glucagon**	Used for acute insulin-induced hypoglycaemia, not chronic hypoglycemia	Injectable	Adipogenesis ↑ An-inflammation ↑ Bodyweight ↓	•Nausea/vomiting and diarrhoea

↑, increase, ↓decrease, —, no effects or no data.

1.5 Macrophage Migration Inhibitory Factor (MIF)

MIF is a pleiotropic cytokine/chemokine that plays a pivotal role in both innate and adaptive immunity. Initially identified in the culture medium of activated T lymphocytes, this soluble factor was noted for its ability to impede the unguided movement of macrophages [163]. This distinctive property led to its nomenclature as macrophage migration inhibitory factor [164 165]. Over time , MIF is constitutively expressed by other immune cells, such as monocytes/macrophages, dendritic cells B lymphocytes and mast cells [166], establishing itself as a crucial element in innate immune and inflammatory responses [163] . Given its proinflammatory nature and involvement in innate immunity, MIF has been implicated in the pathogenesis of diverse diseases, ranging from acute and chronic infectious conditions to inflammatory and autoimmune disorders [166]. These include septic shock, asthma, acute respiratory distress syndrome, rheumatoid arthritis, glomerulonephritis, and inflammatory bowel diseases [166]. In addition to immune cells, MIF expression was also found in non-immune cells, such as adipocytes [167], pancreatic β cell [168 169], hepatocytes [166], and neurons [170], which plays significant roles in metabolic regulation, neurogenesis, fibrosis and insulin section within these cell types [171 172].

1.5.1 The Basic Structure and Function of MIF

MIF exhibits a distinctive tautomerase enzymatic activity and remains highly conserved across evolutionary scales, present in a wide array of organisms from unicellular to vertebrate species [173 174]. Despite this conservation, the gene sequence of MIF displays variability among species [175], e.g. mammal, amphibian (frog), fish, arthropods, helminths, molluscs, protozoa (Leishmania and Plasmodium) with several diverged variants, fungi, bacteria and plants [21] [22], but not in Drosophila and yeast where MIF appears more dispensable [23]. Situated on human chromosome 22q11.2, the MIF gene encodes a non-glycosylated protein of 114 amino acids,

equivalent to 12.5 kDa in molecular weight. The MIF protein has a homotrimeric structure, wherein each monomer is constituted by two antiparallel α-helices (residues 18-31 and 89-72) and a central four-stranded β-sheet [176]. The total six α helix and three β sheets collectively form a barrel-like configuration, featuring a solvent-accessible channel [177] [178]. This channel is intricately linked to the catalytic function of MIF and its binding affinity with its receptor, cluster of differentiation 74 (CD74) [179].

MIF plays a pivotal role in modulating the migration of macrophages particularly evident during the delayed-type hypersensitivity response. However, its contribution extends beyond mere regulation of macrophage migration within inflammatory processes. MIF exerts an amplifying effect on the production of various cytokines, including but not limited to TNF-α, interferon-γ, and interleukins (IL-1β, IL-2, IL-6, IL-8) [180]. Furthermore, MIF actively participates in inflammatory signaling pathways regulated by toll-like receptor 4 (TLR4) or TNF-α receptor [181] [182]. These pro-inflammatory properties of MIF might elucidate its counter-regulatory role, effectively attenuating the immunosuppressive effects induced by glucocorticoids [183].

1.5.2 The Cellular Signaling Transduction of MIF

MIF exerts its cellular functions through both extracellular and intracellular mechanisms. As an extracellular agent, MIF functions as a ligand by binding to cell membrane receptors, notably CD74 and C-X-C chemokine receptors 2/4/7 (CXCR2/4/7). Additionally, it possesses the capacity to be internalized directly by cells, enabling interactions with a diverse array of intracellular proteins.

1.5.2.1 Cluster of differentiation 74 (CD74)/ cluster of differentiation 44 (CD44) receptors

CD74, recognized as a major histocompatibility complex (MHC) class II chaperone, assumes a pivotal role as a cell surface receptor for MIF [184]. Within immune cells, CD74 plays a crucial part in propagating MIF-induced inflammatory responses [184] [185]. Conversely, in non-immune cells, CD74 is implicated in metabolic processes [186] [187] as well as arrhythmia in the presence of MIF [188]. However, CD74 lacks inherent tyrosine or serine/threonine kinase activity in its intracellular domain, thus precluding direct triggering of intracellular signaling pathways. Thus, it typically initiates downstream cellular activities through either co-activator recruitment or intracellular domain cleavage. In the former mode, CD74 necessitates association with CD44 to form a functional complex, activating the extracellular signal-regulated kinase (ERK) signaling pathway in the presence of Src tyrosine kinase [189]. This complex also mediates B lymphocyte proliferation and survival by activating the tyrosine-protein kinase (Syk)-Akt-nuclear factor kappa B (NF-κB) signaling cascade in the presence of MIF [190]. Moreover, upon binding with MIF, CD74 undergoes cleavage, liberating its cytosolic domain known as intracellular domain of CD74 (CD74-ICD). The CD74-ICD engages with runt related transcription factor (RUNX) and NF-κB, thereby enhancing B cell survival [191].

1.5.2.2 C-X-C chemokine receptors (CXCRs)

MIF monomer shares a similar structure as the dimer of C-X-C motif chemokine ligand 8 (CXCL8) [192] [193]. Thus, the chemokine receptors, CXCRs have been identified as the second category of MIF receptors [192]. However, these chemokine receptors are often coupled with CD74 for cellular functions. For example, MIF recruits atherogenic or inflammatory monocytes through binding with both CXCRs and CD74, which are colocalized on cell membrane to form a functional complex [192] [194]. MIF/CD74 stimulated Akt activation is inhibited by the blockade of CXCR4 in T

lymphocytes, suggesting that the CD74/CXCR4 complex involves in MIF signaling pathways [194]. CXCR7 also mediates B cell migration [195] [196] [197] and it is involved in anti-apoptotic and cell survival signaling pathways induced by MIF in platelets [195]. However, due to the limited expression of CXCRs in some tissues, MIF-regulated cellular functions through CXCRs are not comparable with those through CD74.

1.5.2.3 Intracellular effects of MIF

MIF also regulates cellular signaling transductions through directly binding with intracellular proteins. Intracellular MIF can either be synthesized within cells or obtained from extracellular sources through endocytosis. The regulation of MIF endocytosis is facilitated by its receptors, CD74 and CXCR4 [198]. For example, intracellular MIF binds with Jun activating binding protein (Jab1, also known as constitutive photomorphogenesis 9 signalosome subunit 5,Csn5) [199] [200] to downregulate JNK activation [199] and contributes to a "transient" ERK activation [201]. Interestingly, Jab1/Csn5 deficiency augments MIF secretion and subsequent Akt phosphorylation, suggesting that the Jab1/Csn5-MIF interaction serves to sequester MIF in the cytosol [202].

Intracellular MIF also has a major effect on regulating tumor development and neural diseases. MIF binds with the tumor suppressor (p53) that regulates proliferation and survival of carcinoma cells [203] [204]. This effect can be reinforced by heat-shock protein 90 (HSP90) which stabilizes MIF and facilitates the interaction between MIF and p53 in cancer cells [205]. In contrast, pharmacological inhibition of HSP90 leads to a reduction in MIF levels and inhibits tumor growth *in vivo* [206]. In the setting of amyotrophic lateral sclerosis (ALS), a neurodegenerative disorder linked to mutations in superoxide dismutase 1 (SOD1), the chaperone activities of intracellular MIF play a protective role by preventing the accumulation of mutant SOD1 in motor neurons, thus

mitigating the progression of ALS [207] [208]. Obviously, the intracellular effects of MIF are intricate and have a multifaceted impact on cellular signalling cascade.

1.5.3 MIF Polymorphisms and Metabolic Dysfunction

MIF exhibits a positive correlation with the onset of metabolic dysfunction [209] [210] [211] [212] [213]. There are two MIF polymorphisms identified on human MIF promoters, the -794 $[CATT]_{5-8}$ repeats [214] and specific single-nucleotide polymorphisms (SNPs) -173 (G/C, rs755622) [215] [216] (Figure 1.7). Both these two MIF polymorphisms affect MIF expression and circulating MIF levels under physiological and pathological conditions. Compared to the lower MIF expressers (G/5-CATT), high MIF expressers (G/6,7,8-CATT) become more susceptible to obesity [217], insulin resistance or hyperlipidemia [31] [218]. MIF-173C allele is also linearly associated with central obesity [219]. Deciphering the precise biological significance of MIF polymorphisms may favor the adoption of tailored approaches to modulate the function of MIF and its associated genes for the treatment of the disease.

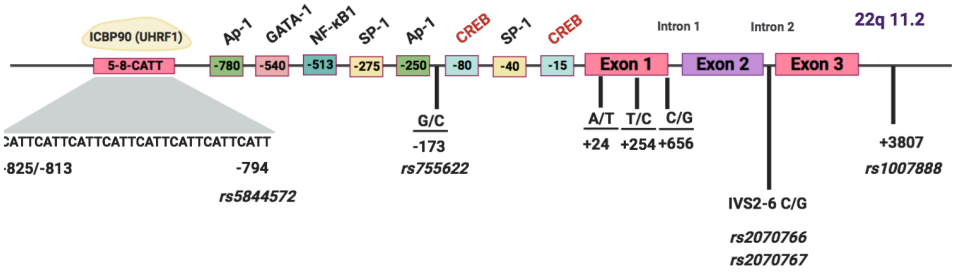

7-Figure 1.7 Schematic representation of the human *Mif* gene: exons, predicted transcription factor-binding sites, and polymorphisms (-173 SNP and -794 CATT) [312].

This figure provides a schematic overview of the human MIF gene, delineating its structure into three exons (labeled as E1, E2, and E3) and highlighting predicted transcription factor–binding sites associated with gene regulation. Additionally, the locations of significant polymorphisms, specifically the -173 single nucleotide polymorphism (SNP) and the -794 CATT polymorphism, are denoted for reference and understanding of genetic variation in the *Mif* gene.

1.6 The Gap of Knowledge

Metabolic dysfunctions, encompassing conditions like obesity, insulin resistance, and NAFLD, pose significant challenges due to their chronic and often asymptomatic progression, making early diagnosis and effective therapeutic interventions difficult. Extensive research over the past decades has shed light on these metabolic disorders [80] [220] [221] [222], yet their underlying molecular mechanisms remain largely elusive. These metabolic conditions are intricately tied to chronic systemic inflammation, particularly within adipose tissue. Remarkably, MIF holds a central position as an upstream regulator in initiating and amplifying the inflammatory response by promoting the production of pro-inflammatory mediators [180]. However, current clinical studies highlight the limitation of targeting specific inflammatory mediators, such as TNF-α, ineffectively addressing adiposity and systemic insulin sensitivity, even when there is an improvement in inflammatory status [223]. Emerging evidence from fundamental research and clinical investigations suggests a positive correlation between circulating MIF levels and metabolic syndromes [209] [210] [211] [212] [213]. Despite studies have primarily focused on MIF within adipose tissue [224], associating its gene expression with adipocyte size, insulin action [225], and adipogenesis [226] [227] [228], there remains an inadequate understanding of its precise role in the regulation of obesity. Moreover, the role of MIF in NAFLD remains a subject of debate, with conflicting findings regarding its contribution to liver fibrogenesis or its potential as a preventive factor [229] [230]. The previous studies have indicated that MIF exacerbates liver fibrogenesis by facilitating the differentiation of immune cells toward a pro-fibrotic phenotype [231] [232]. MIF has also been shown to be involved in preventing liver fibrosis by activating AMPK signaling pathway in hepatocytes [232] [233]. These inconsistent findings concerning the role of MIF in liver fibrosis motivate us for further exploration of new molecular mechanisms and a comprehensive clarification of MIF's role in NAFLD. In light of this, our studies are

strategically devised to bridge this knowledge gap and comprehensively investigate the molecular mechanisms through which MIF initiates and promotes obesity and NAFLD. This research endeavor holds the promise of delivering innovative insights into the functional role of the cytokine MIF in metabolism.

1.7 Overarching Hypotheses, Research Goals and Specific Aims

1.7.1 Research Hypotheses

(1) MIF inhibition of HSL within adipose tissue leads to adipocyte hypertrophy, consequently contributing to the development of obesity.

(2) MIF influences CD74 stability, thereby triggering to the development NAFLD.

1.7.2 Overarching Research Goals and Specific Aims

The first *overarching research goal* of my dissertation is to investigate the regulatory mechanisms governing MIF and the associated signaling pathways crucial in modulating HSL activity during lipolysis. Understanding these regulatory molecular mechanisms is pivotal in comprehending adipocyte hypertrophy and its consequential contribution to obesity.

The *second overarching research goal* is to elucidate the contributions of MIF and its receptor CD74 in NAFLD. This research aims to provide clarity on the ambiguous role of MIF in regulating pathogenesis in the liver.

The above goals were investigated via the following specific aims:

(1) Investigate the molecular signaling pathway involving MIF-AMPK and its downstream effects on HSL in 3T3-L1 differentiated adipocytes *in vitro*.

(2) Examine the molecular mechanisms underlying MIF regulation of HSL in diverse obese animal models *in vivo*.

(3) Assess the influence of MIF on increasing CD74 protein levels in hepatic cells.

(4) Investigate the association between MIF-related CD74 protein accumulation and the progression of NAFLD in murine models.

(5) Elucidate the intricate molecular mechanisms by which MIF contributes to the stabilization of CD74 in in hepatic cells.

CHAPTER 2: MATERIALS AND METHODS

2.1 Antibodies and Reagents

Antibodies against phosphor-AMPK (Thr^{172}) (catalog # 2531), phosphor-Akt (Ser^{473}) (catalog # 9271), phosphor-HSL (Ser^{563}) (catalog # 4139), phosphor-HSL (Ser^{565}) (catalog # 4137) phosphor-PKA (Thr^{197}) (catalog # 4781) phosphor-CREB (Ser^{133}) (catalog # 9198), phosphor-JNK (catalog #4668), phosphor-c-Jun (catalog #9164) and total AMPK (catalog # 2532), PKA (catalog # 4782), Akt (catalog # 9272), CREB (catalog # 99578), Jab1 (catalog # 9444), JNK (catalog # 9252), HSL (catalog # 4107), GAPDH (catalog # 2118S), and secondary antibodies (anti-rabbit IgG, HRP-linked, catalog #7074, anti-mouse IgG, HRP-linked, catalog #7076) were purchased from Cell Signaling. Antibodies against α-Sma (alpha-smooth muscle actin, catalog # MA5-15871) and caspase-4 (catalog # PA5-118880) were purchased from Thermo-Fisher. The antibody against CD74 was a gift generously provided by Dr. Richard Bucala at Yale University. The human recombinant MIF and mouse recombinant MIF proteins were obtained through purification from a high-yield *E. coli* expression system. The purification process involved fast protein liquid chromatography (FPLC), followed by C8 chromatography to eliminate endotoxin [234].

2.2 Experimental Animals

MIF knockout ($Mif^{-/-}$), CD74 knockout ($Cd74^{-/-}$), MIF lung transgenic (*Mif* Lung Tg) and wild type littermate (WT) male mice on a pure C57BL/6 background [235] [236] were bred at the Health Science Center Animal Facility in Memorial University of Newfoundland or the Animal Care Centre of University of Manitoba, Canada. $Mif^{-/-}$, $Cd74^{-/-}$, and their WT littermates at 3 weeks were fed with either normal chow (NC) or high caloric diet (HFD) (#12492, Research Diets, Inc., New Brunswick, NJ, USA) for 12 weeks. *Mif* Lung Tg and its littermate were fed with NC for 25 weeks. All experimental procedures were carried out in compliance with the Guidelines for the Care and

Use of Laboratory Animals set forth by the National Institutes of Health. The protocols were approved by the Internal Animal Committee Review Board of either Memorial University of Newfoundland or University of Manitoba.

2.3 Cell Culture

2.3.1 3T3-L1 Cell Culture

3T3-L1 cells (3T3-L1, ATCC® CL-173TM)) were cultured and differentiated as described previously [237] [238], which the cells used for experiments will be limited within 8th cell passages to prevent population and genetic drift, and ideally, experiments performed with similar passage numbers. Initially, 3T3-L1 preadipocytes were seeded into 6-well plates or 12-well plates and maintained in 37 °C in a humidified 5% CO_2 incubator. The culture medium consisted of Dulbecco's Modified Eagle Medium (DMEM, 11995-040, Gibco™) supplemented with 10% newborn calf serum (16010159, Gibco™) until the culture reaches 100% confluence.

The induction of adipocytic differentiation was achieved through the addition of adipogenic agents as the differentiation medium, including 0.5 mM 3-Isobutyl-1-methylxanthine (IBMX, I-7018, Sigma), 1 μM dexamethasone (DEX, D-4902, Sigma), and 5 μg/mL insulin (I-5500, Sigma), to the culture medium containing 10% fetal bovine serum (FBS, A3160401, Gibco™), for a duration of 48 hours. Following this initial induction phase, the culture medium was switched to maintenance medium supplemented with 10% FBS and 5 μg/mL insulin for another 48 hours, repeated twice. The differentiated 3T3-L1 adipocytes, characterized by the presence of conspicuous lipid droplets observed under a microscope, were then prepared for subsequent experimental treatments.

Prior to commencing all experiments, cells were subjected to an 8-hour serum-starvation period in DMEM-0.5% FBS cell culture medium.

2.3.2 HepG2 Cell Culture

HepG2 cells (ATCC, HB-8065) were cultured in Minimum Essential Medium (10-009-CV, Corning) supplemented with 10% Fetal Bovine Serum (FBS, Gibco™, Canada). Upon reaching a cell confluence of 70~80%, cells were subjected to serum fasting by replacing the medium with one containing 0.5% FBS, and this condition was maintained for 8 hours. Subsequently, the cells were exposed to various treatments, including human rMIF at a concentration of 400 ng/ml, MIF098 (10 μM, compound 5 [239], generously provided by Dr. Richard Bucala), Z-LEVD-FMK (20 μM, ab120489, Abcam), and FITC-labeled rMIF.

2.4 MIF Neutralization with Anti-MIF Antibody

As previously outlined [240], C57BL/6 WT mice were individually housed in IVC cages under a controlled 12:12 hr light-dark cycle at room temperature (RT). These mice were subjected to either a standard chow diet or for a duration of 12 weeks, commencing at the age of 3 weeks. Intraperitoneal injections (i.p.) were administered to the WT mice (at 7 weeks) in the last 5 weeks of the 12 weeks HFD regimen. The injections included a mouse anti-MIF monoclonal antibody, generously provided by Dr. Richard Bucala, as the experimental treatment, and non-specific IgG (MAB002, R&D) as a control treatment. Each injection was administered at a dosage of 20 mg/kg, and these injections were conducted twice weekly. Body weights of these mice were assessed on a weekly basis. Upon the conclusion of the 15-week study, which included 12 weeks of HFD feeding, the mice were euthanized, and both blood samples and tissues (such as adipose tissue, liver, skeletal muscle) were collected and subsequently preserved at -80 °C for subsequent analysis.

2.5 Histology

2.5.1 Oil red O Staining

2.5.1.1 Oil red O staining of 3T3-L1 adipocytes

Given that lipid synthesis and accumulation represent protracted processes within the cell, the following treatment regimen was pursued: 3T3-L1 preadipocytes were cultured in 6-well plates, maintaining them in DMEM supplemented with 10% bovine calf serum until the culture reaches 100% confluence. Adipocytic differentiation was induced by differentiation medium for 48 hours. Following this, the medium was transitioned to a maintenance medium comprised of 10% FBS, 5μg/mL insulin and 100μM palmitic acid (P0500, Sigma) with or without 250 μM AICAR (A9978-5MG, Sigma) or 10 μM SP600125 (JNK Inhibitor II, 420128, Calbiochem®). The culture medium was refreshed every 48 hours to maintain treatment consistency. Palmitic acid was employed to mimic a high-lipid plasma environment *in vivo*. Cell harvesting was conducted 72 hours following the initiation of differentiation and was ready for the Oil red O staining for the intracellular lipid accumulation.

The Oil red O (A12989.22, Thermo Scientific Chemicals) working solution was prepared by initially dissolving 0.5 g of Oil Red O powder in 100 mL of isopropanol, resulting in a 0.5% stock solution. Subsequently, this stock solution was diluted with double distilled water (ddH_2O) in a 3:2 ratio. The working solution was then filtered and allowed to stand for a minimum of 10 minutes at RT [241].

Cells were subjected to two washes with phosphate-buffered saline (PBS, pH 7.4) and subsequently fixed using 4% paraformaldehyde (PFA) for a duration of 15 minutes at RT. After a double wash with ddH2O, the cells were covered with the Oil Red O working solution for a period

of 10 minutes. Following this, the cells underwent washes under running tap water for 5~10 minutes. Finally, the stained cells were observed under a microscope, and characteristic images were captured for analysis.

2.5.1.2 Oil red O staining of Tissues

Tissues, including liver and skeletal muscle, were initially fixed by immersion in 10% neutral formalin and allowed to undergo fixation overnight. Subsequently, these tissues were subjected to cryoprotection through immersion in a 30% sucrose (w/v) solution prepared in 1× phosphate-buffered saline (PBS). Following cryoprotection, the tissues were embedded in OCT compound (Sakura Finetek, 4583, CA, United States) and frozen [242]. The tissue specimens were sectioned into 5-10 μM slices, followed by visualization, and staining of intracellular lipids using the Oil Red O method, as previously detailed in literature. Microscopy was utilized to capture representative images of these tissue sections, with a specific focus on obtaining characteristic visuals for subsequent analysis [243].

2.5.2 Hematoxylin-eosin (H&E) Staining

H&E staining was employed to facilitate the identification of adipocyte hypertrophy within adipose tissue, following established protocols [244]. In brief, glass slides containing paraffin-embedded sections were subjected to a series of treatments. First, they were immersed in xylene three times for 5 minutes each to eliminate the paraffin. Then, the samples underwent hydration through sequential immersion in 100% ethanol, 95% ethanol, and 70% ethanol, each for 5 minutes. Following this, the slides were rinsed under running tap water for 2 minutes.

Next, the slides were immersed in hematoxylin solution for a duration of 3 minutes, followed by a thorough washing under running tap water for 5 minutes. After that, the samples

were stained with eosin Y solution for a period of 2 minutes and dehydrated by sequentially dipping the slides into 70% ethanol for 20 times, and transferring to 95% ethanol, 100% ethanol, and finally into xylene for three changes of 2 minutes each. Lastly, the prepared slides were mounted with a suitable mounting medium, cover slips were placed on them, and the edges of the coverslips were sealed with nail polish to ensure an airtight seal, facilitating image acquisition and quantification under a microscope.

2.5.3 Trichrome Staining [245]

Trichrome staining is employed to visualize tissue sections, specifically emphasizing collagen fibers and connective tissues, following established protocols [245]. The samples were deparaffinized by submerging into 3 times of the xylene for 5minutes/time, followed by 100%, 95%, and 70% of ethanol for 5 minutes/change to hydrate the samples. The slides then were put in the Bouin's solution at 60 °C for 45 minutes. Next, slides were washed in running tap water until yellow colour in samples disappeared. Slides were immersed in Weigert's haematoxylin for 8 minutes to differentiate nuclei and followed with 2 minutes washing under tap water. To stain the cytoplasm and erythrocytes, slides were initially immersed in anionic dyes, acid fuchsin for a duration of 5 minutes. Next, the slides were rinsed with running tap water for 2 minutes. Following this, the slides were exposed to a phosphomolybdic acid solution as a mordant for 10 minutes. Immediately thereafter, the slides were immersed in methyl blue solution) for 5 minutes to facilitate the staining of fibroblasts and collagen. Following this step, the slides were once again washed under running water for 2 minutes. Finally, they were treated with a 1% acetic acid solution for a duration of 1 minute. Subsequently, the slides underwent a dehydration process using a series of alcohol solutions, each with a 5-minute duration at percentages of 70%, 95%, and finally 100%.

Before observation, the slides were briefly dipped into absolute xylene for 1 minute. Finally, they were mounted with a cover slip using mounting medium.

2.6 The Lipid Profiles Quantification

Following established procedures [246], 3T3-L1 adipocytes underwent an initial PBS wash to eliminate phenol red. They were then subjected to various treatments, including vehicle, AICAR (250μM), recombinant mouse MIF proteins (400ng/ml, generously provided by Dr. Richard Bucala), or isoproterenol (10μM). These treatments were individually administered to phenol red-free high glucose DMEM supplemented with 2% BSA, and the cells were exposed for a duration of 24 hours. These interventions were conducted both in the presence and absence of high palmitic acid (100μM). The culture medium was subsequently collected for the quantification of glycerol and fatty acid levels using commercially available kits from Sigma (F6428, free glycerol reagent) and Fuji Film (NEFA-HR (2) assay). These quantifications were carried out in strict accordance with the manufacturer's provided protocols.

2.7 Enzyme-Linked Immunosorbent Assay (ELISA)

Mouse MIF concentrations were measured by a one-step sandwich enzyme-linked immunosorbent assay according to manufacturer’s protocol (Mouse MIF DuoSet ELISA, R&D, DY1978) as previously described [227].

2.8 siRNA Transfection

In order to transiently inhibit the expression of MIF and AMPK in 3T3-L1 adipocytes, the cells were transfected with 1nM *Mif* siRNA (N405895, ThermoFisher), 30μM AMPK Alpha 1/2 siRNA (sc-45313, Santa Cruz), or a non-silencing control siRNA (AM4611, ThermoFisher) using Lipofectamine™ RNAiMAX Transfection Reagent (13778075, Invitrogen) in a medium devoid

of FBS and antibiotics, following the manufacturer's instructions. In summary, the procedure involves the preparation of two solutions: Solution 1 containing diluted RNAiMAX Transfection reagent and Solution 2 containing siRNA, both prepared in blank DMEM medium. Subsequently, these two solutions are combined in a 1:1 ratio and allowed to incubate at room temperature for 5 minutes. Finally, the resulting mixture is added to the cells and incubated for 1-3 days, followed by various treatments as required.

2.9 Samples Preparation and Assessment

2.9.1 RNA Extraction

Total RNA was extracted by a TRIzol method. Briefly, cells were washed with ice cold 1× PBS, and then 500 μL TRIzol™ reagent (15596026, Invitrogen™) was added to each well of a 6-well or 12-well plates containing cells subjected to various treatments. The cell lysate was thoroughly homogenized by pipetting up and down several times and incubated at RT for 10 minutes to ensure complete dissociation of the nucleoproteins complex. After that, the lysate was transferred to a 1.7 mL Eppendorf tube. To remove lipid content, the lysate was centrifuged at 12,000 × g for 5 minutes at 4 °C. The upper fat layer was discarded, and the pink layer was retained. To this layer, 100 μL of chloroform was added, gently shaken by hand, and incubated for 10 minutes at RT. Following incubation, the samples were centrifuged for 15 minutes at 12,000 × g at 4 °C. This centrifugation resulted in phase separation, with a lower phenol-chloroform layer, an interphase, and a colorless upper aqueous phase. The aqueous phase, which contained RNA, was carefully transferred to a new tube, and mixed with an equal volume of isopropanol. The mixture was incubated at 4 °C for 10 minutes and then centrifuged for 10 minutes at 12,000 × g at 4 °C. This step led to the precipitation of total RNA, forming a white, gel-like pellet at the tube's bottom. The supernatant was discarded, and the RNA pellet was washed twice with 1 mL of 75% ethanol.

Following washing, the RNA pellet was air-dried. Finally, the RNA was resuspended in 30 µL of RNase-free water. The quantity and quality of the isolated mRNA were determined using a NanoDrop 2000 spectrophotometer.

Tissue RNA extraction commenced with homogenizing 50 mg of tissue in 1 mL of TRIzol™ reagent using sonication. Afterward, the RNA extraction procedure for cells was followed.

2.9.2 Reverse Transcription (RT) of RNA to Obtain cDNA

The cDNA synthesis from the total RNA was carried out using the RevertAid First Strand cDNA Synthesis Kit (K1621, Thermo Scientific™) following the manufacturer's protocol. In summary, 500 ng of total RNA was combined with 1 µL random hexamer primer, 4 µL 5 × reaction buffer, 1 µL ribolock RNase inhibitor (20 U/µL), 2 µL of 10 mM dNTP mix, and 1 µL revertAid M-MulV RT (200U/ µL) to a total volume of 20 µL. The mixture was gently mixed and briefly centrifuged. The reverse transcription reaction followed the program below: 1) incubate for 5 minutes at 25 °C; 2) followed by 60 minutes at 42 °C) terminate the reaction by heating at 70 °C for 5 minutes.

4-Table 2.1. List of PCR primer sequences

Gene Name	Sequences (5'–3')
Mouse ATGL	GAG ACC AAG TGG AAC ATC GTA GAT GTG AGT GGC GTT
Mouse HSL	CAG AAG GCA CTA GGC GTG ATG GGG CTT GCG TCC ACT TAG TTC

Mouse PPARγ	ACA GAC AAA TCA CCA TTC GT CTC TTT GCT CTG CTC CTG
Mouse FASN	CAT GAC CTC GTG ATG AAC GTGT CGG GTG AGG ACG TTT ACA AAG
Mouse LPL	AGA GCC AAA AGA AGC AG GGC AGA GTG AAT GGG AT
Mouse CD36	TTG AAA AGT CTC GGA CAT TGA T TCA GAT CCG AAC ACA GCG TA
Mouse PPARa	TGG TGT TCG CAG CTG TTT TG AGA TAC GCC CAA ATG CAC CA
Mouse CPT1	ACT CCG CTC GCT CAT TCC G TGT TTG AGG GCT TCA TGG CT
Human-Cd74	GGC AAC AT GAC AGA GGA CCA CAG GAT GTT GAA GAC CGC CT
Mouse-Cd74	ACG CTC CAC CGA AAG AGT C CGT AGA ATC GAG ACC GAG GA
Human-TNF-α	TGT AGC CCA TGT TGT AGC AAA CC GAG GAC CTG GGA GTA GAT GAG GTA
Mouse-TNF-α	CAG GCG GTG CCT ATG TCT C CGA TCA CCC CGA AGT TCA GTA G
Human-IL-1β	CAG AAG TAC CTG AGC TCG CC AGA TTC GTA GCT GGA TGC CG

Mouse-IL-1β	TGG TGT GTG ACG TTC CCA TT CAG CAC GAG GCT TTT TTG TTG
Human-IL-6	TGG CTG AAA AAG ATG GAT GCT TCT GCA CAG CTCT GGC TTGT
Mouse-IL-6	GAG GAT ACC ACT CCC AAC AGA CC AAG TGC ATC ATC GTT GTT CAT ACA
Human-Caspase-4	TTC CCT ATG GCA GAA GGC AAC TGC CAT GAC CCG AAC TTT GT
Mouse-Caspase 11	AGA GGT GGG AAC TCT GGA GAA AGC CTC CTG TTT TGT CTC GG
Mouse-Col1A1	TCG CTT CAC CTA CAG CAC CC TGA CTG TCT TGC CCC AAG TTC
Mouse-Acta2	CGT GGA TGC CCG CTG A TAC GCT TCC GCT GCC C
Mouse-Tgfβ	GGA CTC TCC ACC TGC AAG ACC GGA TGG CTT CGA TGC GC
Human-β-actin	CCT GTA CGC CAA CAC AGT GC ATA CTC CTG CTT GCT GAT CC
Human-HSL	CCA CGA GCC CTA CCT CAA GA CCA GGG AGT AGT CGA TGG AGA
Mouse-*GAPDH*	ATG TGT CCG TCG TGG ATC TGA TGC CTG CTT CAC CAC CTT CTT

2.9.3 Quantitative qPCR

The reaction was performed with a SsoAdvanced Universal SYBR® Green Supermix (Bio-RAD, 1725274) in a total 20 μL reaction system according to the manufacturer's instruction. Transcript levels of *ATGL*, *PPARγ*, *Cd36*, *FASN*, *PPARα*, *CPT1*, *HSL*, *Cd74*, *Tnf-α*, *IL-1β*, *IL-6*, *Acta2*, *Col1A1*, *Tgfb* and *Caspase-4*genes (Table 2.1) were quantified through qPCR using a ViiA™ 7 Real-time PCR System. The data obtained were subjected to analysis using QuantStudio™ Real-Time PCR Software [31]. The cycle threshold (CT) value of the target gene was normalized to either *GAPDH* or *β-actin*. Gene expressions were determined utilizing the relative quantification method ($2^{-\Delta CT}$). The fold changes in the expression of the genes of interest were assessed using the ($2^{-\Delta\Delta CT}$) method.

2.9.4 Protein Extraction

Total proteins were extracted from adherent cells cultured in plates using a lysis buffer composed of 20 mM, Hepes, pH7,4; 50 mM, β- Glycerol phosphate; 2 mM, EGTA; 1mM, DTT; 10mM, NaF; 1mM, $NaVO_4$; 1% triton X-100; 10% glycerol. This lysis buffer was supplemented with 1 × concentration of cOmplete EDTA-free protease inhibitors cocktail (Roche, cat. #11836170001) and phosphatase inhibitors (PhosSTOP, Roche, cat. #4906845001).

Briefly, cells were washed with ice cold 1× PBS, after which 100~200 μL lysis buffer was added to each well of a 6-well or 12-well plates where the cells were previously seeded and subjected to various treatments. These plates were then placed on ice and allowed to incubate for 10 minutes prior to cell detachment using cell scrapers. The resulting cell lysate underwent multiple rounds of gentle pipetting to ensure thorough homogenization before being transferred to 1.7 mL Eppendorf tubes. The lysates were then subjected to centrifugation at 14,000 × g for 10

minutes at 4 °C. Supernatants were meticulously collected from the samples, ensuring the avoidance of disturbance to the upper beige fat layer.

The protein concentration was determined by the protein assay dye reagent (5000006, Bio-Rad). Specifically, triplicate preparations were made for each sample by combining 10 μL of diluted cell lysate (1:49 diluted with dd H_2O) with 200 μL dye (1:4 diluted with dd H_2O), followed by a 5-minute incubation at RT. The absorbance was measured at 595 nm using a microplate reader (Synergy™ H1, BioTeK).

In the case of tissue samples, the amount of tissue was quantified by weight before being mixed with lysis buffer and subsequently subjected to the same standardized procedure.

2.9.5 Co-immunoprecipitation

Adipose tissues from WT and *Mif*$^{-/-}$ mice were subjected to lysis utilizing a lysis buffer, with resulting lysates standardized to a concentration of 1mg/mL. Immunoprecipitation was conducted in accordance with the prescribed protocol outlined in the Dynabeads™ Protein G Immunoprecipitation Kit (10007D) from Thermo Fisher.

In brief, the preparation of the Dynabeads-antibody (Ab) complex commenced with incubation, involving a specific antibody directed against Jab1 (9444, CST) (diluted at 1:200), along with Dynabeads™ magnetic beads, under constant rotation for a period of 30 minutes at RT. The Dynabeads™-Ab complex then was washed twice with a washing buffer. Following the removal of the supernatant, the Dynabeads™-Ab-antigen complex was generated by introducing freshly prepared lysates from adipose tissue, with incubation involving rotation extended overnight at 4 °C. After a further cycle of washing with the washing buffer repeated thrice, the Dynabeads™-Ab-antigen complex was treated with 4 × SDS loading buffer. Analysis via Western blotting [247]

enabled the assessment of the levels of total JNK, phosphorylated JNK, and MIF proteins, which were captured through antibody targeting Jab1.

2.9.6 Western Blot Analysis

Protein samples were prepared by mixing them with 4× Laemmli sample buffer to achieve a working concentration of 1-2 μg/μl for subsequent analysis. These samples underwent denaturation at 95°C for 10 minutes. In parallel, a 10~12% SDS-PAGE handcast gel was submerged in 1× sodium dodecyl sulfate (SDS) running buffer within a western blot system (Bio-Rad). A dual color standard protein ladder (PM008-0500, Froggabio) and the pre-heated samples were loaded and run following the program (100V, 90 minutes). The separated proteins in the gel were electrically transferred to a 0.22 μm PVDF membrane (8cm × 7cm) in 1× transferring buffer at 100V for 60 minutes. Following transfer, the membranes were blocked with 5% skim milk in TBS-Tween (TBST) for 60 minutes at RT. The membranes were then incubated overnight at 4°C with primary antibodies, each prepared in 5% BSA in 1× TBST. The following day, the membranes were subjected to three 10-minute washes with 1× TBST before being incubated with HRP-linked secondary antibodies in 5% skim milk in 1× TBST for 60 minutes at RT. After three additional 10-minute washes with 1× TBST, the protein bands were visualized using an ECL Substrate (1705061, Bio-Rad). Signal detection was performed utilizing an iBright™ FL1500 Imaging System (Invitrogen™). The levels of phosphorylated and total protein in adipose tissue or cells were assessed, and signal quantification was carried out using ImageJ software.

2.10 Statistical Analysis

Differences between group mean values were assessed using either one-way ANOVA followed by Tukey’s post-hoc tests or a Student's t-test, as appropriate. The level of statistical

significance was set at $p<0.05$.

CHAPTER 3: Different Roles of Extracellular and Intracellular MIF in Mediating Adipose Hormone-sensitive Lipase During the Development of Obesity

3.1 ABSTRACT

Attenuation of adipose HSL may impair lipolysis and exacerbate obesity. We investigate the role of cytokine MIF in regulating adipose HSL and adipocyte hypertrophy. MIF released from the adipocytes downregulates HSL in an autocrine fashion, by activating the AMPK/JNK signaling pathway upon binding to its membrane receptor, CD74. Wild type (WT) mice fed HFD, as well as mice overexpressing MIF, both of them had high circulating MIF levels and showed suppression of HSL during the development of obesity. Blocking the extracellular action of MIF by a neutralizing MIF antibody significantly reduced obesity in HFD mice. Interestingly, intracellular MIF binds with Jab1 and JNK, which leads to an opposing effect to inhibit JNK phosphorylation. With global MIF deletion, adipocyte JNK phosphorylation increased, resulting in decreased HSL expression, suggesting that the loss of MIF's intracellular inhibitory action on JNK was dominant in *Mif*$^{-/-}$ mice. Adipose tissue from *Mif*$^{-/-}$ mice also exhibited higher Akt and lower PKA phosphorylation following HFD feeding compared with WT, which may contribute to the downregulation of HSL activation during more severe obesity. Thus, intracellular and extracellular MIF have opposing effects to balance HSL function, but extracellular actions physiologically predominate to downregulate HSL and exacerbate the development of obesity during HFD.

3.2 INTRODUCTION

Fatty acid mobilization from adipose tissue is a key mechanism contributing to the development of insulin resistance in liver and skeletal muscle [248]. Hormone sensitive lipase (HSL) mediates fatty acid release from adipose tissue by catalyzing hydrolysis of triglycerides and diacylglycerides [249]. Insulin resistance is negatively correlated with HSL gene and protein expression independent of fat mass [250]. Obesity also downregulates HSL activity and norepinephrine-induced lipolysis [251]. The reduction in HSL may contribute to adipocyte hypertrophy and obesity in the setting of HFD and caloric excess. HSL undergoes both transcriptional and non-transcriptional regulation, however, the precise cellular mechanisms underlying the regulation of HSL in obesity are largely unknown.

Metabolic disorders are associated with chronic underlying inflammation in adipose tissue. The cytokine TNF-α has lipolytic actions [252], suggesting that adipose inflammation and inflammatory factors may regulate lipolysis, and endotoxin, which is a potent stimulus of TNF-α release, increased HSL phosphorylation, and stimulated lipolysis in adipose tissue [93]. Thus, classic inflammatory factors appear to regulate lipolysis by activating HSL in adipose tissue.

The previous studies suggest that MIF is positively correlated with adipose tissue mass [253], and obesity induces adipose MIF expression and cellular release [224]. Our recent work has shown that the antipsychotic olanzapine inhibits HSL and lipolysis in adipose tissue through increasing MIF action and promotes insulin resistance [31]. However, it is currently unknown whether MIF directly downregulates HSL and thus the development of adipocyte hypertrophy during obesity.

MIF has both intracellular and extracellular actions to regulate cell signaling. In immune cells and cardiomyocytes, MIF activates ERK and AMPK signaling pathways through binding with its cell surface receptor, CD74. MIF additionally demonstrates chemokine-like properties via

non-cognate interactions with chemokine receptors CXCR2 and CXCR4. However, in Hela cells, intracellular MIF directly interacts with Jab1, a coactivator facilitating JNK activation. MIF arrests Jab1/Csn5 resulting in the downregulation of JNK signaling pathway. In the present study, we investigated the transcriptional and non-transcriptional effects of extracellular and intracellular MIF in regulating HSL in adipose tissue. We also examined whether MIF inhibition of HSL contributes to lipid accumulation in adipose tissue. Our data suggest that HSL regulation by MIF is an important molecular mechanism that could exacerbate obesity in HFD.

3.3 RESULTS

3.3.1 The Activation of AMPK Inhibits HSL and Lipolysis through JNK in Adipocytes

We first investigated the molecular signals contributed to the HSL mediated lipolysis in the adipocytes *in vitro*. This is based on prior studies showing that MIF activates AMPK in the heart and liver that promotes fatty acid oxidation [254] [255], and AMPK also inhibits lipolysis by downregulating HSL activation in adipose tissue [256]. While the HSL and lipolysis were well established that HSL phosphorylation at Ser^{563} via PKA stimulates HSL activity whereas AMPK phosphorylates HSL at Ser^{565}, which leads to reduced phosphorylation of Ser^{563} and lipolysis [256]. To this end, we started to test and verify our hypothesis in the differentiated 3T3-L1 adipocytes, we found that AMPK activation induced by AICAR treatment (250μM, Figure 3.3.2A) was associated with a reduction in HSL gene and protein expression (Figure 3.3.1A and B) but did not change the expression of adipose triglyceride lipase (ATGL) (Figure 3.3.1A). In parallel, AICAR also upregulated the inhibitory phosphorylation of HSL at Ser^{565} (Figure 3.3.1C). These effects of AMPK activation together reduced activating phosphorylation of HSL at Ser^{563} (Figure 3.3.1C) and were associated with a decrease in glycerol and fatty acid release from adipocytes (Figure 3.3.1D). The results suggest that both transcriptional and non-transcriptional effects of AMPK mediate the inhibition of HSL activation which downregulates adipocyte lipolysis.

To determine the transcription factors involved in the gene-level regulation of AMPK action on HSL. We found that AICAR treatment also upregulated phosphorylation of JNK and its downstream protein, a nuclear transcriptional factor, c-Jun (Figure 3.3.1E). Notably, these effects were inhibited by *AMPK-siRNA*, indicating that this action was mediated by AMPK (Figure 3.3.1E). Intriguingly, the inhibition of JNK by SP600125 did not impact AMPK activation by AICAR (Figure 3.3.1F). Still, it effectively prevented the effects of AICAR on HSL expression

and phosphorylation and adipocyte lipolysis (Figure 3.3.1G to I). Importantly, The AMPK/JNK regulated HSL signaling pathway occurred without changes in the PKA signaling pathway (Figure 3.3.2B). Furthermore, in the presence of high fatty acid (100μM palmitic acid), AICAR augmented lipid storage, and this effect was notably inhibited by SP600125 (Figure 3.3.1J). These collective results suggest that AMPK/JNK activation contributes to adipocyte hypertrophy through its inhibitory effects on HSL expression and activation.

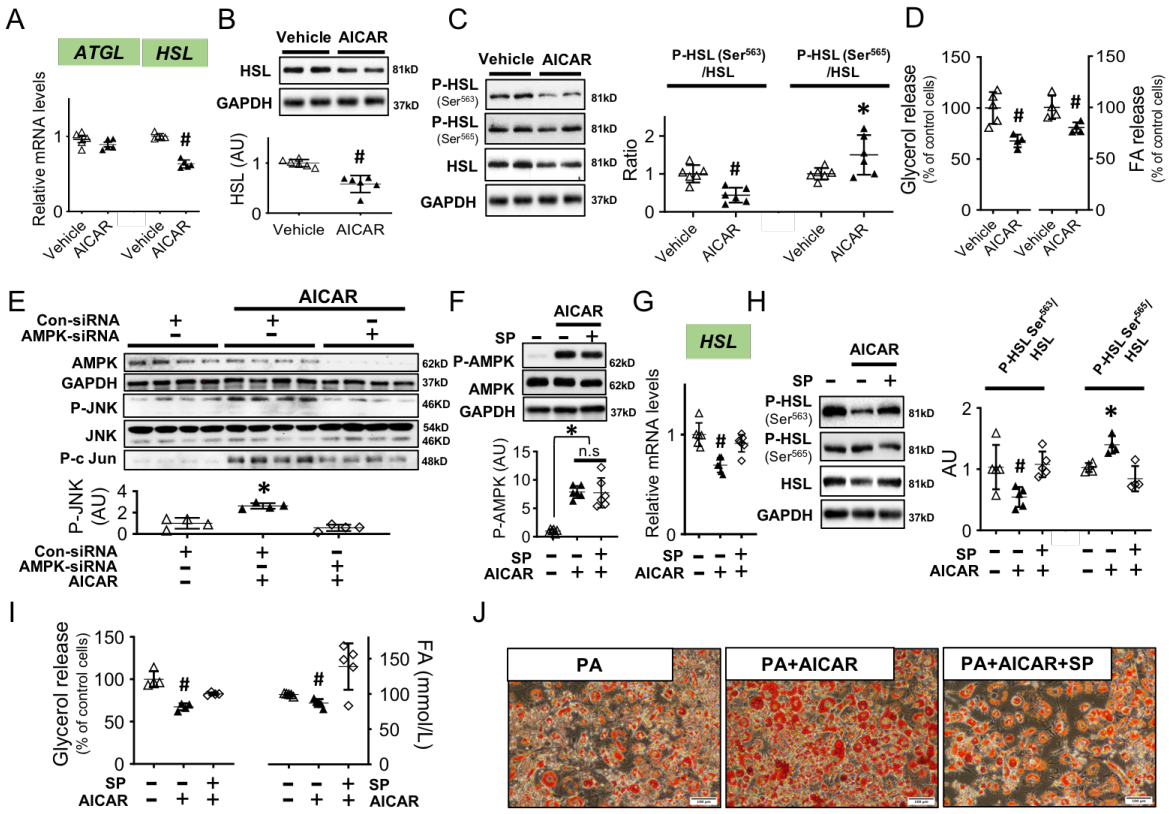

8-Figure 3.3.1. AMPK activation inhibits HSL and lipolysis through JNK in adipocytes.

3T3-L1 cells were differentiated and incubated with an AMPK activator, AICAR (250µM) for 24 hours. *ATGL* and *HSL* gene expression was quantified with qPCR (A). Total and phosphor-HSL protein levels were measured with western blot (B and C). Glycerol and fatty acid (FA) release was evaluated in (D). Following knockdown of *AMPKα1* and *α2* isoforms by siRNA, AMPK, phosphor- and total JNK, and p-c Jun were examined in adipocytes following vehicle and AICAR treatment (E). In a separate experiment, the JNK inhibitor, SP600125 (10µM) was incubated with AICAR and AMPK phosphorylation, *HSL* gene and protein expression and HSL phosphorylation were subsequently evaluated from (F) to (H). Glycerol and FA were quantified in (I). In the presence of high palmitic acid (PA, 100µM), Oil red O staining was performed to evaluate lipid accumulation in adipocytes following AICAR with or without SP600125 treatment. All data are Mean ± SD. *$P \leq 0.05$ increase and $^{\#}P \leq 0.05$ reduction vs. vehicle in A-D and F; vs. other groups in E, G-I.

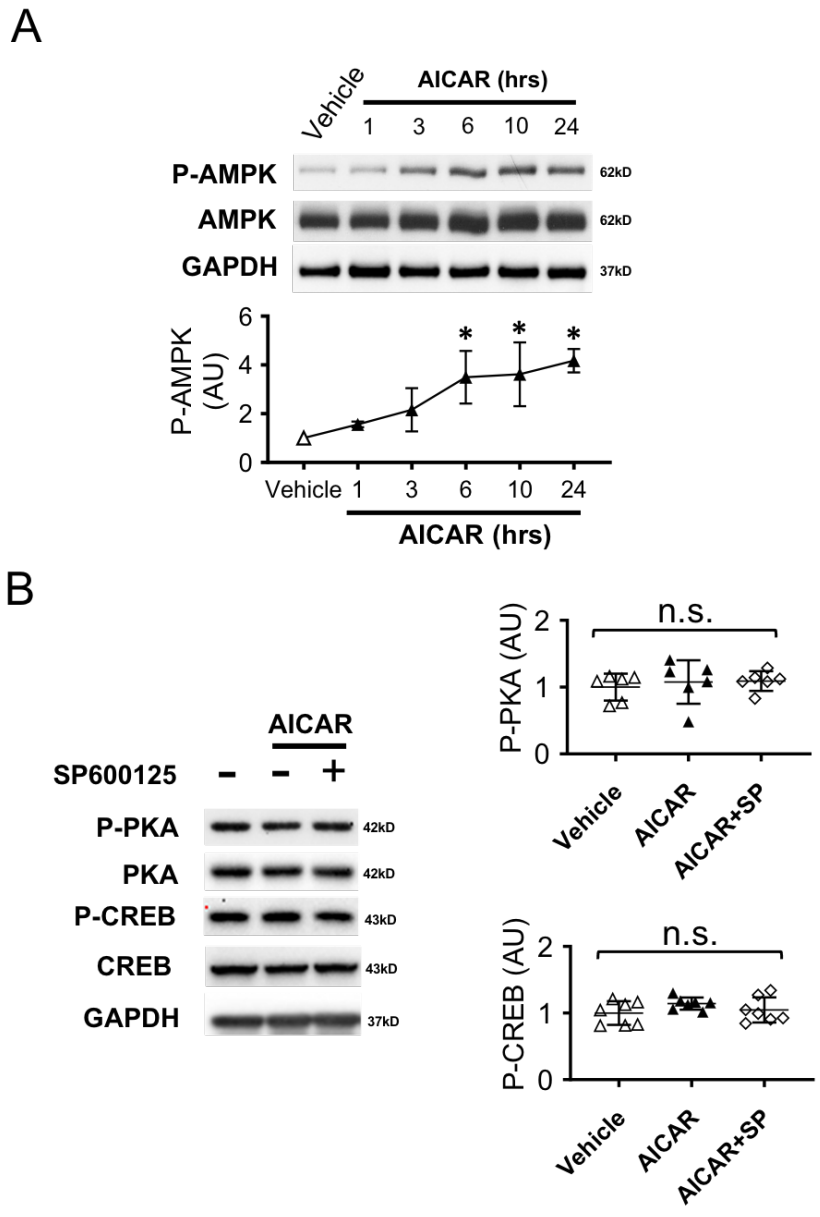

9-Figure 3.3.2. The effects of AICAR on AMPK and PKA/CREB.

AICAR stimulates AMPK phosphorylation in a time-dependent manner (A) without affecting PKA and CREB phosphorylation (B). JNK inhibition by SP600125 does not change the PKA/CREB signaling pathway (B). All data are presented as mean ± SD. *P ≤ 0.05 increase vs. vehicle. n.s. represents no significance.

3.3.2 Extracellular MIF Downregulates Lipolysis through the AMPK/HSL Pathway Which Facilitates Lipid Storage in Adipocytes following High Palmitic Acid Treatment

Our previous studies indicated that MIF regulates metabolism through activating AMPK signaling pathway in the heart and hypothalamus [31] [187]. Hence, we extended our studies by treating the 3T3-L1 adipocytes with MIF (400ng/ml) for 24 hours. Evidently, we found MIF elicited a robust stimulation of AMPK phosphorylation (Figure 3.3.3A). In concert with this, there was a significant reduction in *HSL* gene and protein expression (Figure 3.3.3B and C), while the expression of the lipolytic enzyme *ATGL* remained unaltered (Figure 3.3.3B). Importantly, MIF-induced AMPK activation also triggered inhibitory phosphorylation of HSL, thereby contributing to an attenuation in HSL activation (Figure 3.3.3D). Further investigations unveiled that MIF treatment exhibited a direct inhibitory effect on Akt phosphorylation in 3T3-L1 adipocytes (Figure 3.3.4A). It is noteworthy, however, that the downregulation of Akt was not associated with any discernible change in the phosphorylation of PKA or its downstream protein CREB (Figure 3.3.3E). This observation strongly suggests that MIF's regulatory influence on HSL operates independently of the traditional Akt/PKA signaling pathway. Moreover, MIF treatment exerted a significant downregulation on the release of glycerol and fatty acids from the cells (Figure 3.3.3H), underscoring its inhibitory effect on lipolysis. Crucially, upon silencing AMPK in adipocytes (Figure 3.3.4C), MIF failed to inhibit either HSL expression or activation (Figure 3.3.3F and G), and the MIF-mediated downregulation of glycerol and fatty acid release was likewise impeded (Figure 3.3.3H). These compelling findings affirm that MIF's regulation of HSL and lipolysis is unequivocally AMPK-dependent.

We also found that MIF activation of phosphorylation of JNK and c-Jun was also inhibited by *AMPK siRNA* (Figure 3.3.3I). Furthermore, the effects of MIF on the expression and activation

of HSL, as well as adipocyte lipolysis, were reversed in response to the JNK inhibitor (Figure 3.3.3J-L), underscoring the pivotal role of JNK in mediating MIF's impact on HSL and lipolysis. This regulatory influence of JNK also operated independently of the PKA signaling pathway (Figure 3.3.4B).

To delve deeper into the consequences of MIF's downregulation of HSL and lipolysis, particularly under conditions of high fatty acid exposure, we incubated 3T3-L1 adipocytes with MIF in the presence of high palmitic acid (PA, 100μM) for 24 hours. While the expression of adipogenesis-related genes such as *PPARγ* and *FASN* remained unchanged, HSL gene expression and phosphorylation were significantly reduced following MIF and high PA treatment (Figure 3.3.3M and N). Intriguingly, isoproterenol, a non-selective β adrenoceptor agonist, effectively reversed the reduction of HSL activation induced by MIF (Figure 3.3.3N). Consequently, isoproterenol significantly reduced MIF-induced enlargement of lipid droplets (Figure 3.3.3O), emphasizing the pivotal role of HSL in regulating lipid accumulation associated adipocyte hypertrophy following MIF exposure.

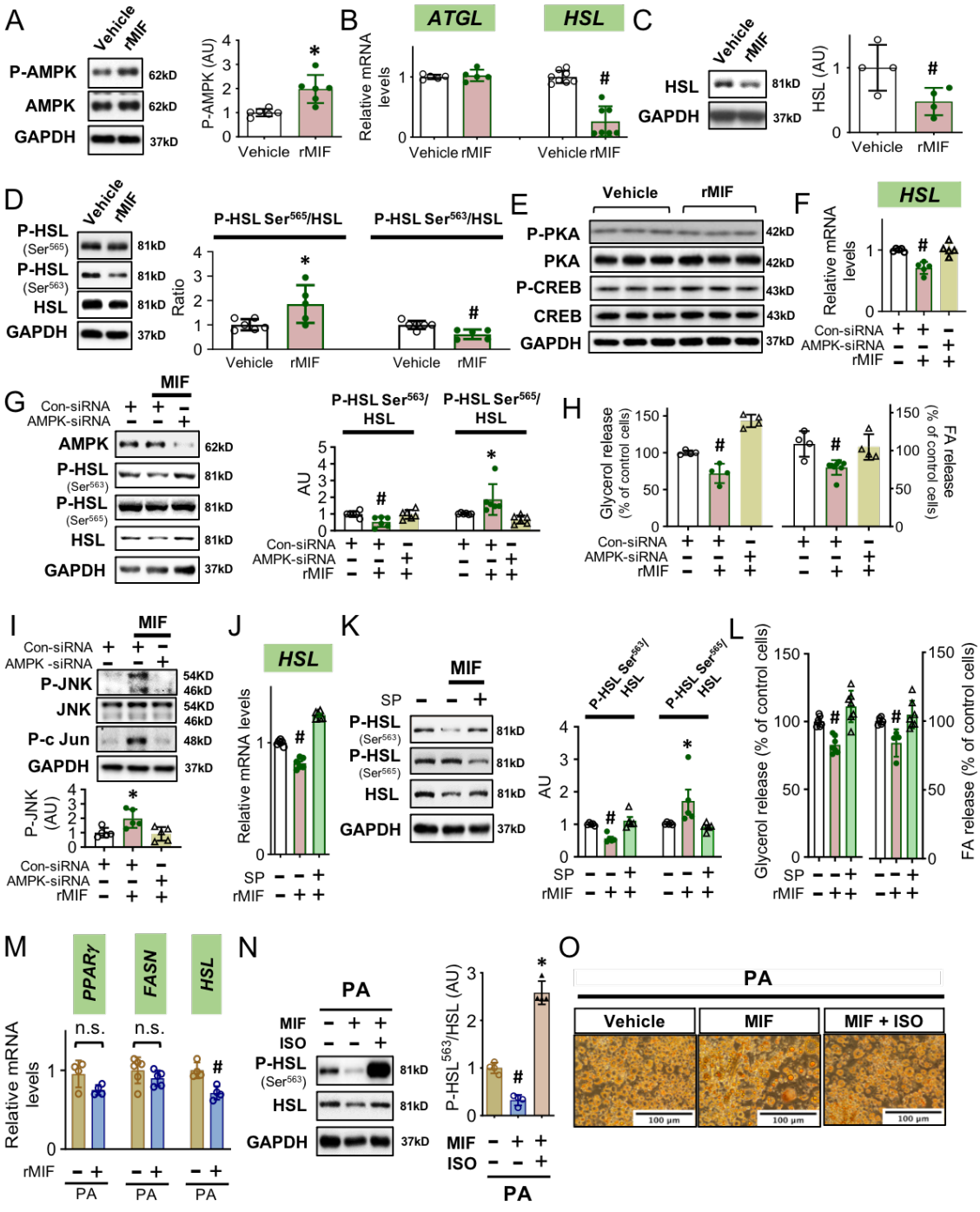
A
Vehicle
rMIF
P-AMPK
AMPK
GAPDH
62kD
62kD
37kD
P-AMPK (AU)
Vehicle
rMIF
B
ATGL
HSL
Relative mRNA levels
Vehicle rMIF
Vehicle rMIF
C
HSL
GAPDH
81kD
37kD
HSL (AU)
Vehicle
rMIF
D
P-HSL (Ser565)
P-HSL (Ser563)
HSL
GAPDH
81kD
81kD
81kD
37kD
P-HSL Ser565/HSL
P-HSL Ser563/HSL
Ratio
Vehicle
rMIF
Vehicle
rMIF
E
Vehicle
rMIF
P-PKA
PKA
P-CREB
CREB
GAPDH
42kD
42kD
43kD
43kD
37kD
F
HSL
Relative mRNA levels
Con-siRNA
AMPK-siRNA
rMIF
G
MIF
Con-siRNA
AMPK-siRNA
AMPK
P-HSL (Ser563)
P-HSL (Ser565)
HSL
GAPDH
62kD
81kD
81kD
81kD
37kD
P-HSL Ser563/ HSL
P-HSL Ser565/ HSL
AU
Con-siRNA
AMPK-siRNA
rMIF
H
Glycerol release (% of control cells)
FA release (% of control cells)
Con-siRNA
AMPK-siRNA
rMIF
I
MIF
Con-siRNA
AMPK -siRNA
P-JNK
JNK
P-c Jun
GAPDH
54KD
46kD
54KD
46kD
48kD
37kD
P-JNK (AU)
Con-siRNA
AMPK-siRNA
rMIF
J
HSL
Relative mRNA levels
SP
rMIF
K
MIF
SP
P-HSL (Ser563)
P-HSL (Ser565)
HSL
GAPDH
81kD
81kD
81kD
37kD
P-HSL Ser563/ HSL
P-HSL Ser565/ HSL
AU
SP
rMIF
L
Glycerol release (% of control cells)
FA release (% of control cells)
SP
rMIF
M
PPARγ
FASN
HSL
Relative mRNA levels
n.s.
n.s.
rMIF
PA
PA
PA
N
PA
MIF
ISO
P-HSL (Ser563)
HSL
GAPDH
81kD
81kD
37kD
P-HSL563/HSL (AU)
MIF
ISO
PA
O
PA
Vehicle
MIF
MIF + ISO
100 μm
100 μm
100 μm

10-Figure 3.3.3. Extracellular MIF downregulates lipolysis through the AMPK/HSL pathway which facilitates lipid storage in adipocytes following high palmitic acid treatment.

Differentiated 3T3-L1 adipocytes were incubated with recombinant mouse MIF protein (rMIF, 400ng/ml) for 24 hours. The phosphorylation of AMPK (A), *ATGL* and *HSL* gene (B), and HSL protein (C) expression was evaluated subsequently with qPCR or western blot. Furthermore, the phosphorylation of HSL at Ser^{565} and Ser^{563} sites was assessed by western blot (D). The activation of HSL upstream enzyme, PKA and its downstream, CREB was quantified in (E). Following knockdown of *AMPKα1* and *α2* isoforms by siRNA, HSL expression and activation were measured in (F) and (G). The relevant glycerol and fatty acid (FA) release was quantified in (H). In the absence of AMPK, phosphor- and total JNK were evaluated by western blot (I). In addition, HSL expression and phosphorylation were quantified by qPCR or western blot following MIF treatment with or without SP600125 (SP) incubation (J and K). Glycerol and FA were also measured in the medium (L). In the presence of high palmitic acid (PA), *PPARγ*, *FASN* and *HSL* gene was quantified following MIF treatment (M). Isoproterenol (ISO) regulated HSL phosphorylation and lipid accumulation following MIF was examined by western blot and Oil red O staining in (N) and (O), respectively. All data are mean ± SD. $^{*}P \leq 0.05$ increase and $^{\#}P \leq 0.05$ reduction vs. vehicle in A-D and M; vs. other groups in F-L and N. n.s. represents no significance.

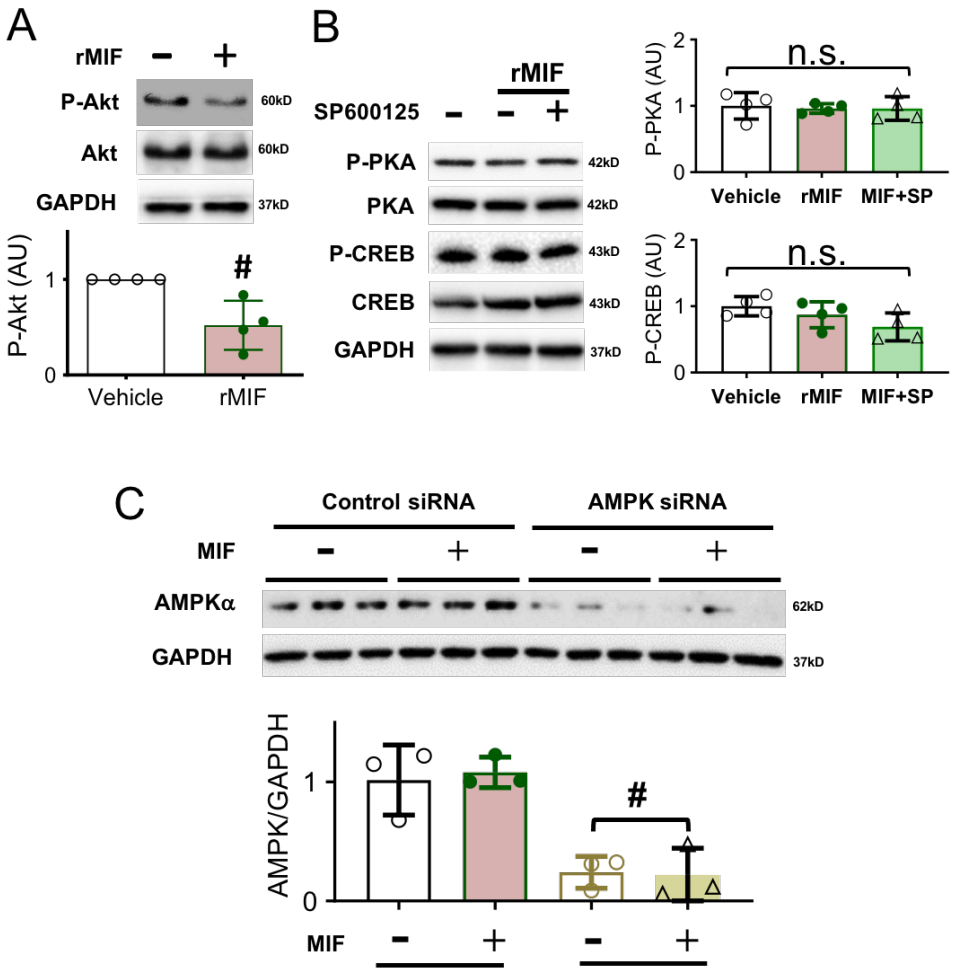

11-Figure 3.3.4. The effects of MIF on phosphorylation of Akt and PKA.

Vehicle or 400ng/ml of recombinant mouse MIF was incubated with 3T3-L1 differentiated adipocytes for 24 hours. Akt (A) and PKA (B) phosphorylation was evaluated by western blot. SP600125 was also incubated with MIF to investigate whether the inhibition of JNK affects PKA and CREB phosphorylation (B). *AMPK α1* and *α2* subunits were knocked by siRNA (C). All data are presented as mean ± SD. $^{\#}P \leq 0.05$ reduction vs. vehicle. $^{\#}P \leq 0.05$ reduction vs. control siRNA. n.s. represents no significance.

3.3.3 High Plasma MIF Induces Adipocyte Hypertrophy and Obesity through Activating the AMPK/JNK Signaling and Inhibiting HSL

The *in vitro* findings provide compelling evidence that MIF activation of AMPK exerts a downregulatory effect on HSL expression and activation, constituting a pivotal molecular mechanism underlying the augmentation of lipid storage within adipocytes. To further elucidate the contribution of the MIF/AMPK/HSL signaling pathway to the development of adipocyte hypertrophy and obesity *in vivo*, we first employed *Mif* lung Tg mice, in which MIF is over-expressed in the lung. These mice characterized with a high plasma MIF levels (Figure 3.3.5A), which coincided with increased phosphorylation of AMPK, JNK, and c-Jun (Figure 3.3.5B), along with decreased HSL expression and activation in adipose tissue (Figure 3.3.5C to E). Concurrently, these mice displayed visibly enlarged adipocyte size (Figure 3.3.5F) and exhibited a higher rate of body weight gain compared to age-matched WT mice (Figure 3.3.5G).

Given the well-established connection between heightened plasma MIF levels and insulin resistance [227], a condition characterized by reduced Akt activation [257], our investigations substantiated the presence of systemic and adipose-specific insulin resistance in the *Mif* lung Tg mice (Figure 3.3.5H and I). Furthermore, it's also noteworthy to highlight that HSL is widely recognized to be dependent on the Akt/PKA pathway [258]. Intriguingly, we observed a notable attenuation of Akt phosphorylation in the adipose tissue of these mice, while the PKA signaling pathway exhibited no discernible alteration (Figure 3.3.5J). Additionally, our findings revealed that the elevated plasma MIF levels did not induce changes in the expression of adipogenesis-related genes, specifically *PPARγ* and *FASN* expression (Figure 3.3.5K). These results suggest that MIF-mediated activation of the AMPK/JNK axis selectively impacts HSL and lipolysis in adipose tissue during the progression of adipocyte hypertrophy and obesity.

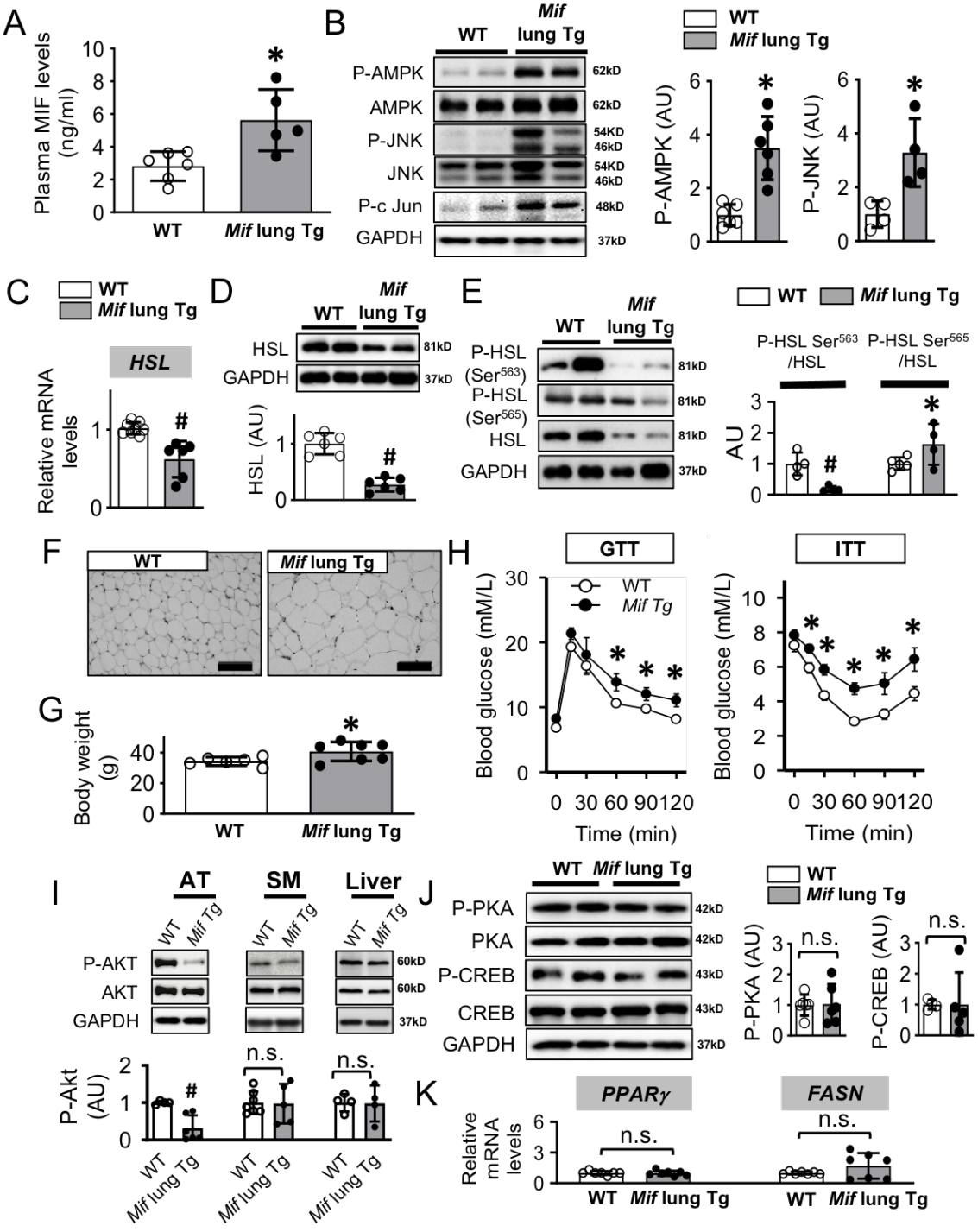
A
Plasma MIF levels (ng/ml)
WT
Mif lung Tg
B
WT
Mif lung Tg
P-AMPK
AMPK
P-JNK
JNK
P-c Jun
GAPDH
62kD
54KD 46kD
48kD
37kD
P-AMPK (AU)
P-JNK (AU)
C
HSL
Relative mRNA levels
D
HSL (AU)
E
P-HSL (Ser563)
P-HSL (Ser565)
P-HSL Ser563 /HSL
P-HSL Ser565 /HSL
AU
F
G
Body weight (g)
H
GTT
ITT
Blood glucose (mM/L)
Time (min)
Mif Tg
I
AT
SM
Liver
P-AKT
AKT
P-Akt (AU)
n.s.
J
P-PKA
PKA
P-CREB
CREB
K
PPARγ
FASN
Relative mRNA levels

12-Figure 3.3.5. High plasma MIF induces adipocyte hypertrophy and obesity through activating the AMPK/JNK/HSL signaling pathway.

Age-matched WT and *Mif* lung Tg mice were euthanized for the quantifications of plasma MIF levels (A), AMPK and JNK activation (B), HSL expression (C and D) and phosphorylation (E), and adipocyte size (F) and body weight (G). Whole-body insulin sensitivity was evaluated by glucose tolerance test (GTT) and insulin tolerance test (ITT) (H). The phosphorylation of Akt in the adipose tissue (AT), smooth muscle (SM) and liver was measured in (I). Phosphorylation of PKA and CREB (J), and gene expression of *PPARγ* and *FASN* (K) were evaluated by western blot and qPCR, respectively. All data are presented as mean ± SD. *$P \leq 0.05$ increase vs. WT in A, B, E, G and H. $^{\#}P \leq 0.05$ reduction vs. WT in C, D and I. n.s. represents no significance, the scale bars are 220 μm.

3.3.4 High Caloric Diet Upregulates Plasma MIF that Activates Adipose AMPK/HSL Signaling and Adipocyte Hypertrophy

In animal models, the consumption of a HFD has been demonstrated to induce a notable elevation in circulating MIF levels [259]. To further elucidate the *in vivo* functionality of the MIF/AMPK/JNK anti-lipolytic pathway, in addition to the *Mif* lung transgenic (Tg) mice model, we subjected C57BL/6 mice to a 12-week HFD regimen (Figure 3.3.6A). Our findings in this HFD-fed mouse model closely resembled the observations in the *Mif* lung Tg mice. Specifically, HFD feeding led to a significant increase in plasma MIF levels (Figure 3.3.7A), accompanied by heightened phosphorylation of AMPK and JNK (Figure 3.3.7B). Concurrently, it resulted in a reduction in both *HSL* gene and protein expression (Figure 3.3.7C and D) compared to the control group maintained on a NC diet. Furthermore, adipose tissue samples collected from the HFD group exhibited increased phosphorylation of HSL at Ser^{565} and decreased phosphorylation at Ser^{563} (Figure 3.3.7E). In addition, HFD induced systemic insulin resistance (Figure 3.3.6B) and reduced Akt phosphorylation in peripheral tissues, including adipose tissue (Figure 3.3.6C-E). However, mirroring our previous observations in the *Mif* lung Tg model, the alterations in adipose HSL expression and phosphorylation in HFD-fed mice were not associated with changes in the PKA signaling pathway (Figure 3.3.7F and G) or adipogenesis-related gene expression (Figure 3.3.7H and I). HFD induced a significant increase in the circulating levels of non-esterified fatty acids (FA) but not triglycerides (Figure 3.3.6F and G). Consequently, in the context of elevated FA levels, the reduction in HSL and lipolysis likely contributed to the enlargement of adipocytes and the consequent increase in body weight observed in HFD-induced obese mice (Figure 3.3.7J and K).

Thus, we next asked if a reduction in circulating MIF levels could alleviate MIF's inhibitory influence on adipose HSL. In this regard, we employed an *in vivo* approach by administering anti-MIF antibodies known to neutralize both circulating and extracellular MIF [240]. These antibodies were administered to mice during the final five weeks of the HFD regimen, a period during which significant differences in body weight emerged between the NC and HFD groups. We found that immunoneutralization of MIF effectively attenuated the activation of the AMPK/JNK signaling pathway (Figure 3.3.7L) and the suppression of HSL (Figure 3.3.7M and N), while also partially mitigating adipocyte hypertrophy (Figure 3.3.7O) and limiting body weight gain (Figure 3.3.7P) during HFD feeding. These results provide further evidence that extracellular MIF plays a pivotal role in mediating the activation of the AMPK/JNK signaling pathway in adipose tissue during HFD. Extracellular MIF also contributes significantly to the downregulation of HSL and lipolysis, thereby promoting adipocyte hypertrophy and obesity under HFD feeding.

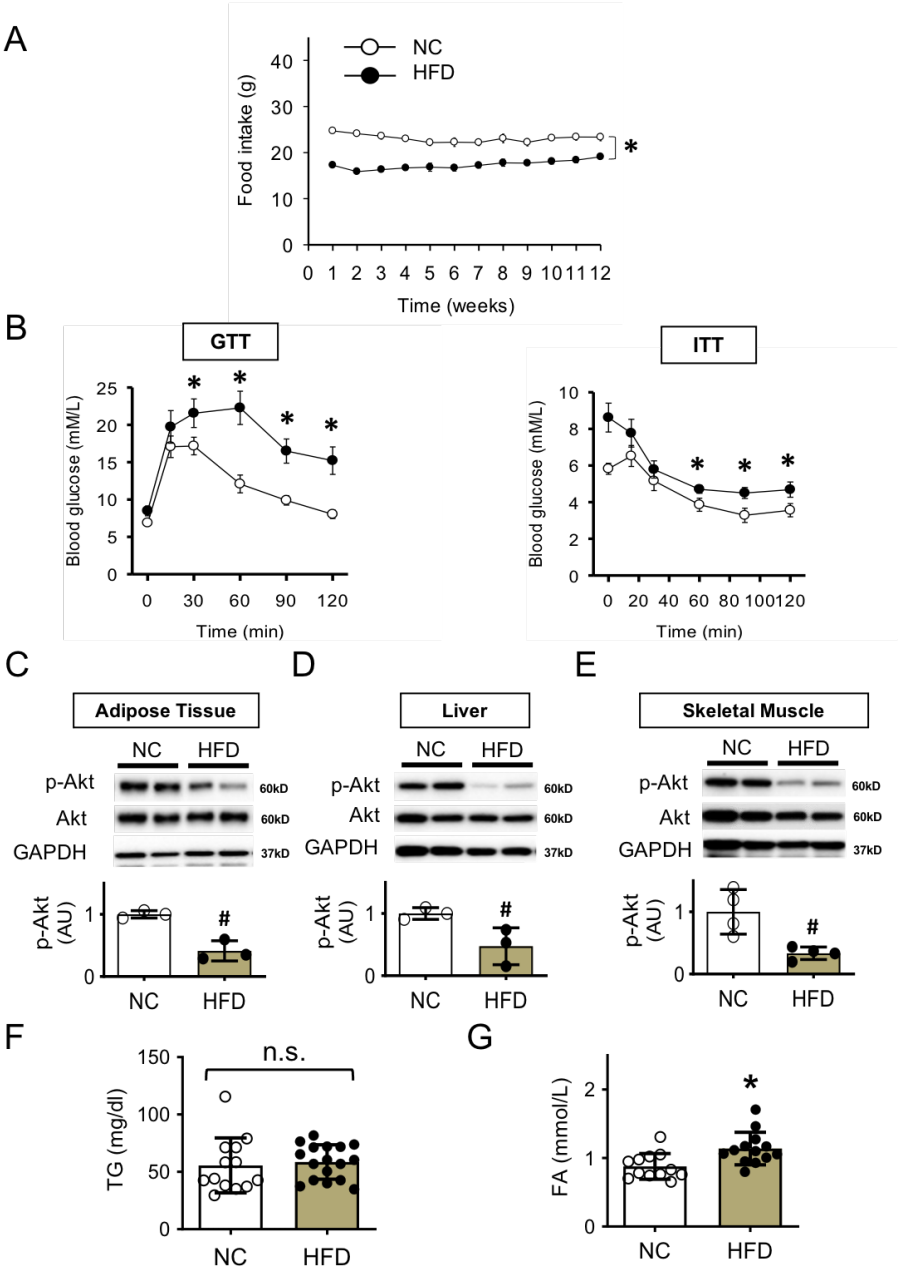

13-Figure 3.3.6. High caloric diet induces insulin resistance and hyperlipidemia.

C57BL/6 mice (3 weeks) were fed NC or HFD for 12 weeks. The food intake was monitored in (A). Whole-body insulin resistance was evaluated by glucose tolerance test (GTT) and insulin tolerance test (ITT) (B). Insulin stimulated Akt phosphorylation in peripheral tissues was measured by western blot (C to E). Serum TG (F) and FA (G) levels were examined by commercial kits. N= 3-11 each animal group. All data are presented as mean ± SD. *$P \leq 0.05$ increase and $^{\#}P \leq 0.05$ reduction vs. NC. n.s. represents no significance.

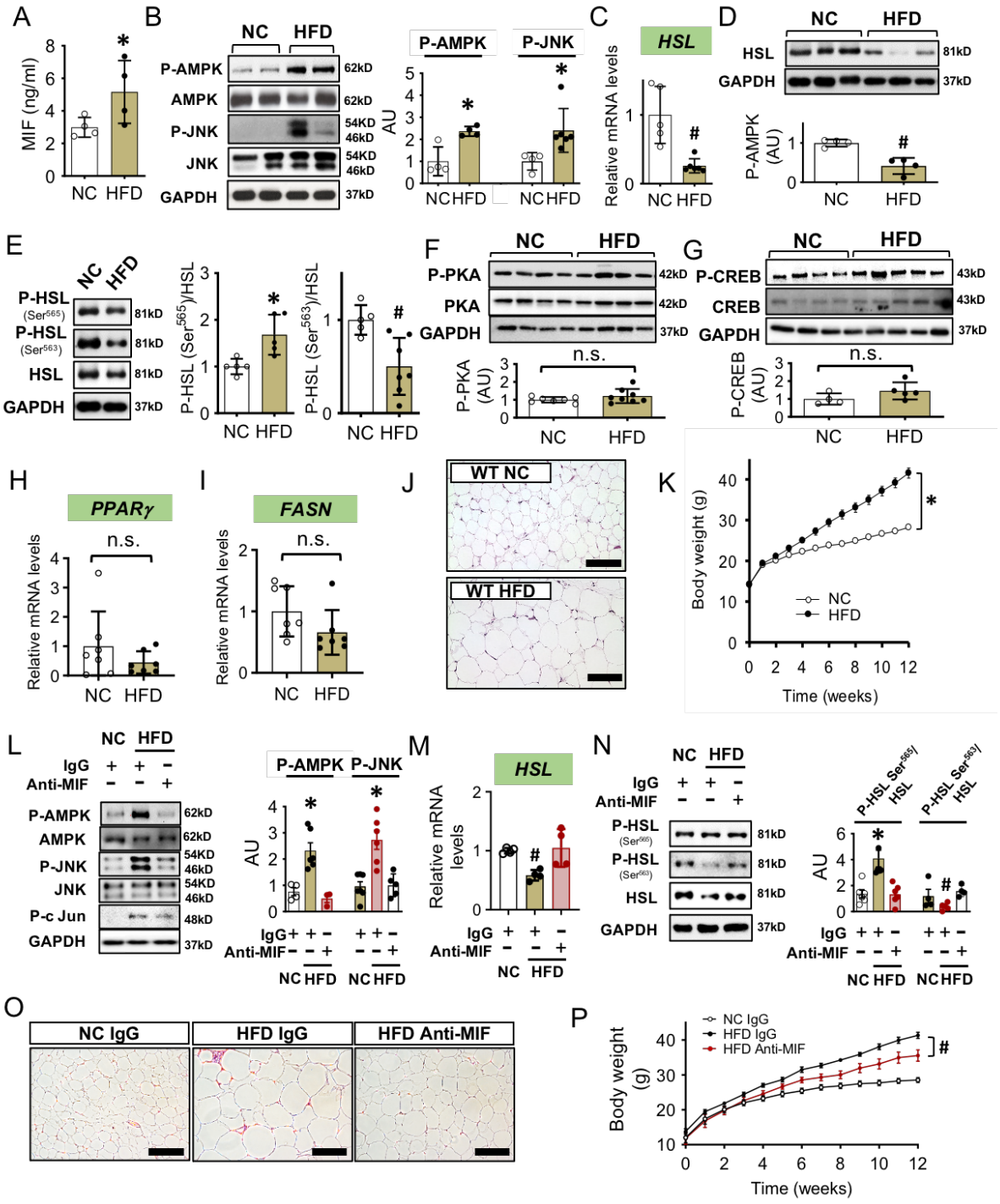
A
MIF (ng/ml)
NC HFD
B
NC HFD
P-AMPK
AMPK
P-JNK
JNK
GAPDH
62kD
54KD
46kD
37kD
P-AMPK P-JNK
AU
C
HSL
Relative mRNA levels
D
HSL
GAPDH
81kD
37kD
P-AMPK (AU)
E
P-HSL (Ser565)
P-HSL (Ser563)
HSL
GAPDH
81kD
37kD
P-HSL (Ser565)/HSL
P-HSL (Ser563)/HSL
F
P-PKA
PKA
GAPDH
42kD
37kD
n.s.
P-PKA (AU)
G
P-CREB
CREB
GAPDH
43kD
37kD
P-CREB (AU)
H
PPARγ
I
FASN
J
WT NC
WT HFD
K
Body weight (g)
Time (weeks)
L
IgG
Anti-MIF
P-c Jun
48kD
M
N
P-HSL Ser565/ HSL
P-HSL Ser563/ HSL
O
NC IgG
HFD IgG
HFD Anti-MIF
P
NC IgG
HFD IgG
HFD Anti-MIF
Body weight (g)
Time (weeks)

14-Figure 3.3.7. High caloric diet upregulates plasma MIF that activates adipose AMPK/HSL signaling pathway and augments adipocyte hypertrophy.

WT mice at 3 weeks were fed with normal chow (NC) or a high caloric diet (HFD) for 12 weeks. Plasma MIF level (A) was measured subsequently. The phosphorylation of AMPK (B), JNK (B) and *HSL* gene (C) and protein (D) expression were quantified in adipose tissue by western blot or qPCR. The phosphorylation of HSL at Ser^{565} and Ser^{563} was evaluated in (E). The phosphorylation of PKA and CREB was also examined by western blot (F and G). The gene expression of *PPARγ* and *FASN* was evaluated by qPCR (H and I). Hematoxylin–eosin (HE) staining was performed to identify adipocyte hypertrophy in (J), and body weight gain was monitored weekly (K). In a separate experiment, non-specific IgG or anti-MIF antibody (20 mg/kg, i.p. twice a week) was injected twice per week accompanied with high fat diet. Phosphor- or total AMPK and JNK and HSL expression and phosphorylation were evaluated in (L to N). Adipocyte size was detected by H&E staining and body weight gain was monitored and shown in (O and P). All data are presented as mean ± SD. $^{*}P \leq 0.05$ increase and $^{\#}P \leq 0.05$ reduction vs. NC in A-K; vs. other groups in L-N; vs. HFD IgG in P. n.s. represents no significance, the scale bars are 220 μm.

Furthermore, it is noteworthy that the administration of anti-MIF antibodies didn't change the TG levels (Figure 3.3.8A) but significantly reduced the elevated levels of circulating fatty acids associated with HFD (Figure 3.3.8B). This reduction in circulating fatty acids led to decreased lipid accumulation in the liver and skeletal muscle (Figure 3.3.8C), thereby enhancing peripheral tissue insulin sensitivity (Figure 3.3.8F-H) and ameliorating whole-body insulin resistance (Figure 3.3.8I). Of particular interest, we observed that the expression of the fatty acid oxidation regulator, *PPARα* in the liver but not in skeletal muscle, was significantly reduced following HFD feeding; however, anti-MIF treatment restored the *PPARα* gene levels in the liver during HFD (Figure 3.3.8D and E). These findings propose that MIF could potentially hinder fatty acid oxidation in the liver, indirectly promoting the accumulation of lipids in the hepatic tissue and consequently raising plasma fatty acid levels. Notably, it's crucial to highlight that the neutralization of circulating MIF did not modify the HFD-induced elevation of inflammatory markers like TNF-α (*Tnfa*), IL1β (*Il1b*), and IL6 (*Il6*), in adipose tissue (Figure 3.3.9). This suggests that the metabolic shifts mediated by MIF were not linked to the induction of other inflammatory factors.

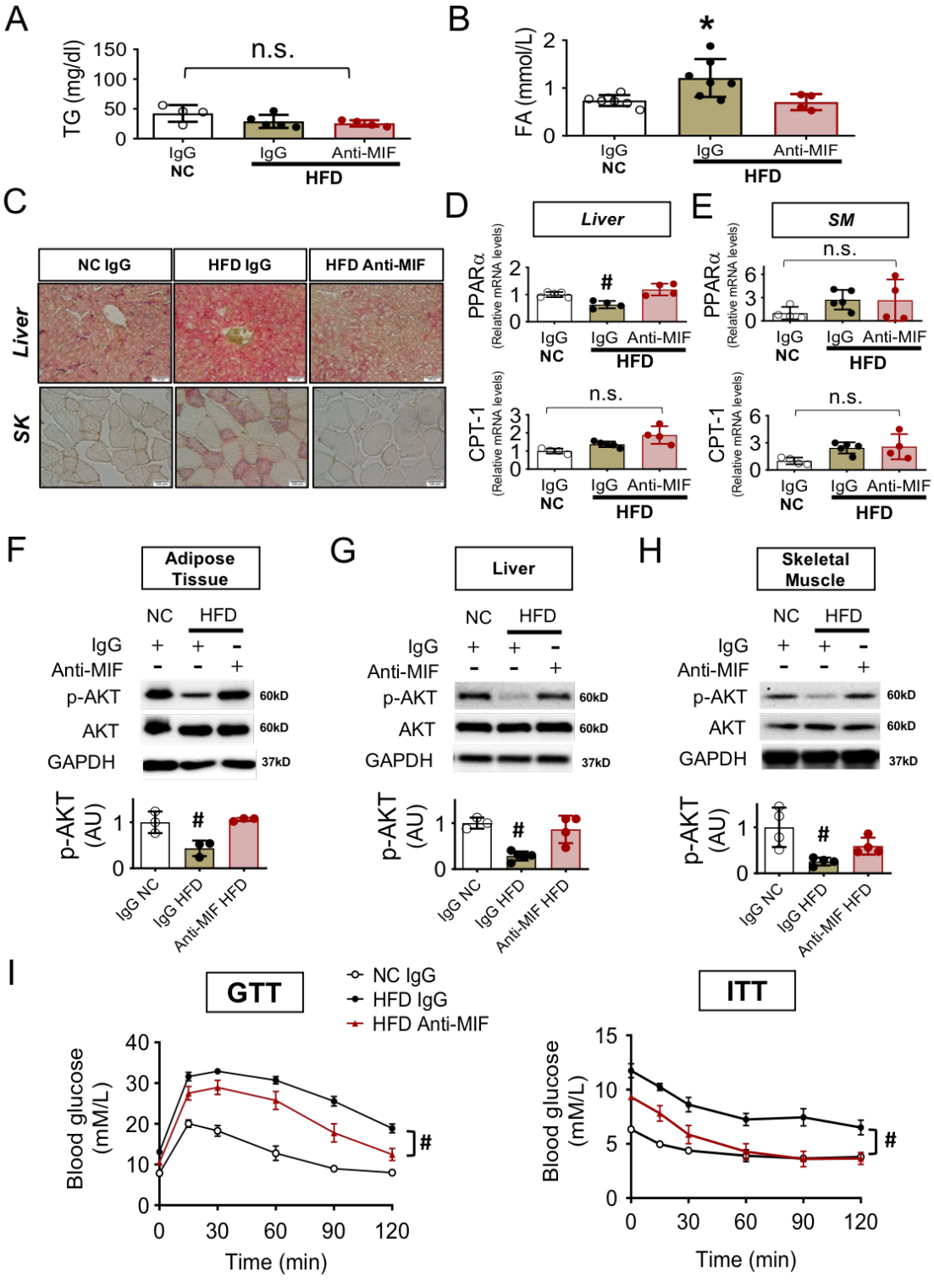
A
TG (mg/dl)
150
100
50
0
n.s.
IgG
NC
IgG
Anti-MIF
HFD
B
FA (mmol/L)
2
1
0
*
IgG
NC
IgG
Anti-MIF
HFD
C
NC IgG
HFD IgG
HFD Anti-MIF
Liver
SK
D
Liver
PPARα
(Relative mRNA levels)
#
CPT-1
(Relative mRNA levels)
n.s.
E
SM
PPARα
(Relative mRNA levels)
n.s.
CPT-1
(Relative mRNA levels)
n.s.
F
Adipose Tissue
NC
HFD
IgG
Anti-MIF
p-AKT
AKT
GAPDH
60kD
60kD
37kD
p-AKT (AU)
#
IgG NC
IgG HFD
Anti-MIF HFD
G
Liver
NC
HFD
IgG
Anti-MIF
p-AKT
AKT
GAPDH
60kD
60kD
37kD
p-AKT (AU)
#
IgG NC
IgG HFD
Anti-MIF HFD
H
Skeletal Muscle
NC
HFD
IgG
Anti-MIF
p-AKT
AKT
GAPDH
60kD
60kD
37kD
p-AKT (AU)
#
IgG NC
IgG HFD
Anti-MIF HFD
I
GTT
NC IgG
HFD IgG
HFD Anti-MIF
Blood glucose (mM/L)
40
30
20
10
0
#
0
30
60
90
120
Time (min)
ITT
Blood glucose (mM/L)
15
10
5
0
#
0
30
60
90
120
Time (min)

15-Figure 3.3.8. Neutralization of MIF reverses HFD induced metabolic dysfunction.

C57BL/6 mice (3 weeks) were fed with NC or HFD with IgG or anti-MIF antibody injection (twice per week) for 12 weeks. Serum TG (A) and FA (B) levels were examined, and Oil red O staining was performed to detect lipid accumulation in the liver and skeletal muscle (C). The gene expression of *PPARα* and *CPT-1* was quantified in the liver and skeletal muscle by qPCR (D and E). Insulin stimulated Akt phosphorylation in peripheral tissues was measured by western blot (F to H). Whole-body insulin resistance was evaluated by glucose tolerance test (GTT) and insulin tolerance test (ITT) (I). N= 3-7 for each animal group. All data are presented as mean ± SD. *$P \leq 0.05$ increase vs. other groups in (B); $^{\#}P \leq 0.05$ reduction vs. other groups in (D), (F) to (H); and $^{\#}P \leq 0.05$ reduction vs. HFD IgG in (I). n.s. represents no significance.

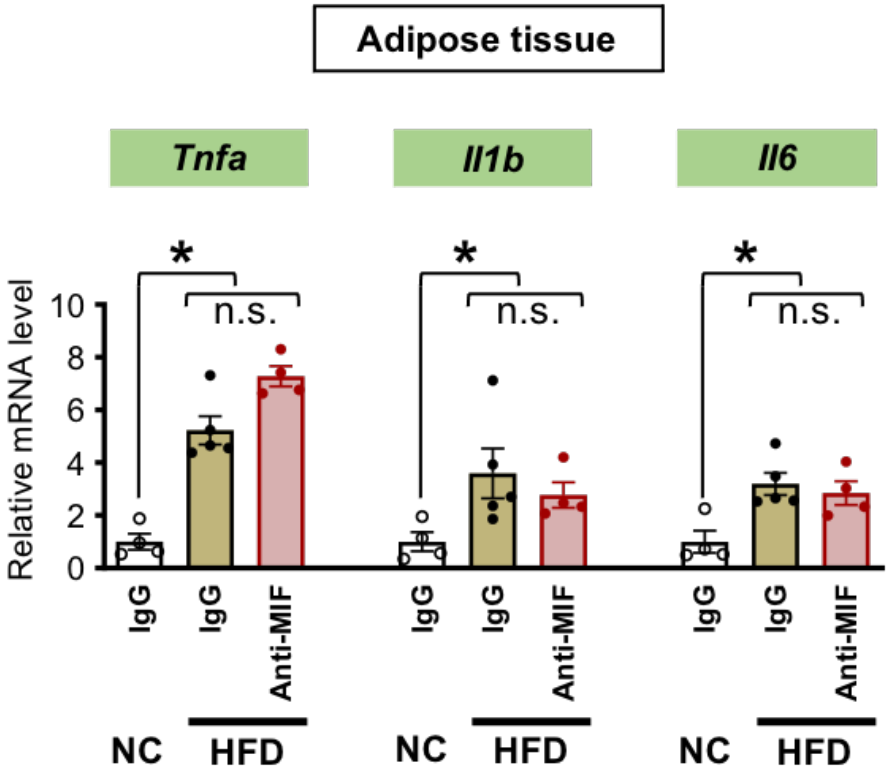

16-Figure 3.3.9. Neutralization of MIF did not affect HFD induced inflammatory gene expression.

C57BL/6 mice (3 weeks) were fed with NC or HFD with IgG or anti-MIF antibody injection (twice per week) for 12 weeks. The gene expressions of inflammatory factors, *Tnfa*, *Il1b* and *Il6* were quantified by qPCR. N= 4-5 each animal group. *P<0.05 increase vs. IgG. n.s. represents no significance.

3.3.5 MIF Receptor, CD74 is Involved in the MIF/AMPK/JNK/HSL Signaling Pathway and Obesity

The CD74 receptor, which serves as the cognate receptor for MIF, was found to be expressed in both 3T3-L1 adipocytes and adipose tissue (Figure 3.3.10A and G). To gain deeper insights into the impact of extracellular MIF on adipose tissue signaling, we employed the MIF inhibitor, MIF098, to disrupt the binding of MIF to the cell surface CD74 receptor [260 261]. We found that MIF098 effectively inhibited MIF-induced activation of the AMPK/JNK signaling pathway (Figure 3.3.10A) in 3T3-L1 adipocytes, thereby counteracting the downstream effects of MIF on reducing HSL expression and activation (Figure 3.3.10B and C). Furthermore, MIF098 mitigated the reduction in adipose glycerol content and fatty acid release induced by MIF (Figure 3.3.10D). Thus, it comes as no surprise that MIF098 was successful in inhibiting MIF-induced lipid accumulation in adipocytes in the presence of PA (Figure 3.3.10E).

To further elucidate the role of CD74 *in vivo*, we conducted parallel experiments using CD74-deficient mice (*Cd74*$^{-/-}$) subjected to HFD. We found the plasma MIF levels remained comparable between WT and *Cd74*$^{-/-}$ mice during HFD (Figure 3.3.10F). However, the absence of CD74 effectively blocked HFD-induced AMPK/JNK activation (Figure 3.3.10G) and prevented the inhibition of HSL (Figure 3.3.10H and I). Similarly, the phosphorylation of both PKA and its downstream target, CREB, showed no significant changes (Figure 3.3.10J). In alignment with the effects observed upon neutralizing MIF, CD74 knockout significantly reduced adipocyte hypertrophy (Figure 3.3.10K) and attenuated body weight gain (Figure 3.3.10L) in response to HFD feeding. These findings collectively suggest that the MIF receptor, CD74 may play a pivotal role in regulating the MIF/AMPK/JNK/HSL axis during obesity.

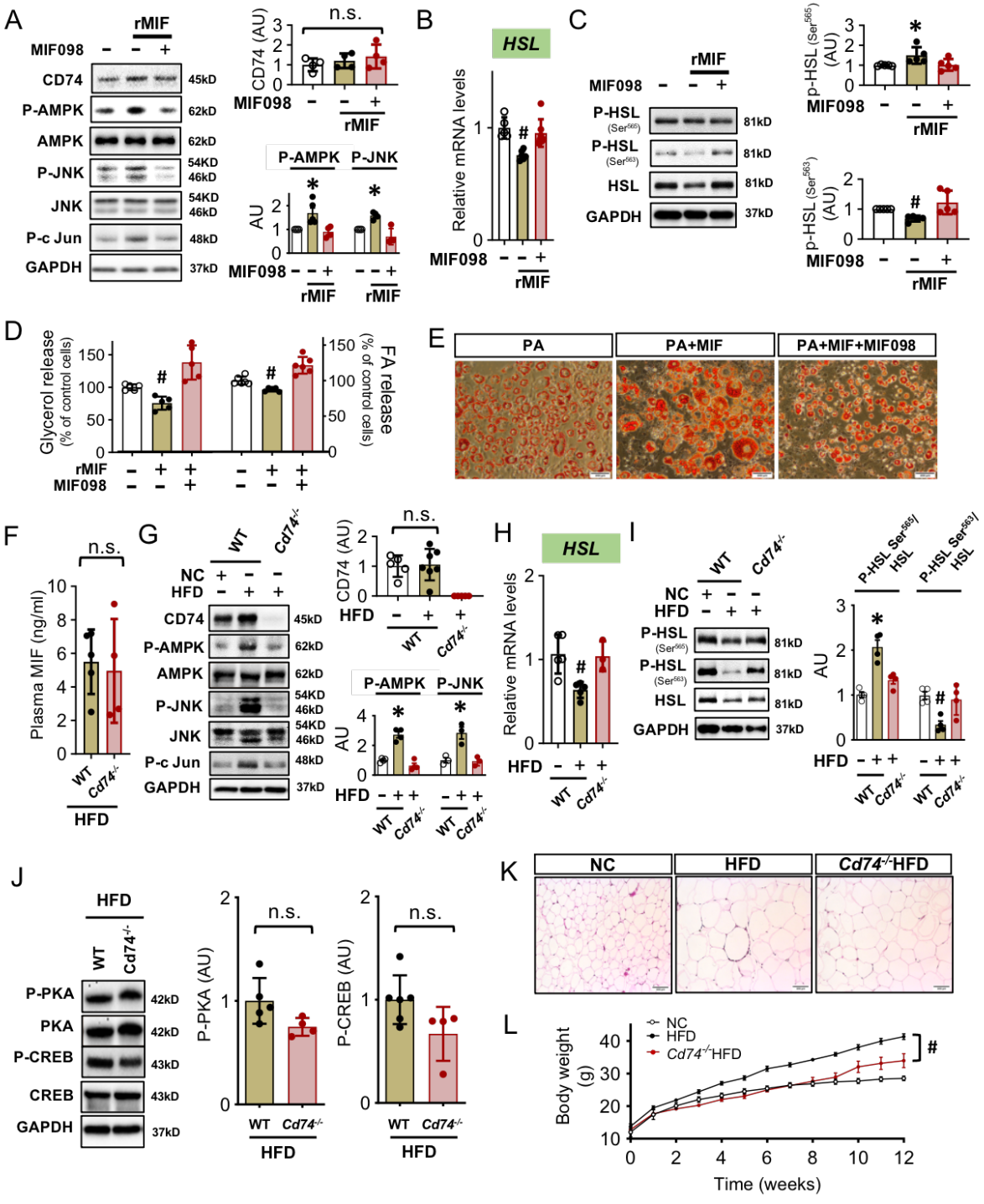
A
rMIF
MIF098
CD74
P-AMPK
AMPK
P-JNK
JNK
P-c Jun
GAPDH
45kD
62kD
54KD
46kD
48kD
37kD
n.s.
CD74 (AU)
P-AMPK
P-JNK
AU
B
HSL
Relative mRNA levels
C
P-HSL (Ser565)
P-HSL (Ser563)
HSL
81kD
p-HSL (Ser565) (AU)
p-HSL (Ser563) (AU)
D
Glycerol release (% of control cells)
FA release (% of control cells)
E
PA
PA+MIF
PA+MIF+MIF098
F
Plasma MIF (ng/ml)
WT
Cd74-/-
HFD
G
NC
HFD
H
I
P-HSL Ser565/ HSL
P-HSL Ser563/ HSL
J
P-PKA
PKA
P-CREB
CREB
42kD
43kD
P-PKA (AU)
P-CREB (AU)
K
NC
HFD
Cd74-/-HFD
L
Body weight (g)
Time (weeks)

17-Figure 3.3.10. The MIF receptor, CD74 is involved in the MIF/AMPK/JNK/HSL signaling pathway.

3T3-L1 adipocytes were incubated with vehicle, rMIF (400mg/ml) or rMIF+MIF098 (10μM) for 24 hours. CD74, AMPK, JNK and c-Jun were evaluated with specific phosphor- or total antibodies (A). *HSL* gene expression and activation were measured by qPCR or Western Blot (B and C). Release of glycerol and FA was quantified in (D). In the presence of high palmitic acid (PA), lipid droplet accumulation regulated by MIF and MIF098 was assessed with Oil red O staining (E). WT and *Cd74*$^{-/-}$ mice were subjected to high fat diet (HFD) feeding for 12 weeks and their bloods were collected for the measurements of plasma MIF levels (F). Their adipose tissues were also harvested for the quantifications of CD74, AMPK, JNK, c Jun (G) and HSL expression and activation (H and I). In addition, phosphorylation of PKA and CREB was assessed in (J). H&E staining in adipose tissues and body weight gain were monitored in WT and *Cd74*$^{-/-}$ mice with or without HFD (K and L). All data are presented as mean ± SD. *$P \leq 0.05$ increase and $^{\#}P \leq 0.05$ reduction vs. other groups in A-D and G-I; vs. other groups in (G) to (I). $^{\#}P \leq 0.05$ reduction vs. HFD in (L). n.s. represents no significance.

3.3.6 Deficiency of Intracellular MIF Inhibits HSL Expression through JNK but Independent of AMPK

To comprehensively investigate the roles of both extracellular and intracellular MIF in HSL regulation and adipose lipid metabolism, we conducted experiments involving *Mif*$^{-/-}$ mice with a global genetic deletion of MIF. Surprisedly, *Mif*$^{-/-}$ mice administered a HFD displayed a reduction in HSL expression and activation in adipose tissue compared to WT mice (Figure 3.3.11A to C). This unexpected finding suggests an integral role for intracellular MIF in the intricate orchestration of HSL expression within adipocytes. As anticipated, *Mif*$^{-/-}$ mice demonstrated a reduced phosphorylation of adipose AMPK (Figure 3.3.11D) compared to WT mice, with a loss of action of extracellular MIF to activate AMPK. Consequently, this reduction of AMPK phosphorylation was associated with a loss of inhibitory phosphorylation of HSL at Ser^{565} (Figure 3.3.12). Unexpectedly, *Mif*$^{-/-}$ mice still demonstrated an increase in JNK phosphorylation in adipose tissue in the absence of AMPK activation (Figure 3.3.11D). In align with the results from the adipose tissue, we also observed enhanced JNK phosphorylation and reduced HSL activation in adipocytes isolated from *Mif*$^{-/-}$ mice compared to WT (Figure 3.3.11E). These findings suggest a potentially paradoxical role for intracellular MIF in regulating HSL. Physiologically, intracellular MIF might suppress JNK signaling, partially counterbalancing the stimulatory effects of extracellular MIF on JNK activation pathways, potentially preventing an overactivation of JNK.

To elucidate how the reduction of intracellular MIF regulates JNK activation, we partially deleted MIF expression in 3T3-L1 adipocytes by *MIF siRNA*. At the same time, those cells also be treated with MIF-098 to block the extracellular effects of MIF. We found that intracellular MIF reduction following *MIF siRNA* treatment led to the overactivation of JNK phosphorylation

(Figure 3.3.11F). These findings provide further support for the notion that intracellular MIF acts as a counterbalance to JNK activation in adipocytes and exerts an opposing effect to extracellular MIF.

Previous research indicates that intracellular MIF exerts its inhibitory influence on JNK activation through direct binding to the transcription factor Jab1[199]. To elucidate this mechanistic, we conducted immunoprecipitation experiments, and found that Jab1 forms complexes with both MIF and JNK in adipose tissue from HFD WT mice (Figure 3.3.11G). This observation prompted the hypothesis that the assembly of a complex involving MIF, Jab1, and JNK might contribute to the downregulation of JNK activation in WT mice. And this inhibitory effect of intracellular MIF might be lost in *Mif*$^{-/-}$ mice. As anticipated, we found that the absence of MIF resulted in heightened JNK phosphorylation (Figure 3.3.11G), despite the continued binding between Jab1 and JNK in *Mif*$^{-/-}$ mice (Figure 3.3.11G). To confirm the missing intercellular MIF-induced the overactivation of JNK is a pivotal factor contributing to the downregulation of HSL expression, we incubated adipose tissues from WT and *Mif*$^{-/-}$ mice with the JNK inhibitor, SP600125 (Figure 3.3.11H). We found that SP600125 treatment reversed both overactivated JNK and the reduction in HSL expression and activation (Figure 3.3.11H). This provides compelling evidence that increased JNK activity *Mif*$^{-/-}$ mice indeed plays a significant role in the downregulation of HSL expression.

We then proceeded to examine how the absence of MIF affected plasma lipid profiles and the insulin sensitivity during HFD. As we had shown before, the administration of a MIF-neutralizing antibody significantly lowered circulating FA concentrations in WT mice following HFD (Figure 3.3.8B), however, this effect on FA levels was not evident in the *Mif*$^{-/-}$ mouse model (Figure 3.3.13A). In addition, *Mif*$^{-/-}$ mice showed significantly increased plasma triglyceride levels (Figure 3.3.13B), indicating more severe hyperlipidemia in *Mif*$^{-/-}$ compared to WT mice.

WT mice subjected to a HFD exhibited reduced Akt phosphorylation in the liver, adipose tissue, and skeletal muscle (Figure 3.3.6C-E). This reduction was more pronounced in the livers of *Mif*$^{-/-}$ mice on a HFD (Figure 3.3.13C), indicating aggravated hepatic insulin resistance due to MIF deletion. Interestingly, in adipose tissue, *Mif*$^{-/-}$ mice demonstrated elevated Akt phosphorylation (Figure 3.3.11I) compared to WT mice following HFD. This increased Akt phosphorylation was linked to a diminished PKA signaling pathway (Figure 3.3.11I), suggesting that MIF deficiency could lead to the downregulation of HSL activation through the Akt/PKA signaling pathway. In contrast, equivalent levels of Akt phosphorylation were observed in the skeletal muscle of *Mif*$^{-/-}$ mice compared to WT mice on a HFD (Figure 3.3.13D).

Phenotypic characterization of MIF deficiency revealed that MIF plays a previously unsuspected role in metabolic health. In *Mif*$^{-/-}$ mice, the inhibition of adipose HSL is due to the overlapping effects of: (1) decreased *HSL* gene expression and (2) attenuated HSL activation by the AKT/PKA signaling pathway. Accordingly, the levels of HSL in MIF deficient mice are lower than those in WT mice (Figure 3.3.11C). These results underscore the crucial role of intracellular MIF in maintaining HSL expression and activation. Additionally, through the analysis of adipogenesis genes, we also found that MIF deletion increased *LPL* gene expression in adipose tissue (Figure 3.3.11J) which may also contribute to the development of adipocyte hypertrophy and obesity. Indeed, *Mif*$^{-/-}$ mice had more pronounced adipocyte hypertrophy compared to WT mice following HFD feeding (Figure 3.3.11K), which was associated with more weight gain (Figure 3.3.11L) and whole-body insulin resistance (Figure 3.3.14).

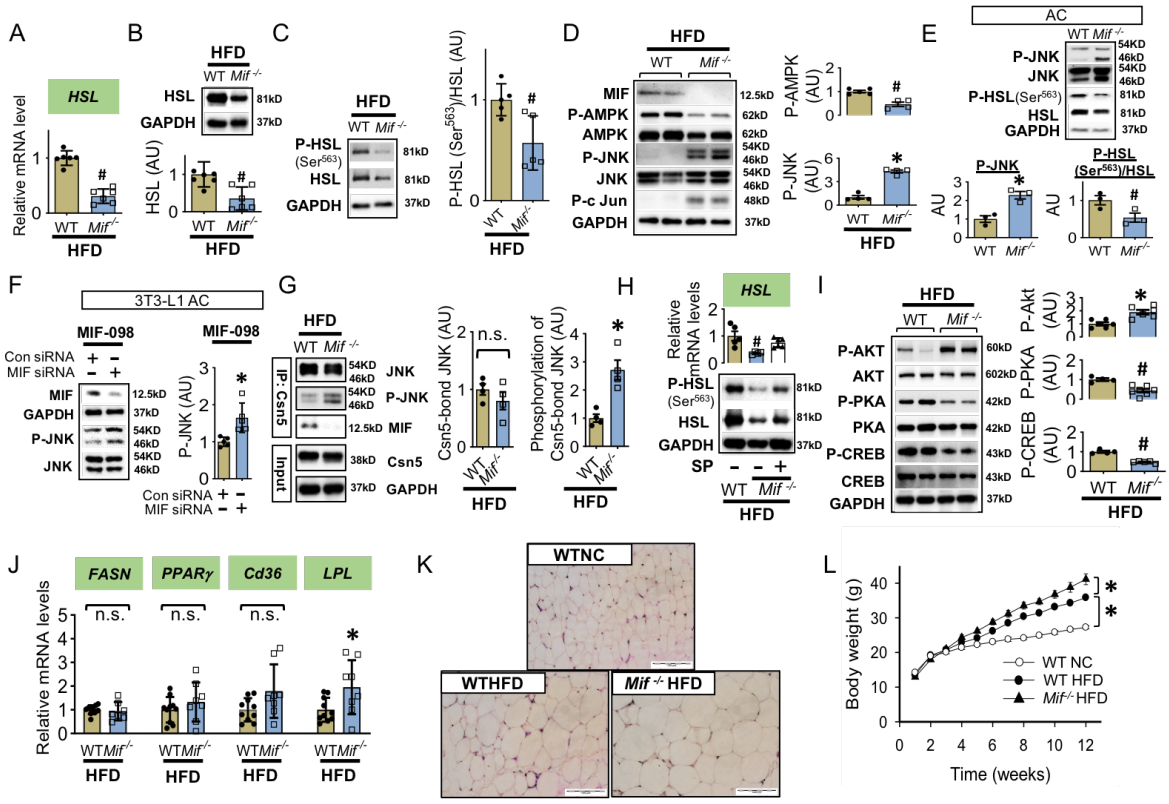

18-Figure 3.3.11. Deficiency of intracellular MIF inhibits HSL expression through JNK but independent of AMPK.

WT and *Mif*$^{-/-}$ mice at 3 weeks were fed with normal chow (NC) or high fat diet (HFD) for 12 weeks. The gene (A) and protein (B) expression of HSL in adipose tissue was quantified with qPCR and western blot, respectively. The phosphorylation of HSL at Ser^{563} (C), AMPK and JNK phosphorylation (D) and MIF levels (D) were also examined. Adipocytes were isolated from WT and *Mif*$^{-/-}$ adipose tissue and the phosphorylation of JNK and HSL Ser^{563}/HSL ratio were evaluated by western blot (E). In 3T3-L1 adipocytes, following knockdown of MIF with MIF siRNA, MIF and JNK phosphorylation in the presence of MIF inhibitor, MIF098 (10μM) were evaluated by western blot in (F). The interaction among JNK, MIF and Jab1 was determined by co-immunoprecipitation (G). Phosphorylation of Jab1-bond JNK was quantified by western blot (G). Adipose tissues were isolated from WT and *Mif*$^{-/-}$ mice following HFD and they were cultured in physiological KREB solution at 37°C for 24 hours in the absence or presence of SP600125. *HSL* gene and protein expression were detected by qPCR and western blot (H). The phosphorylation of Akt and PKA was examined in (I). Adipogenesis gene expressions, such as *FASN*, *PPARγ*, *CD36* and *LPL* were quantified by qPCR (J). H&E staining was performed to identify adipocyte hypertrophy in (K), and body weight gain was monitored in (L) weekly. All data are presented as mean ± SD. *P ≤ 0.05 increase and $^{\#}$P ≤ 0.05 reduction vs. WT or WTHFD. n.s. represents no significance.

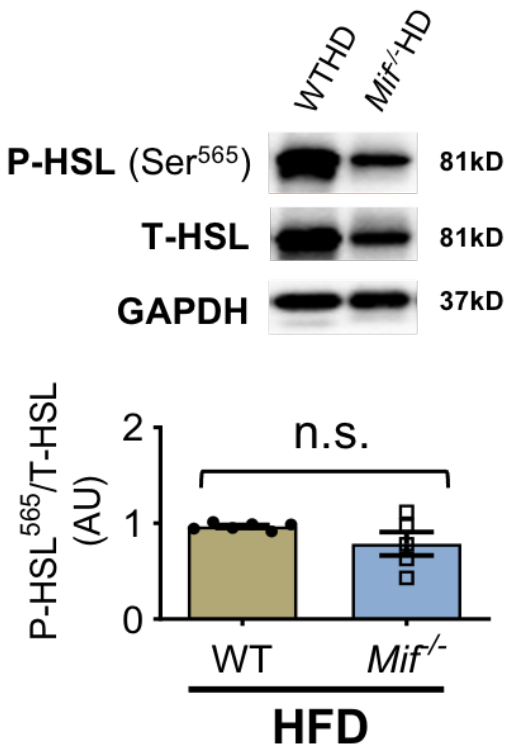

19-Figure 3.3.12. *Mif*$^{-/-}$ mice have unchanged HSL phosphorylation at the site of Ser^{565} following HFD compared to WT.

WT and *Mif*$^{-/-}$ mice (3 weeks) were fed with HFD for 12 weeks. HSL phosphorylation at the site of Ser^{565} was quantified by western blot. N= 5-6 each animal group. n.s. represents no significance.

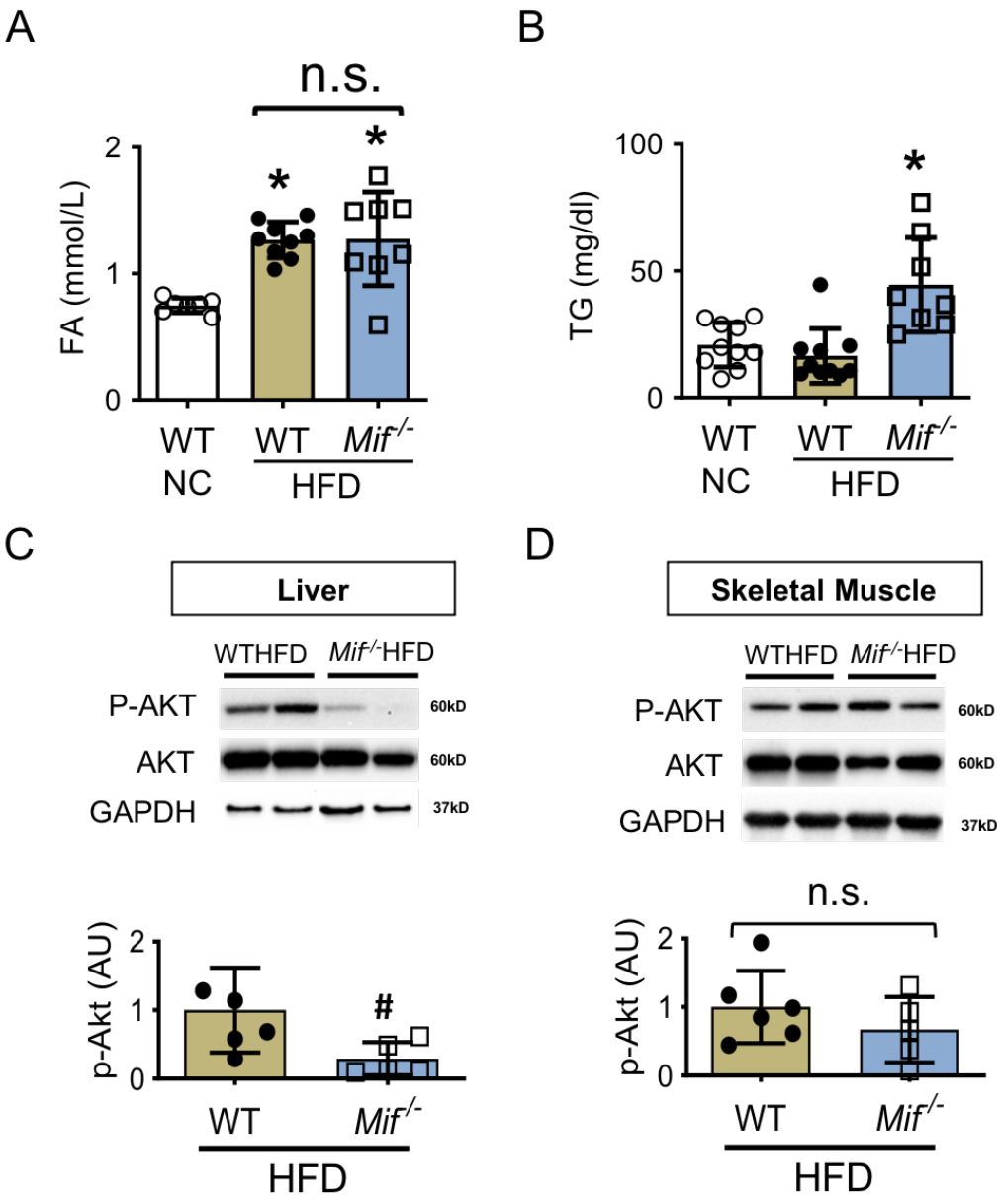

20-Figure 3.3.13. *Mif*$^{-/-}$ mice have exacerbated hyperlipidemia and tissue specific insulin resistance in liver and skeletal muscle.

WT and *Mif*$^{-/-}$ mice (3 weeks) were fed with HFD for 12 weeks. Serum TG (A) and FA (B), and Akt phosphorylation in the liver (C) and skeletal muscle (D) were quantified. N= 5-10 each animal group. *P $\leq$ 0.05 increase vs. WT NC in (A) and (B); and $^{\#}$P $\leq$ 0.05 reduction vs. WT HFD. n.s. represents no significance.

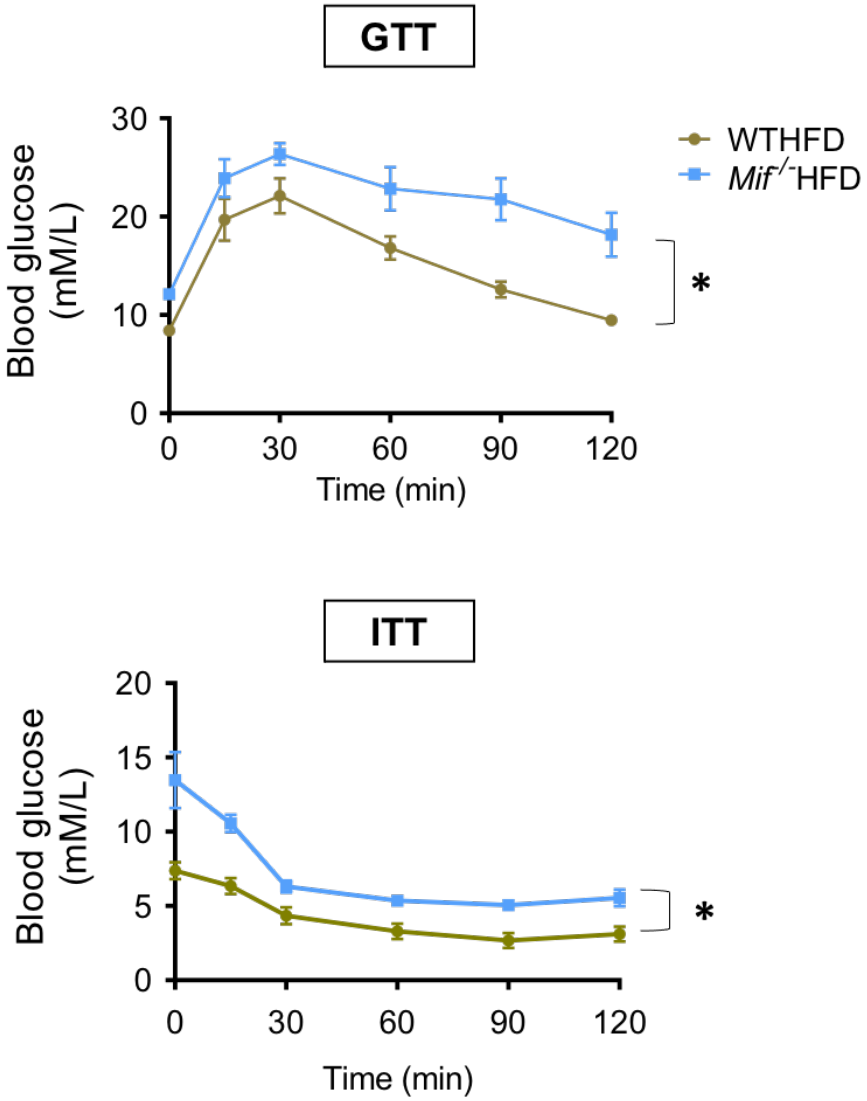

21-Figure 3.3.14. *Mif*$^{-/-}$ mice have more severe whole-body insulin resistance compared to WT following HFD.

WT and *Mif*$^{-/-}$ mice (3 weeks) were fed with high caloric diet (HFD) for 12 weeks. GTT and ITT (D) were then quantified by i.p. injection of high glucose or insulin. N= 6 for each animal group. *P ≤ 0.05 increase vs. WT HFD.

3.4 DISCUSSION

Lipolysis is accelerated by inflammatory cytokines, such as TNF-α and IL-4 [93] [252] , and this process may be related to the activation of HSL [93]. However, the current results show that the cytokine, MIF, expressed upstream of these cytokines [262] [263], inhibits HSL and lipolysis in adipose tissue, thereby exacerbating adipocyte hypertrophy and contributing to the development of obesity. MIF is released from pre-formed storage pools in response to stimuli and has autocrine-paracrine actions to regulate cellular function and metabolism by binding to the cell membrane receptor, CD74. We show that extracellular MIF released from adipocytes has autocrine actions to downregulate HSL through activation of AMPK/JNK signaling after binding to CD74. Mice overexpressing MIF, as well as WT mice fed a HFD that caused high circulating MIF levels, showed suppression of HSL, which was associated with the development of obesity. Blocking the extracellular action of MIF by a neutralizing anti-MIF antibody significantly prevented the development of HFD-induced obesity which is associated with reduced adipose AMPK/JNK signaling and reversed HSL in HFD mice, further suggesting a role for extracellular MIF in downregulating HSL. Unexpectedly, however, mice with MIF global deletion also had reduced HSL activation and expression in adipose tissue. This finding led us to investigate the role of a potential distinct MIF regulatory pathway, in which intracellular MIF downregulates JNK activation by binding to the intracellular protein, Jab1[199]. Knockdown of MIF had additional effects after blockade of the extracellular pathway, which recapitulated changes in global *Mif*$^{-/-}$ mice. Global deletion of MIF led to hyperactivation of JNK, resulting in reduced HSL gene and protein expression. MIF deficiency also increased Akt and downregulated PKA signaling compared to WT mice fed an HFD. Inhibition of PKA downregulated HSL activation and enhanced adipocyte hypertrophy. Thus, our present data suggest that the intracellular and

extracellular MIF have opposing effects to downregulate HSL and exacerbate the development of obesity during HFD.

Metabolic dysfunction, including obesity and insulin resistance, is associated with reduced HSL expression in adipose tissue [250]. *HSL* mRNA expression is diminished in visceral adipose tissues from obese subjects and is strongly correlated with human adipocyte size and plasma insulin concentrations [264]. Interestingly, insulin resistance is inversely associated with adipose HSL expression but not with adipocyte size and body composition [250]. Together, these data suggest that regulation of HSL in adipose tissue may contribute to adipocyte hypertrophy and the development of insulin resistance. However, the underlying mechanisms by which HSL is regulated are largely unknown. Our present study is the first to investigate the regulation of adipose HSL expression by the immune cytokine MIF. In metabolic disorders, MIF may be released from circulating monocytes and adipose tissue, leading to high plasma MIF levels [265]. We found that extracellular MIF inhibits the expression and activation of HSL and lipolysis in adipocytes by binding to its cell membrane receptor, CD74. This effect of MIF leads to augmented adipocyte hypertrophy in the presence of high fatty acid or a high fat diet. Interestingly, this effect was independent of alterations in the expression of adipogenesis genes. Furthermore, blocking the extracellular action of MIF by a neutralizing MIF antibody significantly reduced obesity and insulin resistance in HFD mice, suggesting a critical role for extracellular MIF in regulating metabolism through the downregulation of HSL.

We found that extracellular MIF downregulates HSL activation and subsequent lipolysis in adipocytes by activating AMPK. MIF is known to stimulate AMPK activation in different cell types, such as cardiomyocytes [187], neurons [31] and liver cells [186] through CD74. Previous studies indicated that AMPK phosphorylates HSL at Ser^{565} and inhibits HSL activity [256]. In this study, we

found that AMPK activation induced by both AICAR and MIF also downregulates *HSL* gene and protein expression. The transcriptional effect of AMPK on HSL seems to be critical with respect to the regulation of lipolysis. Interestingly, AMPK activation did not affect the expression of the lipolytic enzyme *ATGL*, suggesting a selective effect on HSL to inhibit lipolysis. MIF is also known to activate JNK in cardiomyocytes and immune cells during myocardial ischemia-reperfusion [266] and inflammation [267], respectively. Here, we show that MIF treatment stimulates JNK phosphorylation through AMPK in adipocytes. Furthermore, AMPK/JNK signaling appears to be regulated by extracellular MIF (through CD74) and has an important transcriptional regulatory effect on HSL that inhibits lipolysis.

Although blocking the extracellular action of MIF by a neutralizing MIF antibody successfully reversed HSL down-regulation and reduced obesity in HFD mice, MIF transgenic knockout mice with global loss of MIF action had an opposing effect. Previous studies indicated that intracellular MIF has an inhibitory effect on the intracellular protein, Jab1 which normally activates JNK activity and enhances phosphor-cJun levels [199]. Although our data indicate that intracellular MIF did not affect the binding between Jab1 and JNK, it inhibited Jab1-mediated JNK phosphorylation and activation. Thus, after global deletion of MIF in *Mif*$^{-/-}$ mice, the loss of intracellular MIF inhibition of adipose Jab1-mediated JNK phosphorylation, augmented JNK phosphorylation compared to WT following high fat diet feeding. Thus, despite the loss of CD74-AMPK activation resulting from the absence of extracellular MIF, intracellular JNK activation remained elevated and *HSL* gene expression was still inhibited in global *Mif*$^{-/-}$ mice. It should be noted that this mechanism was only observed during global MIF deletion and is unlikely to occur under more physiological conditions. This might suggest that enhanced body weight gain observed

in global *Mif*$^{-/-}$ mice during HFD [232], was probably due to the activation of the JNK/HSL signaling pathway in mice with global deletion of intracellular MIF.

Normally, MIF attenuates insulin sensitivity by inducing insulin receptor substrate (IRS) serine phosphorylation in adipocytes [227]. Although whole-body insulin resistance in *Mif*$^{-/-}$ mice fed a high fat diet is even worse due to exacerbated insulin resistance in the liver, they have improved adipose Akt phosphorylation compared to WT. Akt-downregulated PKA also contribute to the inhibition of HSL in the *Mif*$^{-/-}$ mice. In addition, the development of obesity is generally regulated by increased adipogenesis and/or decreased lipolysis. Extracellular MIF inhibits HSL and lipolysis without associated changes in adipogenesis gene expression. However, with a reduction in HSL, the deficiency of intracellular MIF leads to an upregulation of *LPL* gene that may augment adipogenesis. Thus, *Mif*$^{-/-}$ mice have more severe obesity compared to WT following high fat diet feeding. Whether this effect results primarily from intracellular or extracellular MIF is currently unknown.

It should be noted that mice [268] with HSL knockout and human subjects with HSL mutations [269] have reduced lipolysis in adipose tissue, but do not develop obesity [270]. Interestingly, mice with global HSL knockout have enlarged adipocytes in white and brown adipose tissues despite the lack of overall obesity [75]. In contrast, our present findings suggest that extracellular MIF contributes to both HSL downregulation related adipocyte hypertrophy and obesity. It is possible that HSL mutations during development cause some degree of loss of adipose cell number and lipodystrophy, which does not occur with post-developmental MIF-mediated loss of HSL during HFD. In addition, MIF neutralization by anti-MIF antibody significantly reversed HSL, but not the expression of *TNF-α*, *IL-1β*, and *IL6*, suggesting that MIF regulated HSL and body weight independent of changes in adipose tissue inflammation.

MIF has different regulatory effects on different organs that express CD74. In the heart, during ischemia-reperfusion, cardiomyocyte-derived MIF promotes glucose metabolism by activating AMPK to compensate for energy deprivation and prevent cardiac injury [187]. In the liver, MIF stimulated AMPK counteracts the development of liver fibrosis [233]. However, MIF derived from adipose tissue has been suggested to be detrimental to the development of metabolic dysfunction [77] [224]. High fat diet induced adipose MIF release is positively associated with insulin resistance in the presence or absence of adipose inflammation [271] [272]. MIF attenuates insulin signaling only in adipocytes but not in liver or skeletal muscle cells [31]. Our present study also indicated that MIF inhibits HSL by activating the AMPK/JNK signaling pathway. The diverse effects of MIF are most likely cell specific, governing in large part by CD74 expression and its coupling to intracellular signaling intermediates. There is also growing evidence that MIF may have both intracellular and extracellular effects on the same cellular signaling targets. For example, the intracellular effect of MIF in inhibiting the JNK signaling pathway was observed in cancer cells [199], but the extracellular effect of MIF in activating JNK through the CD74 receptor was reported in T cells and fibroblasts [267]. Interestingly, our present data show for the first time that both intracellular and extracellular MIF are present in adipocytes and appear to have opposing effects on HSL and lipolysis. JNK is a key mediator of both effects. Previous studies have showed that glucocorticoids can bind to membrane glucocorticoid receptors or cytosolic glucocorticoid receptors thereby exerting multiple effects in regulating inflammation [273]. Serotonin has extracellular effects in regulating heart valve development, but it also has intracellular effects on heart valve remodeling during disease [274]. Therefore, MIF may be one of the secreted factors that exhibit both extracellular and intracellular effects under physiological and pathological conditions in the human body. Although intracellular regulation of JNK by MIF is only revealed under the

extreme condition of complete MIF absence, strategies to selectively inhibit extracellular MIF with neutralizing antibody or small molecule antagonism of MIF interaction with cell surface CD74 appear to have more beneficial metabolic actions. The strategy to develop CD74 inhibitors for the treatment of metabolic dysfunction may be most effective in subjects with high MIF expression, for instance due to their genetic predisposition for a high expression MIF allele [31].

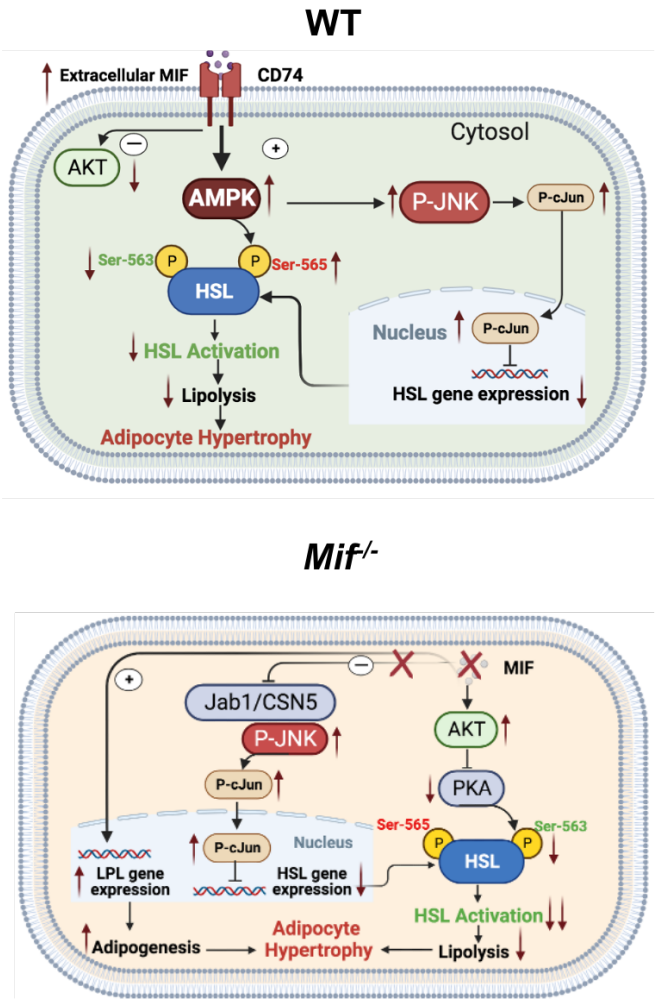

22-Figure 3.3.15. The schematic diagram regarding the effects of extracellular and intracellular MIF on regulating HSL.

High fat diet stimulates MIF release which activates AMPK and JNK in adipocytes, leading to an inhibition of HSL expression and upregulation of inhibitory phosphorylation of HSL. The attenuated HSL activation is associated with adipocyte hypertrophy. In the absence of intracellular MIF, JNK will be also activated by Jab1 and it therefore downregulates HSL expression. Following high fat diet feeding, *Mif*$^{-/-}$ mice demonstrated a higher Akt phosphorylation compared to WT. Akt inhibits the upstream enzyme of HSL, PKA and eventually downregulates the active phosphor-site of HSL (Ser^{563}). Intracellular MIF deficiency also upregulates LPL gene expression which may increase adipogenesis. All these mechanisms together contribute to adipocyte hypertrophy in the absence of MIF.

CHAPTER 4: The Role of MIF in Stabilizing CD74: A Novel Mechanism Contributes to the Development of NAFLD

4.1 ABSTRACT

Non-alcoholic fatty liver disease (NAFLD) is associated with metabolic dysfunctions, such as obesity and diabetes. Macrophage migration inhibitory factor (MIF), an innate cytokine, has also been identified to influence the development of NAFLD, but its molecular mechanism remains unclear. We now show that MIF has a non-inflammatory role in triggering NAFLD by upregulating its cognate membrane receptor, CD74. MIF increased CD74 protein contents but not gene expression in hepatocytes. Changes in CD74 were not associated with any changes in the expression of the inflammatory factors, such as *TNFα*, *IL-6*, or *IL-1β*. In an animal model of MIF overexpression (*Mif* lung Tg), high circulating MIF levels were also associated with increased hepatic CD74 proteins, but not mRNA levels in the absence of liver inflammation. A high fat diet increased circulating MIF levels in WT mice, leading to the upregulation of hepatic CD74. Both animal models with high circulating MIF and hepatic CD74 were associated with hepatic steatosis and fibrosis. Alterations in CD74 and liver phenotype could be reversed by MIF neutralization or MIF gene deletion. Caspase-4 promotes the degradation of CD74. We found that MIF endocytosis inhibited caspase-4 cleavage and its activation. Thus, inhibition of MIF upregulated cleaved caspase-4, leading to CD74 degradation. Collectively, our findings suggest that MIF stabilizes CD74 through the inhibition of caspase-4, which may be an important mechanism for regulating NAFLD in the absence of inflammation.

4.2 INTRODUCTION

NAFLD is a broad term that describes a range of liver conditions, such as fibrosis, cirrhosis, NASH, and hepatocellular carcinomas, which are caused by the accumulation of fat in the liver [3]. NAFLD typically occurs in obese or overweight individuals, and its epidemic continues as the number of obese people worldwide continues to increase [113]. The occurrence and development of NAFLD is associated with chronic liver inflammation [275], and triggered by metabolites and exogenous antigens. Following macrophage infiltration, the liver produces pro-inflammatory cytokines such as IL-1β, IL-6 and TNF-α, which maintain chronic low-grade inflammation, leading to disease progression from steatosis to fibrosis [276].

Macrophage migration inhibitory factor (MIF) is a pleiotropic inflammatory cytokine that regulates both innate and adaptive immunity [187] [265]. Thus, MIF has been implicated in sepsis, autoimmune inflammatory conditions, and atherosclerosis. MIF also modulates ethanol or non-ethanol induced liver injury [230] [232]. MIF promotes liver fibrogenesis by promoting the differentiation of NKT cells toward a pro-fibrotic phenotype during chronic liver injury [231]. Loss of MIF shifts the hepatic macrophage phenotype from M1 to M2 following high fat diet feeding [232]. The effect of MIF on the development of NAFLDD is largely mediated by the interaction between MIF and its cognate membrane receptor, CD74 [230] [232] [233].

CD74 is a nonpolymorphic type II integral membrane protein characterized by its structure: it features a concise N-terminal cytoplasmic tail of 28 amino acids, succeeded by a solitary 24 amino acid transmembrane region, and an approximately 150 amino acid lumenal domain. Initially, CD74 was recognized for its role in governing intracellular trafficking and functioning as both a chaperone and a cell membrane receptor, exerting regulatory influence over B, T, and dendritic cell responses [163] [277]. Furthermore, it has been associated with fostering tumor growth by

enhancing tumor cell survival and proliferation [278]. CD74 was thought to function as an MHC class II chaperone in antigen-presenting cells [277], but it initiates a MIF dependent signaling cascade in concert with CD44 [189]. Interestingly, CD74 can be cleaved upon binding MIF in B cells [191] to release an intracellular domain, CD74-ICD that undergoes nuclear translocation to activate transcription factors, such as RUNX (Runt related transcription factor) and NF-κB to enhance B cell survival [191]. MIF-induced CD74 cleavage may also affect CD74 stabilization inside the cytosol. However, whether this mechanism contributes to the development of NAFLD progression is unknown.

Caspase-4 ((known as human homologs caspase-4 and caspase-5, and its murine homolog caspase-11) belongs to the caspase 1 subfamily and plays a key role in regulating pyroptosis [279]. However, accumulating evidence also supports the direct involvement of caspase-4 in inflammation [280]. LPS induces caspase-4 expression, upregulating the production of inflammatory cytokines as IL-18 and IL-1β, which require proteolytic processing for secretion [281]. Interestingly, caspase-4 also promotes the degradation of CD74 during dendritic cell development [282]. Therefore, whether MIF regulates CD74 stability through caspase-4 is of interest for our current study. We investigated the effect of MIF on stabilizing hepatic CD74 and describe a novel regulatory mechanism that contributes to the development of NAFLD. Our study provides new insight into NAFLD pathogenesis as well as suggests new opportunities for therapeutics.

4.3 RESULTS

4.3.1 MIF Upregulates Non-Transcriptional Hepatic CD74 Levels in the Absence of Inflammation

In numerous organ systems, the expression pattern of CD74 has been observed to closely parallel that of its ligand, MIF [184]. Nevertheless, the precise regulatory relationship between MIF and CD74 remains inadequately understood. We found that a conspicuous and time-dependent augmentation of CD74 content in HepG2 cells following MIF exposure (Figure 4.3.1A). Crucially, alterations in CD74 protein were associated with unchanged *Cd74* gene expression and proinflammatory genes, such as *Tnf-α*, *IL-1β*, *IL-6* (Figure 4.3.1A and B). To further delineate the impact of elevated MIF levels on hepatic CD74 regulation *in vivo*, we employed a transgenic MIF-overexpressing animal model known as *Mif* lung Tg. These mice exhibit elevated circulating MIF levels (Figure 4.3.1C) while maintaining steady MIF expression (Figure 4.3.2) and experiencing an absence of inflammatory conditions in the liver (Figure 3.4.1D). But the *Mif* Lung Tg mice displayed heightened CD74 protein levels in the liver, despite the absence of changes in *Cd74* gene expression in comparison to compared to WT (Figure 4.3.1E and F). Collectively, our combined *in vitro* and *in vivo* findings strongly suggest that MIF exerts a direct influence on hepatic CD74 protein levels through a non-transcriptional mechanism.

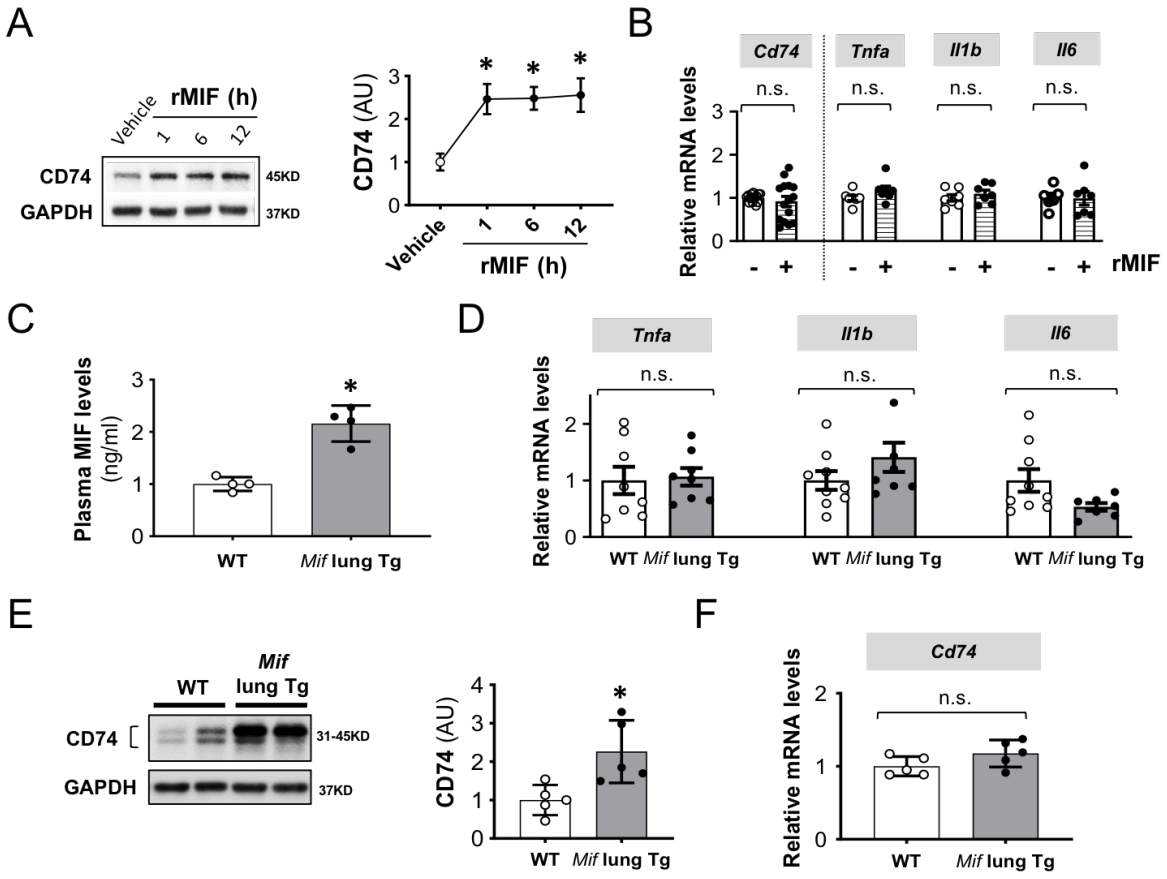

23-Figure 4.3.1. MIF increases non-transcriptional CD74 protein levels *in vitro* and *in vivo*.

HepG2 cells were initially cultured in Minimum Essential Medium with 10% FBS and following fasting (0.5% FBS) overnight, the cells were incubated with vehicle or human recombinant MIF (rMIF, 400ng/ml) for 1-12 hours. CD74 protein levels were then evaluated by western blot (A) and the gene expression of *Cd74* and inflammatory genes *TNF-α*, *IL-1β*, and *IL-6* (B) was quantified by qPCR (B). The levels of plasma MIF in WT and *Mif* Tg mice (15 weeks) were quantified by ELISA (C) and inflammatory factor gene expression was measured in the liver at (D) by qPCR. CD74 protein and gene expression was also quantified (E and F). All the values are mean ± SD. *P ≤ 0.05 increase vs. Vehicle in (A), vs. WT in (C) or (E). n.s. represents no significance.

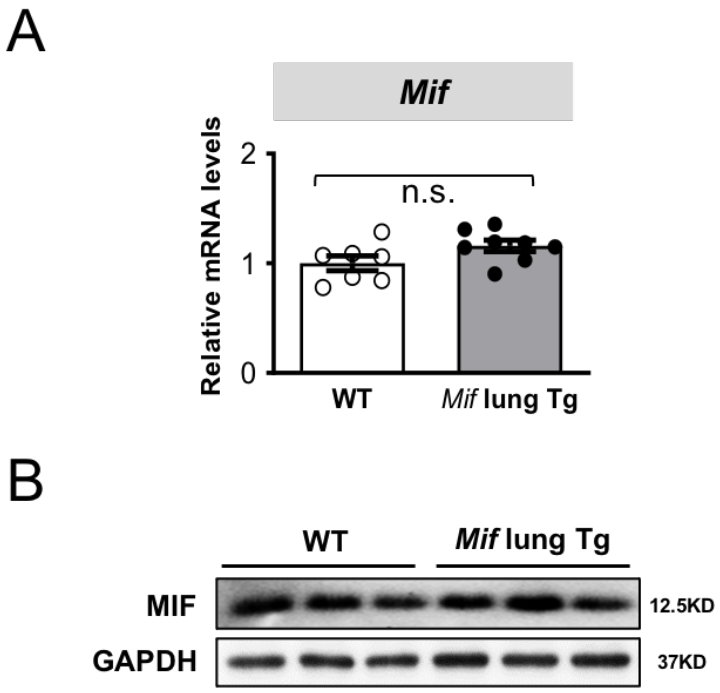

24-Figure 4.3.2. Hepatic MIF expression in WT and *Mif* lung Tg mice.

C57BL/6 mice (WT) and *Mif* lung Tg mice (3 weeks) were fed with normal chow (NC) for 12 weeks and then euthanized for quantifications of hepatic *Mif* gene by qPCR (A) and protein by WB (B). N= 4-5 each animal group. All the values are mean ± SD, *P<0.05 increase vs. WT. n.s. represents no significance.

4.3.2 Transgenic Upregulation of Circulating MIF Levels Increases Lipid Accumulation and Fibrosis in Liver

In *Mif* Lung Tg mice, characterized by elevated circulating MIF levels, we observed a multifaceted impact on hepatic physiology. A prominent consequence of this heightened MIF environment was the conspicuous accumulation of lipid droplets within hepatic tissues (Figure 4.3.3A). Intriguingly, this lipid deposition was concomitant with the upregulation of genes involved in lipid synthesis, including *PPARγ* and fatty acid synthase (*FAS*) (Figure 4.3.3B). These findings collectively suggest that elevated MIF levels may stimulate hepatic lipid biosynthesis. Moreover, the influence of elevated circulating MIF extended to the realm of hepatic fibrosis (Figure 4.3.3C). This fibrotic condition was characterized by increased gene expression of fibrosis makers, *actin alpha 2 (Acta2)*, alpha-1 type I collagen (*Col1A1)*, and transforming growth factor beta (*Tgfb)* (Figure 4.3.3D). And the alpha-smooth muscle actin (α-Sma, also known as Acta2) protein, a well-established marker of fibrosis primarily expressed in vascular smooth muscle cells [283], exhibited a significant upregulation in the liver from *Mif* Lung Tg mice in comparison to that in WT liver (Figure 4.3.3E). This observation suggests that the heightened MIF levels, either directly or through the MIF-upregulated CD74 pathway, may contribute significantly to the development of hepatic steatosis and fibrosis.

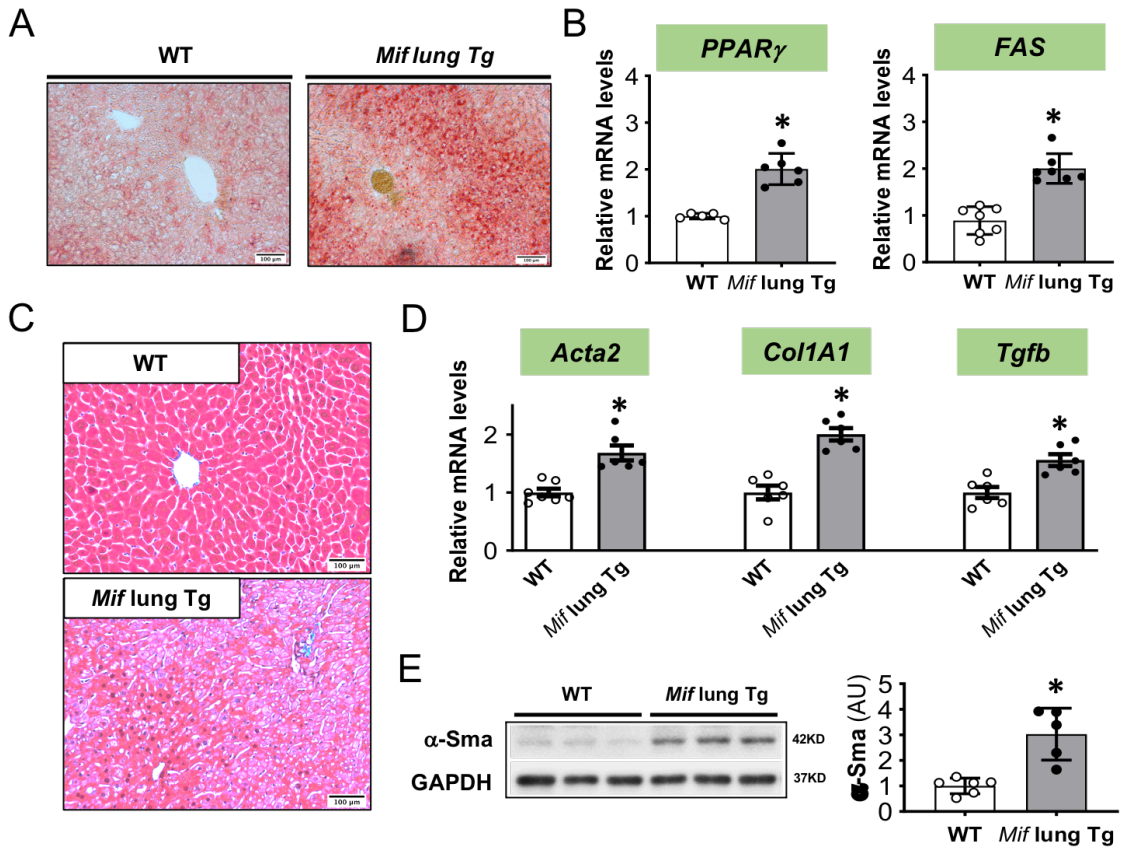

25-Figure 4.3.3. Transgenic upregulation of circulating MIF levels increases lipid accumulation and fibrosis in the liver.

Age-matched WT and *Mif* lung Tg mice (15 weeks) were euthanized for the quantifications of hepatic lipid storage by Oil red O staining (A), the lipid synthesis genes of *PPARγ* and *FAS* by qPCR (B), liver fibrosis by Trichrome staining (C) and the expression of *Acta2*, *Col1A1* and *Tgfb* (D) and α-Sma (E). All the values are mean ± SD. *P ≤ 0.05 increase vs. WT in (B), (D) and (E). n.s. represents no significance.

4.3.3 High Circulating MIF Levels following High Fat Diet (HFD) Upregulate Non-Inflammatory and Non-Transcriptional Hepatic CD74 Levels that Contribute to the Development of Liver Steatosis and Fibrosis

Intriguingly, it has been well-established that the consumption of a high-fat diet has the propensity to induce a marked increase in circulating MIF levels within murine models [259]. To comprehensively investigate this phenomenon, the C57BL/6 WT mice was fed with a high-caloric dietary regimen at the age of 3 weeks for 12 weeks. Astonishingly, these mice with HFD interventions resulted in a remarkable augmentation, exceeding one-fold, in the levels of plasma MIF when compared to WT with NC (Figure 4.3.4A). And this surge in circulating MIF levels was observed in tandem with a conspicuous elevation in CD74 protein in the liver but not its mRNA (Figure 4.3.4B and C). It is noteworthy that this increase in CD74 protein did not correlate with alterations in the expression of other key proinflammatory cytokine genes such as *TNF-α, IL6*, *IL1β* (Figure 4.3.4D). Expanding upon these observations, we delved into the pathophysiological implications of such alterations in MIF and CD74 in response to HFD consumption. Akin to our findings in the *Mif* Lung Tg mice, the WT mice subjected to HFD exhibited heightened hepatic steatosis and fibrosis (Figure 4.3.4E to I). Collectively, these intriguing results strongly advocate for a putative role of MIF-driven CD74 upregulation in the pathogenesis of hepatic pathological changes in response to a HFD feeding.

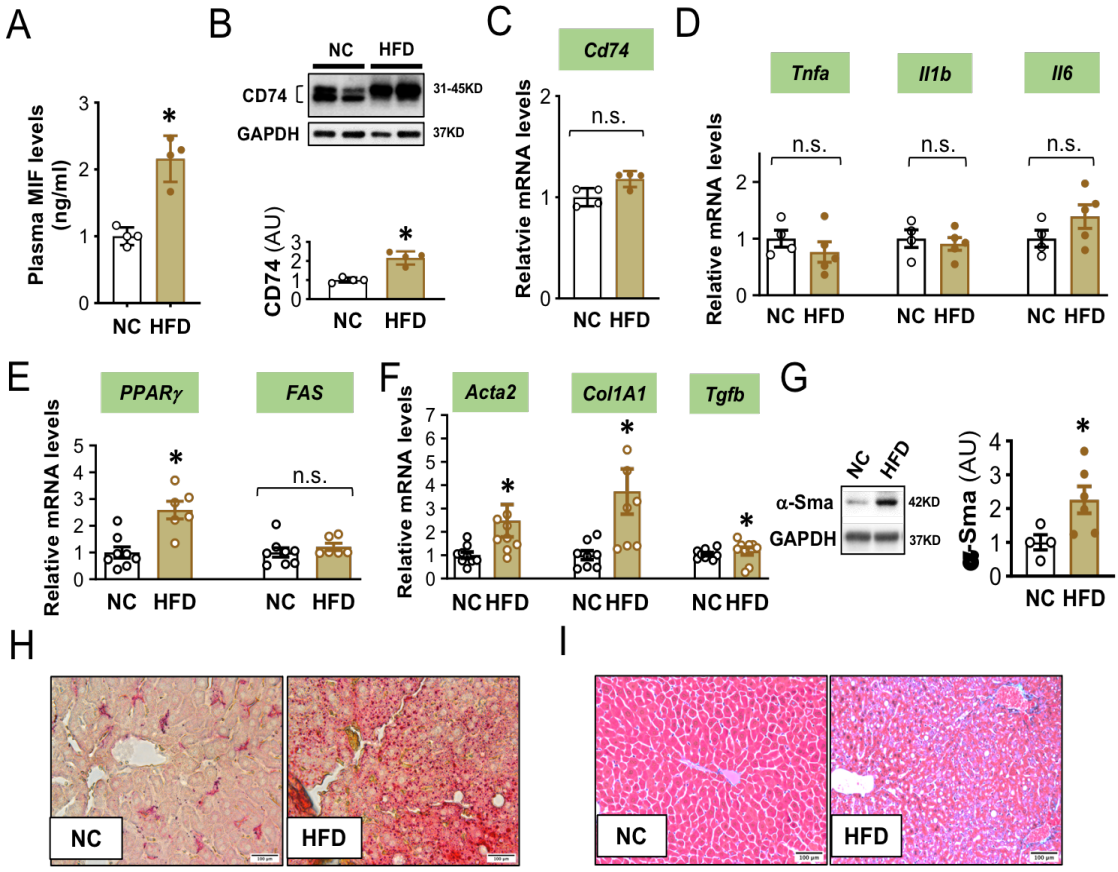

26-Figure 4.3.4. High circulating MIF levels following a HFD upregulate non-inflammatory and non-transcriptional hepatic CD74 levels, leading to the development of hepatic steatosis and fibrosis.

WT mice at 3 weeks were fed with normal chow (NC) or high caloric diet (HFD) for 12 weeks. Plasma MIF levels were quantified by ELISA (A) and the protein and gene levels of CD74 in the liver were measured by western blot and qPCR in (B) and (C), respectively. The hepatic inflammation was evaluated by the quantification of *TNF-α*, *IL-1β*, and *IL-6* (D). Lipid accumulation was assessed by the quantification of *PPARγ* and *FAS* (E) and Oil red O staining (H). Eventually, liver fibrosis was evaluated by the quantification of *Acta2, Col1A1, Tgfb* and α-Sma and visualized by Trichrome staining (F and G). All the values are mean ± SD. *P ≤ 0.05 increase vs. NC in (A), (B), (E), (F) and (G). n.s. represents no significance.

4.3.4. Neutralization of MIF Reverses HFD-Induced Upregulation of Non-Transcriptional CD74 Levels and Attenuates NAFLD Development

Thus, we next asked whether the reduction of circulating MIF levels could mitigate MIF-driven CD74 accumulation within the liver. To address this question, we employed an *in vivo* approach by administering anti-MIF antibodies to neutralize the MIF [240]. Our present study illuminated the profound effects of anti-MIF antibodies in mitigating hepatic CD74 protein within liver (Figure 4.3.5A). This notable reduction in CD74 content was independent to the hepatic inflammation. (Figure 4.3.5B). The improvement of NAFLD was evidenced by the downregulation of key genes pivotal in the context of hepatic pathology, including the lipid synthesis and fibrosis marker genes, including *PPARγ*, *Acta2*, *Col1A1*, and *Tgfb* ((Figure 4.3.5C and D). Complementing these gene expression changes, the marker of fibrosis protein levels of α-Sma was substantially diminished following anti-MIF antibody treatment in the liver (Figure 4.3.5E). Importantly, these molecular alterations precipitated by anti-MIF antibodies were further corroborated by histological assessments of the liver. Specifically, hepatic steatosis and fibrosis, two cardinal features of NAFLD, were appreciably attenuated in response to anti-MIF treatment (Figure 4.3.5F and G). These compelling findings collectively underscore the hitherto unexplored role of MIF in the regulation of non-transcribed CD74 levels and its consequential impact on the pathogenesis of NAFLD.

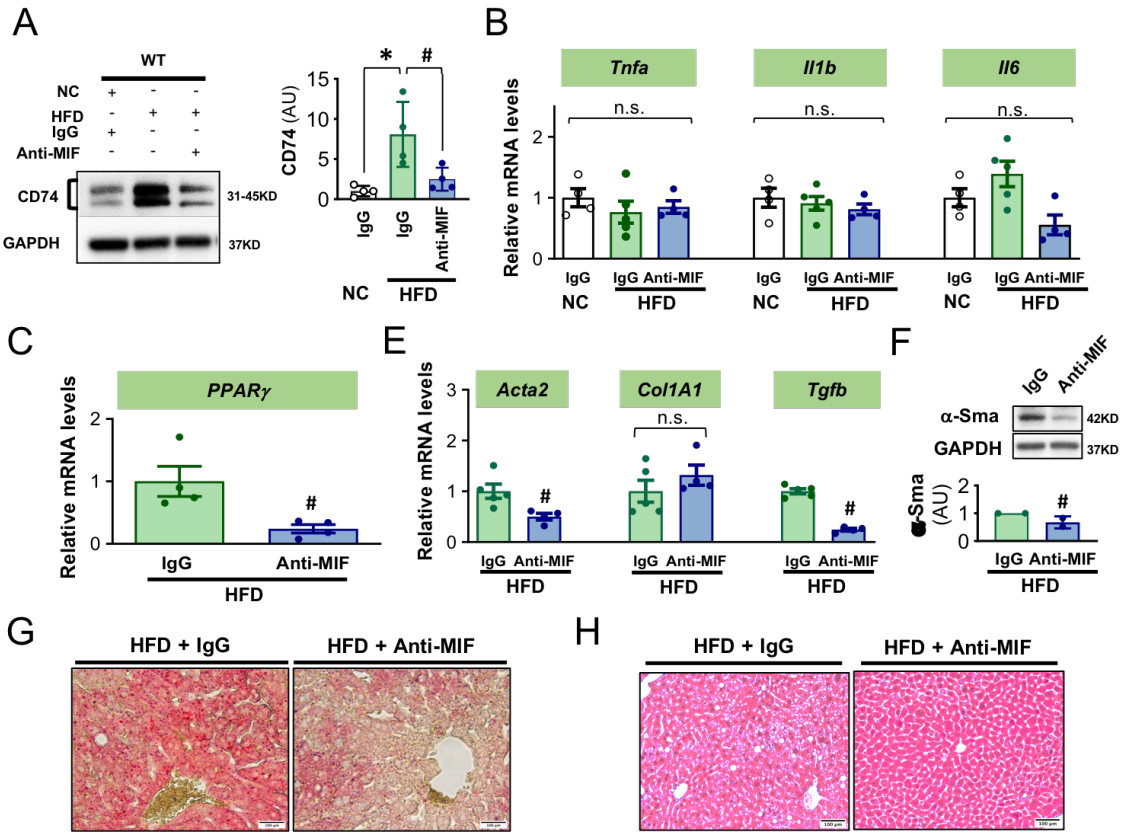

27-Figure 4.3.5. The neutralization of MIF reverses HFD-induced upregulation of non-transcribed CD74 levels and attenuates NAFLD development.

WT mice at 3 weeks were initially fed with normal chow (NC) or high caloric diet (HFD) for 7 weeks and then they were randomly divided to two groups injected with non-specific IgG or anti-MIF antibody (20 mg/kg, i.p. twice a week) accompanied with diet feeding for 5 weeks. The protein levels of CD74 (A) and expression of inflammatory genes, *TNFα*, *IL-1β*, *IL-6* (B) were quantified by western blot and qPCR, respectively. Lipid accumulation and fibrosis makers, *PPARγ*, *Acta2, Col1A1, Tgfb* and α-Sma were evaluated from (C) to (E) and histological changes were identified by Oil red O (F) or Trichrome staining (G). All the values are mean ± SD. *P ≤ 0.05 increase vs. IgG NC in (A). #P ≤ 0.05 reduction vs. IgG HFD in (A), (C), (E) and (F). n.s. represents no significance.

4.3.5 Genetic Deficiency of MIF Reduces Hepatic CD74 Levels and NAFLD following HFD Feeding

To comprehensively investigate the impact of MIF deficiency on CD74 protein levels in the liver, we utilized *Mif*$^{-/-}$ mice, characterized by a global deficiency in MIF. Our findings revealed that global MIF deficiency significantly downregulated non-transcribed CD74 protein levels in the liver following a HFD feeding in *Mif*$^{-/-}$ mice compared with WT mice with HFD (Figure 4.3.6A). This reduction in CD74 protein was associated with a notable downregulation in the gene expression of key markers linked to lipogenesis and liver fibrosis (Figure 4.3.6B and D). Furthermore, the protein levels of α-Sma, a marker of fibrosis, exhibited a similar reduction, aligning with the levels observed in both *Mif*$^{-/-}$ mice and *Cd74*$^{-/-}$ mice subjected to an HFD (Figure 4.3.6E). As expected, the histological analysis of the livers from *Mif*$^{-/-}$ mice revealed improvements in lipid accumulation and collagen formation relative to their WT counterparts when exposed to an HFD (Figure 4.3.6C and F). These findings corroborate our previous observations in models involving MIF neutralization. Collectively, these results underscore the importance of targeting the MIF/CD74 axis to ameliorate hepatic steatosis and fibrosis in the context of complications arising from diet-induced obesity, particularly NAFLD.

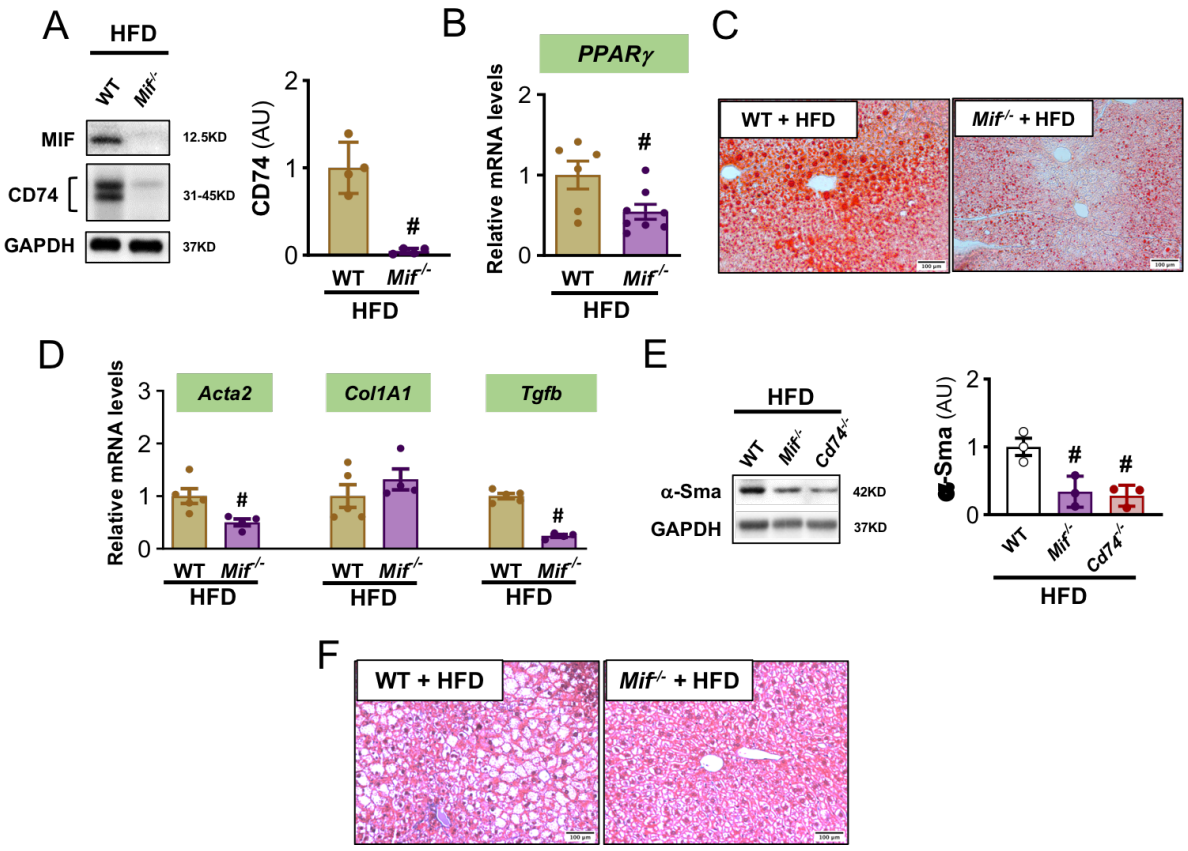

28-Figure 4.3.6. Transgenic deficiency of MIF downregulates hepatic CD74 levels and NAFLD following HFD feeding.

WT and *Mif*$^{-/-}$ mice at 3 weeks were fed with high caloric diet (HFD) for 8 weeks and then hepatic CD74 was quantified by western blot (A). Lipid accumulation and fibrosis makers, *PPARγ*, *Acta2, Col1A1, Tgfb* and α-Sma were evaluated in (B), (D) and (E). Histological changes were identified by Oil red O (C) or Trichrome staining (F). All the values are mean ± SD. #P ≤ 0.05 reduction vs. WT HFD in (A), (B), (D) and (E).

4.3.6 MIF Inhibits Cleavage of Caspase-4 that Facilitates the Degradation of CD74 in Liver

The preceding *in vitro* and *in vivo* findings collectively underscore the pivotal role of MIF in stabilizing its receptor, CD74, thereby leading to a substantial accumulation of CD74 within the liver. This accumulation is strongly associated with the development of NAFLD. Our following objective is to investigate the molecular mechanisms that underlie how MIF influences the stabilization of CD74 in hepatic cells. Initially, our hypothesis revolved around the possibility that MIF achieves CD74 stabilization through direct binding to CD74 on the cell membrane. To investigate this hypothesis, we employed a specific MIF inhibitor, MIF098, known for its ability to obstruct the binding activity between MIF and CD74 [239]. Intriguingly, the levels of CD74, which are augmented by MIF, remained unaffected in the presence of the MIF inhibitor MIF098 (Figure 4.3.7A). This intriguing observation suggests that the regulation of non-transcribed CD74 by MIF operates independently of the conventional ligand-receptor binding mode between MIF and CD74. Furthermore, we incubated the HepG2 liver cell with FITC-labelled rMIF for 1 hour, which distinctly exhibited endocytosis as the mode of cellular entry (Figure 4.3.7B). This mode of entry hinted at the possibility that, aside from the MIF-CD74 binding mechanism, endocytic MIF may govern other factors responsible for CD74 stabilization. Caspase-4 promotes the degradation of CD74 in developing dendritic cells [282], and caspase-4 is normally activated by its cleavage or tis precursor, pro-caspase-4. To facilitate these investigations, we employed a caspase-4-specific inhibitor, Z-LEVD-FMK, in HepG2 liver cells. We found that caspase-4 inhibition significantly heightened CD74 protein levels (Figure 4.3.7C), while gene expression remained unaltered (Figure 4.3.7D). That suggested caspase-4 negatively regulates CD74 levels post-transcriptionally. Additionally, the treatment of HepG2 cells with rMIF exhibited a downregulation of cleaved caspase-4 alongside an upregulation of pro-caspase-4 (Figure 4.3.7E). These *in vitro* observations

were further validated *in vivo*, we found that the inhibition of MIF effects by neutralizing antibodies or genetic deletion of *Mif* in mice relatively increased cleaved caspase-4 compared with the WT group following HFD (Figure 4.3.7F). These results suggested that caspase-4 signaling is postulated to contribute to the degradation of CD74, ultimately resulting in decreased hepatic CD74 levels. While MIF inhibit caspase-4 activation to protect CD 74 from degradation in liver cells (Figure 3.4.4 and 3.4.5).

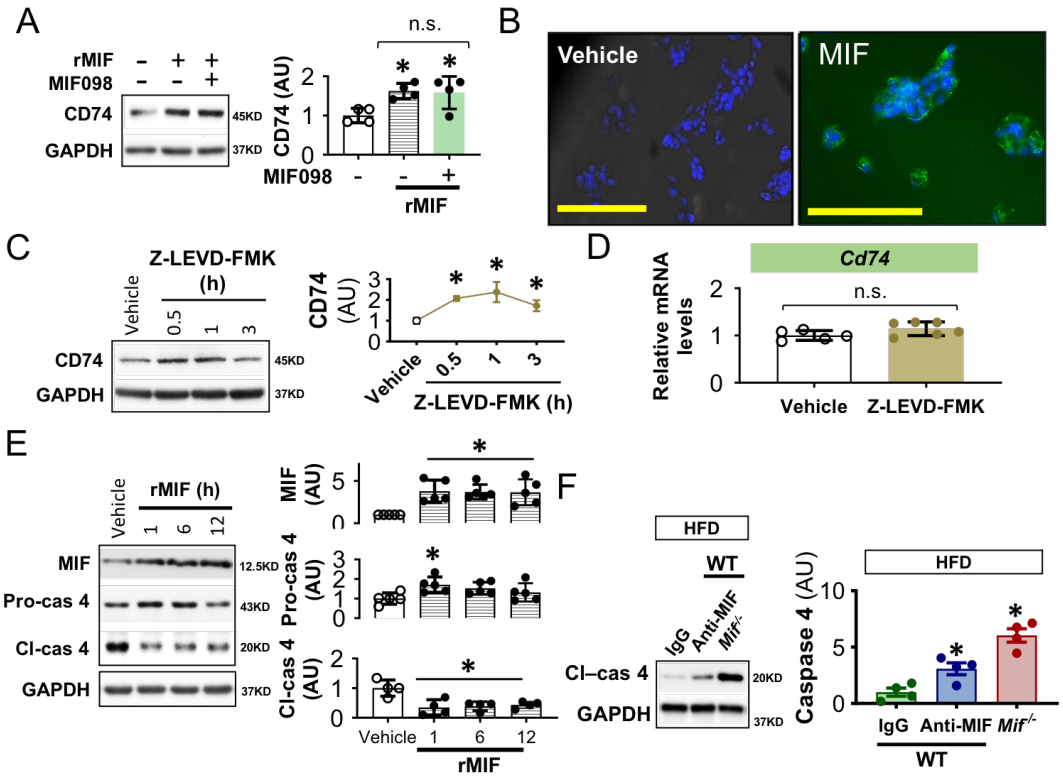

29-Figure 4.3.7. MIF inhibits cleavage of caspase-4 that promotes the stability of CD74 in liver.

HepG2 cells were incubated with vehicle or recombinant MIF (400ng/ml) in the presence or absence of MIF098 (10μM) for 12 hours. CD74 protein levels were then evaluated in (A). FITC labeled rMIF were treated with HepG2 cells for 2 hours and visualized with confocal microscope (B). The cells were also treated with vehicle or the inhibitor of caspase-4, Z-LEVD-FMK (20μM) from 0.5 to 3 hours and the protein (C) and gene (D) levels of CD74 were quantified by western blot and qPCR. In a separate experiment, rMIF was treated with cells from 1 to 12 hours and then MIF, pro-caspase-4 and cleaved caspase-4 were quantified by western blot (E). Following high cleric diet feeding (HFD), cleaved caspase-4 was evaluated in the livers from WT IgG, anti-MIF and *Mif*$^{-/-}$ groups. All the values are mean ± SD. *P ≤ 0.05 increase vs. vehicle in (A), (C) and (E); vs. IgG in (F). #P ≤ 0.05 reduction vs. vehicle in (E). n.s. represents no significance.

4.4 DISCUSSION

NAFLD is a liver disease triggered by obesity-related metabolic dysfunction [113] [284]. Although lifestyle interventions, including exercise and weight loss, may have beneficial effects on NAFLD, the molecular mechanisms regulating NAFLD onset and progression remain largely unknown. Our current study found the cytokine MIF has a regulatory role in NAFLD by the upregulating its cognate receptor, CD74. In mice overexpressing MIF or fed a high-fat diet, MIF increased CD74 protein content but not *Cd74* gene expression which was associated with steatosis and fibrosis. Upregulation of CD74 and hepatic phenotypes can be reversed by blocking MIF with an anti-MIF antibody or *Mif* gene deletion. Caspase-4 promotes the degradation of CD74, and MIF endocytosis inhibits caspase-4 cleavage and activation, leading to enhanced to CD74 degradation. Collectively, our findings suggest that MIF stabilizes CD74 through inhibition of caspase-4, which may be an important mechanism for regulating NAFLD in the absence of liver inflammation.

NAFLD is associated with abnormal lipid metabolism [285], leading to excess accumulation of triglyceride in hepatocytes, resulting in impaired insulin sensitivity and cell damage [102] [286]. Systemic low grade chronic inflammation in the liver also contributes to the development of NAFLD [287]. Obesity is often associated with low-grade inflammation in adipose tissue, which increases the secretion of cytokines, including TNF-α, IL-6, IL-1β and MCP1 [78] [79] [80] [81] [82]. These released cytokines may contribute to inflammatory and immune signaling pathways in hepatocytes, but their relative importance and at which stage they contribute to NAFLD are unknown.

MIF was originally discovered in immune cells (macrophage/monocyte) as an upstream regulator of the innate immune response [265]. It is also widely expressed in metabolically active tissues including adipose tissue, heart, and liver [227]. Of these, adipose tissue appears to be a major source of plasma MIF. *MIF* gene expression in visceral and subcutaneous adipose tissue is

positively correlated with weight gain [211] [288]. Adipose-derived MIF attenuates insulin signaling and regulates lipid metabolism [224] [272]. These lines of evidence suggest that MIF plays a key role in energy metabolism. However, the role of MIF in regulating NAFLD is controversial. Early studies have shown that MIF protects against hepatic steatosis and fibrosis by activating the AMPK signaling pathway [186]. Thus, genetic deficiency of MIF exacerbates the hepatic steatosis phenotype after chronic HFD feeding [233]. However, several other studies indicated that MIF expression in hepatocytes is induced by chronic metabolic injury and that MIF promotes liver fibrogenesis by shifting the polarization of natural killer T cells toward a pro-fibrotic phenotype [231]. Interestingly, although the conclusions are different, both studies suggest that the MIF cell membrane receptor, CD74 is involved in the development of NAFLD [232] [233].

CD74 functions intracellularly antigen-presenting cells as the MHC class II invariant chain, but it has also been identified as a MIF receptor. Upon binding to MIF, CD74 recruits the co-activator CD44 to activate the ERK signaling pathway in both myeloid and stromal cell types [189]. In B cells, CD74 can also be cleaved to release a cytosolic domain CD74-ICD, which interacts with transcriptional factors and enhance cell survival [191]. Therefore, the stability and expression level of CD74 at the cell membrane is important for regulating MIF signal transduction. Our current study shows that MIF contributes to the development of hepatic steatosis and fibrosis, which is associated with post-transcriptional upregulation of CD74 in hepatocytes. CD74 reduction inhibited by anti-MIF antibody or MIF gene deletion significantly attenuates the hepatic phenotype, suggesting that the post-transcriptional stabilization of CD74 by MIF is a key mechanism in disease development.

Caspase-4/11 participates in inflammation [280] by regulating the secretion of IL-18 and IL-1β [281], which contributes to pyroptosis [279]. Caspase-4 also promotes the degradation of CD74

during dendritic cell development [282]. Our present findings suggest that MIF inhibits caspase-4 cleavage which may inhibit its activity to degrade CD74. In contrast, the blockade of caspase-4 increases CD74 levels in hepatocytes. MIF inhibits caspase-4 cleavage, thereby upregulating CD74 and exacerbating the hepatic phenotype. Previous studies have found that caspase-4/11 deficiency enhanced lipid accumulation in the liver [289], suggesting that caspase-4 plays an important role in regulating the development of NAFLD.

It should be noted that MIF can also enter cells through endocytosis [199]. Our present findings indicate that MIF entry into hepatocytes is associated with a downregulates caspase-4 cleavage and an upregulation of cellular CD74 protein. MIF blockade in mice by anti-MIF antibody or MIF gene deletion upregulates cleaved caspase-4 associated with CD74 reduction. Notably, the MIF and CD74 binding inhibitor, MIF098, didn't appear to affect MIF-induced increase in CD74 in hepatocytes. Therefore, we suspect that MIF-mediated CD74 stability in hepatocytes is primarily due to its influx into cells rather than binding to the CD74 receptors.

Overall, we show that MIF-mediated NAFLD pathogenesis is dependent on CD74. Downregulation of CD74 improves hepatic steatosis and fibrosis. Caspase-4 contributes to CD74 degradation, but MIF inhibits caspase-4 cleavage and activation. Thus, inhibition of MIF upregulates caspase-4 activation and stabilizes CD74. This may be an important mechanism to regulate NAFLD in the absence of liver inflammation (Figure 4.3.8).

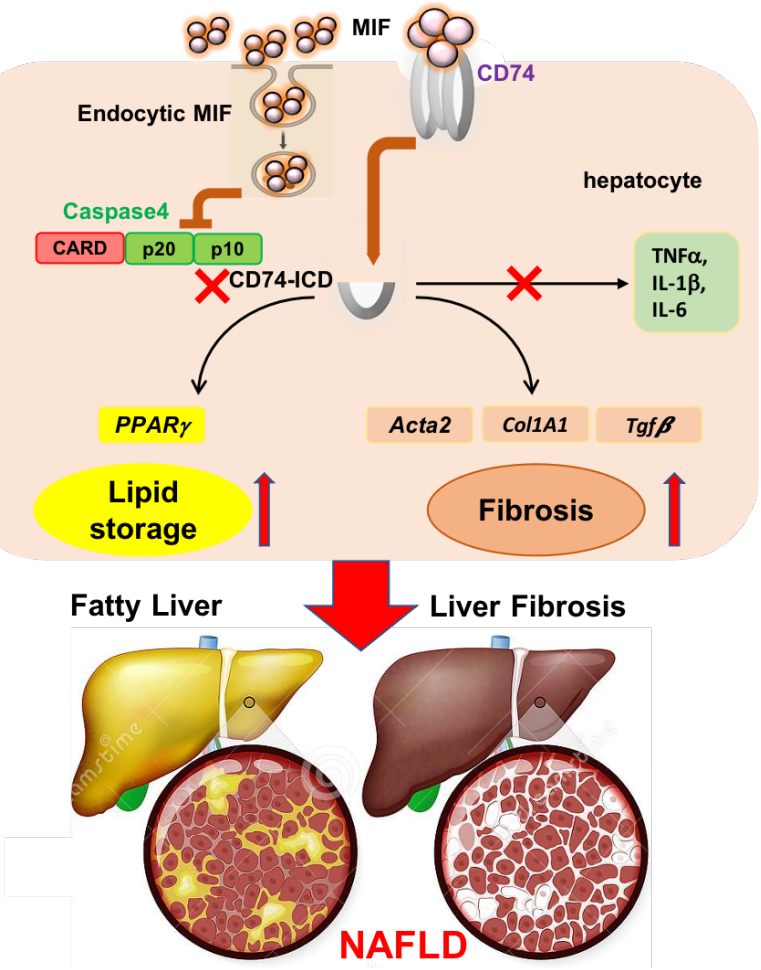

30-Figure 4.3.8 Graphical abstract summarizing the role of MIF in NAFLD and proposed underlying mechanism

MIF triggers NAFLD by upregulating CD74, its membrane receptor, through a non-inflammatory pathway. Specifically, MIF increased CD74 protein levels in a time-dependent manner without affecting *CD74* gene expression or the expression of proinflammatory factors, including *TNFα*, *IL-6*, and *IL-1β*, in hepatocytes. Moreover, in animal models of MIF overexpression or high-fat diet feeding, elevated circulating MIF levels were associated with increased hepatic CD74 protein levels and subsequent hepatic steatosis and fibrosis, independently of liver inflammation. Notably, MIF neutralization or knockout reversed the alterations in CD74 and liver phenotype. We further demonstrated that MIF inhibited caspase-4 cleavage and activation, thereby stabilizing CD74 via endocytosis. Conversely, inhibition of MIF upregulated cleaved caspase-4/11, leading to CD74 degradation. Collectively, our findings suggest that MIF promotes NAFLD by stabilizing CD74 through caspase-4 inhibition, highlighting a non-inflammatory mechanism underlying the regulation of NAFLD.

CHAPTER 5: DISCUSSION AND CONCLUSION

5.1 General Discussion and Conclusion

The metabolic syndrome, though multifaceted, primarily revolves around obesity and insulin resistance as the leading culprits[1]. Obesity induces significant alterations in adipose tissue function, releasing a torrent of fatty acids, hormones, and proinflammatory factors, thereby triggering complications like insulin resistance and fatty liver disease [95] [290]. MIF is one key player in this complex interplay. MIF is an inflammatory cytokine, renowned for its potent pro-inflammatory properties [214] [291] [292]. Moreover, it is acknowledged as trigger of obesity related insulin resistance [31] [272] [293]. However, current research offer limited insights into the mechanisms by which MIF contributes to obesity onset. Additionally, there are conflicting observations regarding MIF's role in advanced liver disease, describing both pro- and anti-fibrotic effects of MIF [231] [232] [233]. This thesis delves into the role of MIF in obesity and NAFLD, aligning with previous studies [31] while expanding our understanding of MIF's metabolic functions in peripheral tissues, including adipose tissue and the liver.

Firstly, this study unveils that MIF suppresses HSL in adipose tissue by activating the AMPK signaling pathway, which, in turn, stimulates JNK. Consequently, JNK activation leads to reduced HSL expression and activity. Both MIF-overexpressing transgenic mice and wild-type mice on a high-calorie diet exhibit inhibited HSL, contributing to obesity development. Interestingly, intracellular MIF interacts with Jab1, inhibiting JNK phosphorylation. Conversely, the absence of intracellular MIF in *Mif*$^{-/-}$ mice enhances JNK phosphorylation and reduces HSL. Furthermore, adipose tissue in *Mif*$^{-/-}$ mice displays increased Akt and reduced PKA phosphorylation compared to WT mice, further dampening HSL activation and worsening obesity.

HSL plays a crucial role in releasing fatty acids from adipose tissue by catalyzing the hydrolysis of triglycerides and diacylglycerol during lipolysis [249]. AMPK has been identified as an inhibitor of lipolysis through its downregulation of HSL activation in adipose tissue [294]. Additionally, AMPK promotes fatty acid oxidation in the liver and muscle [254 255]. Normally, HSL activity is stimulated by PKA-mediated phosphorylation at Ser^{563} but counteracted by AMPK, which phosphorylates HSL at Ser^{565}, reducing Ser^{563} phosphorylation and lipolysis [258]. Usually, insulin activates AKT to inhibit PKA, thereby suppressing lipolysis through the inhibition of HSL activation. Interestingly, we observed an unchanged PKA activation in the presence of MIF treatment and high plasma MIF levels, which might be elucidated by considering the negative regulation between AMPK activity and PKA [295]. Notably, the deficiency of MIF led to a decline in AMPK activation, rendering PKA responsive to AKT activation within adipose tissue (Figure 3.3.11I), further supporting this counter-regulatory relationship between AMPK and PKA. In addition, previous studies have indicated that HSL-deficient mice, including *HSL*$^{-/-}$, *HSL* haploinsufficient and adipose tissue-specific deletion of *HSL* mice, show resistance to HFD-induced weight gain mice [70 76 268 296]. Despite having less abdominal fat mass and normal body weight, these mice display higher core body temperatures, increased brown adipose tissue, and ectopic fat storage, particularly in the liver [70 268 270 297 298]. These complex phenotypes, potentially including a higher baseline of thermogenesis and the development of fatty liver as a compensatory mechanism alongside lipodystrophy [269], in which might make it challenging for these models to mimic post-developmental MIF-mediated HSL loss during the development of obesity.

Adipose tissue dysfunction is intricately linked to fatty liver disease development due to the liver's high susceptibility to fatty acids. Chapter 3 of our study comprehensively elucidates the role of MIF/HSL in mediating adipocyte hypertrophy. We also notice that anti-MIF antibody

neutralization significantly restores adipose tissue function and reduces HFD-induced circulating fatty acids (Figure 3.3.8B), ultimately decreasing hepatic lipid accumulation, potentially by enhancing liver fatty acid oxidation (Figure 3.3.8C). Furthermore, MIF neutralization also enhances peripheral tissue insulin sensitivity, including the adipose tissue, liver, and skeletal muscle (Figure 3.3.8F-H). These results underscore the importance of unraveling the complexities of MIF in fatty liver disease.

Next, we further uncover that MIF induces NAFLD by stabilizing CD74. MIF treatment increases CD74 protein levels in hepatocytes, without altering CD74 gene expression. Both MIF overexpression and a HFD elevate hepatic CD74 protein levels, accompanied by hepatic steatosis and fibrosis. In contrast, MIF neutralization effectively reverses CD74 and liver phenotype. Caspase-4 is responsible for CD74 degradation, but MIF inhibits caspase-4 cleavage and activation, thereby stabilizing CD74 and leading to its accumulation. The inhibition of MIF consequently upregulates cleaved caspase-4, causing CD74 degradation and reduced CD74 protein in hepatocytes. Our findings suggest that MIF may induce NAFLD by stabilizing CD74.

CD74 serves as a pivotal protein in antigen-presenting cells, acting as both a chaperone and aiding in MHC class II (MHCII) complex trafficking. During antigen processing, CD74 undergoes sequential degradation involving different proteases, in which cathepsin S (CatS) [299] [300] and the intramembrane protease signal peptide peptidase-like 2a (SPPL2a) [300] are indispensable for cleavage and turnover of CD74 N-terminal fragment in human [301] and mice [302]. During this dynamic process, newly synthesized CD74 molecules transiently appear on the cell surface followed by rapid internalization to the endosomal pathway [303], with a surface half-life of approximately 10 minutes [304] [305]. Furthermore, CD74 serves as both a receptor (full CD74) for MIF, initiating signaling cascade transmission [306], and as a transcription regulator (CD74-ICD)

implicated in gene expressions [191]. We disclosed that MIF treatment increase CD74 protein in the liver without gene expression alteration. This finding uncover that MIF may exert non-transcriptional effects on CD74, specifically contributing to the stabilization of CD74 within liver cells. The MIF induced disruption of CD74 degradation is linked to the activation of genes involved in lipid synthesis and fibrosis within the liver, ultimately driving the development of NAFLD. Furthermore, our research identified that this regulatory process operates through MIF inhibition on caspase-4 within the cytoplasm by MIF endocytosis, rather than a direct physical binding effect between MIF and CD74. This novel discovery expands our understanding of caspase-4's role in CD74 degradation [282].

Recent studies have shown that excessive activation of caspase-4/5/11-mediated inflammasomes can lead to liver inflammation, resulting in liver injury and subsequent fibrosis. This contributes to the development of NAFLD [307 308]. Our research reveals that MIF-mediated NAFLD pathogenesis is distinct from liver inflammation even though in the presence of adipose tissue inflammation within the HFD group (Figure 3.3.9) without hepatic inflammation (Figures 4.3.1, 4, and 5). It's worth noting that prior research has reported that obese *caspases 1/11*$^{-/-}$ primarily exhibit hepatic steatosis as the most prominent phenotype alteration [289], indicating a protective role of caspase-4/5/11 in NAFLD. In our study, we've uncovered that MIF inhibits caspase-4 activation, disrupting caspase-4-mediated CD74 degradation. Intriguingly, we observed that caspase-4 activity rebounds when MIF levels are reduced through the administration of anti-MIF antibodies or *Mif* gene deletion.

In conclusion, our research reveals the pivotal role of MIF in metabolic dysfunction, particularly in the context of obesity and NAFLD. MIF, both intracellular and extracellular, significantly influences adipose HSL contributing to the adipocyte hypertrophy. Extracellular MIF,

released from adipocytes, suppresses HSL through AMPK/JNK signaling by binding to its receptor, CD74. During obesity development, this extracellular action of MIF is predominant and exacerbates HSL suppression under physiologically condition. While intercellular MIF acts more function in counteracting with the extracellular effect of MIF on HSL over suppression. Our research further expands the understanding of MIF's role in liver diseases. In the context of NAFLD, we discovered that MIF upregulates its receptor, CD74, in hepatocytes, contributing to hepatic steatosis and fibrosis. Caspase-4 is involved in CD74 degradation, and MIF, via endocytosis, inhibits caspase-4, stabilizing CD74. Overall, our findings highlight MIF's complex role in metabolic disorders and underscore the potential therapeutic importance of targeting the MIF/CD74 axis in managing obesity and NAFLD.

5.2 Strengths and Limitations

5.2.1 Strengths:

The primary objective of this thesis was to contribute to our understanding of the role of MIF in metabolic dysfunction, particularly in the context of obesity and its complications, such as NAFLD. This research achieved several notable advancements:

(1) It elucidated, for the first time, the dual impact of MIF on HSL, involving both transcriptional and non-transcriptional regulatory mechanisms; (2) It pioneered the revelation of MIF's distinct extracellular and intracellular effects on HSL, shedding light on its multifaceted role in lipid metabolism; (3) This work expanded our comprehension of the intricate interaction between MIF and Jab1/Csn5, demonstrating that MIF modulates JNK activation and associated processes through a mechanism that extends beyond a mere binding competition between MIF and JNK on Jab1/Csn5. Instead, it involves a nuanced modulation of Jab1's functional effects; (4) It provided novel insights by showcasing MIF's function as a stabilizer of its receptor within liver cells, an observation that had not been previously reported; (5) This study also uncovered a previously undocumented role of MIF in inhibiting caspase-4 activity within liver cells, adding a new dimension to our understanding of MIF's impact on cellular processes.

These findings collectively enhance our comprehension of the multifaceted roles played by MIF in metabolic disorders, opening avenues for further research in this field.

5.2.2 Limitations:

(1) The different animal models. For example, the lack of the basic metabolic data about these animals (*Mif*$^{-/-}$, *Cd74*$^{-/-}$, *Mif* Lung Tg and WT mice with antibody administration under HFD feeding), such behavioral assessments the ratio of the fat mass and lean mass, bone density,

locomotor activities, energy expenditure, includes basal metabolic rate (BMR), resting metabolic rate (RMR), and total daily energy expenditure (TDEE), respiratory parameters, including oxygen consumption (VO_2) and carbon dioxide production (VCO_2) due to the lack of techniques, like indirect calorimetry or metabolic cages. With these basic metabolic data would provide a more comprehensive understanding of the findings in this thesis. Our lab will update these in the future; (2) Gene Expression: it will better confirm our finding target on *Mif*, *HSL*, *CD74*.etc, expressions in adipose tissue, liver to identify the changes in the metabolic pathway and related genes. With this kind of supportive results will strength our discoveries, which might shift the light to the function of MIF in metabolism and attract more attention in it. (3) In Chapter 3, Unfortunately, due to the unavailability of adipose biopsy samples, we were unable to validate this molecular mechanism in humans. (4) In Chapter 4, it would be advantageous and intriguing to investigate CD74 protein levels in mice subjected to caspase-4 inhibitor administration. This approach would yield valuable insights into the *in vivo* degradation of CD74 by caspase-4.

5.3 Therapeutic Implications

Considering the intricate molecular mechanisms through which MIF regulates adipose HSL and hepatic CD74, subsequently contributing to the development of obesity and NAFLD, our findings hold significant implications. They underscore the potential for targeting MIF as a promising therapeutic avenue for addressing metabolic dysfunction, including the use of anti-MIF antibody neutralization.

5.4 Future Work

The current research has shed significant light on the intricate roles of MIF in metabolic regulation, particularly within adipose tissue, liver, and skeletal muscle. However, numerous aspects warrant further exploration to deepen our understanding of MIF's involvement in metabolic dysfunctions.

(1) MIF in Hypothalamic Regulation of Obesity: Our findings indicate a central role of MIF in regulating food intake in the hypothalamus, potentially exacerbating obesity. Future research should delve into whether increased circulating MIF levels can access the hypothalamus and modulate hyperphagia. Understanding how this central effect of MIF interacts with its peripheral effects in adipose tissue and liver is paramount in comprehending the full scope of MIF's impact on obesity. **(2) MIF's Impact on CD74 Stability in Various Organ Systems**: The observed effects of MIF on CD74 stability in the liver raise intriguing possibilities regarding its influence on other organ systems. Future research should expand this investigation to ascertain if MIF's impacts on CD74 extend to other vital organs, potentially uncovering broader implications of MIF beyond adipose tissue and the liver. Understanding how MIF influences metabolism in these tissues and potentially identifying tissue-specific roles will enhance our overall understanding of MIF's systemic impact on metabolism. ***(3) Clinical Relevance and Therapeutic Strategies:*** Translating our research findings into clinical applications is a critical step. Future work should focus on validating our laboratory findings in human subjects and establishing correlations between MIF levels and metabolic status. Additionally, exploring potential therapeutic interventions targeting MIF or its downstream pathways in animal models and eventually in clinical trials could offer promising strategies for managing metabolic dysfunctions.

In conclusion, having successfully uncovered the pivotal role and molecular intricacies of MIF in obesity, the proposed future research areas aim to broaden our understanding, encompassing the central nervous system and multiple metabolic tissues. Furthermore, bridging this understanding to clinical implications holds promise for advancing the field and ultimately benefitting individuals grappling with metabolic disorders.

BIBLIOGRAPHY:

1. Neuhauser, H. K. The metabolic syndrome. *Lancet* **366**, 1415–1428 (2005).

2. Duckworth, W. C. Hyperglycemia and cardiovascular disease. *Curr. Atheroscler. Rep.* **3**, 383–391 (2001).

3. Yi, Y. S. Regulatory Roles of Caspase-11 Non-Canonical inflammasome in inflammatory liver diseases. *Int. J. Mol. Sci.* **23**, (2022).

4. Finucane, O. M., Reynolds, C. M., McGillicuddy, F. C. & Roche, H. M. Insights into the role of macrophage migration inhibitory factor in obesity and insulin resistance. *Proc. Nutr. Soc.* **71**, 622–633 (2012).

5. Hannah Ritchie and Max Roser. Obesity. *Our World in Data* https://ourworldindata.org/obesity (2017).

6. WHO. Obesity and overweight. https://www.who.int/news-room/fact-sheets/detail/obesity-and-overweight.

7. McArdle, M. A., Finucane, O. M., Connaughton, R. M., McMorrow, A. M. & Roche, H. M. Mechanisms of obesity-induced inflammation and insulin resistance: Insights into the emerging role of nutritional strategies. **4**, 1–23 (2013).

8. Ahmad, N. N., Butsch, W. S. & Aidarous, S. Clinical management of obesity in women: Addressing a lifecycle of risk. *Obstet. Gynecol. Clin. North Am.* **43**, 201–230 (2016).

9. Foucan, L. *et al.* High prevalence of rare monogenic forms of obesity in obese guadeloupean afro-caribbean children. *J. Clin. Endocrinol. Metab.* **103**, 539–545 (2018).

10. Loos, R. J. F. & Yeo, G. S. H. The genetics of obesity: from discovery to biology. *Nat.*

Rev. Genet. **23**, 120–133 (2022).

11. Heymsfield, S. B. & Wadden, T. A. Mechanisms, pathophysiology, and management of obesity. *N. Engl. J. Med.* **376**, 254–266 (2017).

12. Kahn, S. E., Hull, R. L. & Utzschneider, K. M. Mechanisms linking obesity to insulin resistance and type 2 diabetes. *Nature* **444**, 840–846 (2006).

13. Pigeyre, M., Yazdi, F. T., Kaur, Y. & Meyre, D. Recent progress in genetics, epigenetics and metagenomics unveils the pathophysiology of human obesity. *Clin. Sci.* **130**, 943–986 (2016).

14. Sadaf Farooqi, I. *et al.* Beneficial effects of leptin on obesity, T cell hyporesponsiveness, and neuroendocrine/metabolic dysfunction of human congenital leptin deficiency. *J. Clin. Invest.* **110**, 1093–1103 (2002).

15. Kühnen, P. *et al.* Proopiomelanocortin deficiency treated with a melanocortin-4 receptor agonist. *N. Engl. J. Med.* **375**, 240–246 (2016).

16. Cummings, D. E. & Schwartz, M. W. Genetics and pathophysiology of human obesity. *Annu. Rev. Med.* **54**, 453–471 (2003).

17. Hruby, A. & Hu, F. B. The Epidemiology of Obesity: A big picture. *Pharmacoeconomics* **33**, 673–689 (2015).

18. Walter, S., Mejia-Guevara, I., Estrada, K., Liu, S. Y. & Glymour, M. M. Association of a genetic risk score with body mass index across different birth cohorts. *JAMA - J. Am. Med. Assoc.* **316**, 63–69 (2016).

19. Dapas, M. *et al.* Distinct subtypes of polycystic ovary syndrome with novel genetic associations: An unsupervised, phenotypic clustering analysis. *PLoS Med.* **17**, 1–28

(2020).

20. Rakhra, V., Galappaththy, S. L., Bulchandani, S. & Cabandugama, P. K. Obesity and the western diet: How we got here. *Mo. Med.* **117**, 536–538 (2020).

21. Kant, A. K. Dietary patterns and health outcomes. *J. Am. Diet. Assoc.* **104**, 615–635 (2004).

22. Heidemann, C. *et al.* Dietary patterns and risk of mortality from cardiovascular disease, cancer, and all causes in a prospective cohort of women. *Circulation* **118**, 230–237 (2008).

23. Mozaffarian, D., Hao, T., Rimm, E. B., Willett, W. C. & Hu, F. B. Changes in diet and lifestyle and long-term weight gain in women and men. *N. Engl. J. Med.* **364**, 2392–2404 (2011).

24. Schnurr, T. M., Stallknecht, B. M., Sørensen, T. I. A., Kilpeläinen, T. O. & Hansen, T. Evidence for shared genetics between physical activity, sedentary behaviour and adiposity-related traits. *Obes. Rev.* **22**, (2021).

25. He, M., Xian, Y., Lv, X., He, J. & Ren, Y. Changes in body weight, physical activity, and lifestyle during the semi-lockdown period after the outbreak of COVID-19 in China: An online survey. *Disaster Med. Public Health Prep.* **15**, E23–E28 (2021).

26. Chang, T. H. *et al.* Weight gain associated with covid-19 lockdown in children and adolescents: A systematic review and meta-analysis. *Nutrients* **13**, 1–10 (2021).

27. Lange, S. J. *et al.* Longitudinal trends in body mass index before and during the COVID-19 pandemic among persons aged 2–19 years — United States, 2018–2020. *MMWR. Morb. Mortal. Wkly. Rep.* **70**, 1278–1283 (2021).

28. Daniels, N. F., Burrin, C., Chan, T. & Fusco, F. A systematic review of the impact of the first year of covid-19 on obesity risk factors: A Pandemic fueling a pandemic? *Curr. Dev. Nutr.* **6**, 1–25 (2022).

29. Al Hourani, H., Alkhatib, B. & Abdullah, M. Impact of COVID-19 lockdown on body weight, eating habits, and physical activity of jordanian children and adolescents. *Disaster Med. Public Health Prep.* **16**, 1855–1863 (2022).

30. Donnelly, J. E. *et al.* Appropriate physical activity intervention strategies for weight loss and prevention of weight regain for adults. *Med. Sci. Sports Exerc.* **41**, 459–471 (2009).

31. Cui, D. *et al.* Macrophage migration inhibitory factor mediates metabolic dysfunction induced by atypical antipsychotic therapy. *J. Clin. Invest.* **128**, 4997–5007 (2018).

32. Wirshing, D. A. *et al.* Novel antipsychotics: Comparison of weight gain liabilities. *J. Clin. Psychiatry* (1999) doi:10.4088/JCP.v60n0602.

33. Pijl, H. & Meinders, A. E. Bodyweight change as an adverse effect of drug treatment: mechanisms and management. *Drug Saf.* **14**, 329–342 (1996).

34. Keteyian, S. J. *et al.* Assessment of body composition in heart transplant patients. *Medicine and Science in Sports and Exercise* vol. 24 247–252 (1992).

35. Zhang, J. L. *et al.* Effect of metformin on weight gain during antihypertensive treatment with a β-blocker in chinese patients. *Am. J. Hypertens.* **22**, 884–890 (2009).

36. Cheskin, L. J. *et al.* Prescription medications: A modifiable contributor to obesity. *South. Med. J.* (1999) doi:10.1097/00007611-199909000-00009.

37. Newcomer, J. W. Antipsychotic medication-induced weight gain and risk for diabetes and cardiovascular disease. in *Energy Metabolism and Obesity: Research and Clinical*

Applications (ed. Donohoue, P. A.) 223–245 (Humana Press, 2008). doi:10.1007/978-1-60327-139-4_12.

38. Virk, S., Schwartz, T. L., Jindal, S., Nihalani, N. & Jones, N. Psychiatric medication induced obesity: An aetiologic review. *Obes. Rev.* **5**, 167–170 (2004).

39. Lindhom, V., Lahti, J., Rahkonen, O., Lahelma, E. & Lallukka, T. Joint association of physical activity and body weight with subsequent physical and mental functioning: a follow-up study. *BMC Public Health* **13**, 197 (2013).

40. Schwartz, T. L., Nihalani, N., Jindal, S., Virk, S. & Jones, N. Psychiatric medication-induced obesity : a review. *Obes. Rev.* 115–121 (2004).

41. Wharton, S., Raiber, L., Serodio, K. J., Lee, J. & Christensen, R. A. G. Medications that cause weight gain and alternatives in Canada: A narrative review. *Diabetes, Metab. Syndr. Obes.* **11**, 427–438 (2018).

42. McKenzie, R. *et al.* Low-dose hydrocortisone for treatment of chronic fatigue syndrome: A randomized controlled trial. *Jama* **280**, 1061–1066 (1998).

43. Chrousos, G. A., Kattah, J. C., Beck, R. W. & Cleary, P. A. Side effects of glucocorticoid treatment: Experience of the optic neuritis treatment trial. *JAMA J. Am. Med. Assoc.* **269**, 2110–2112 (1993).

44. Aljebab, F., Choonara, I. & Conroy, S. Systematic review of the toxicity of long- course oral corticosteroids in children. *PLoS One* **12**, 1–18 (2017).

45. Diaconu, C. *et al.* Beta-blockers in cardiovascular therapy: A review. *J. Mind Med. Sci.* **6**, 216–223 (2019).

46. Holman, R. *et al.* Efficacy of atenolol and captopril in reducing risk of macrovascular and

microvascular complications in type 2 diabetes: UKPDS 39. *Br. Med. J.* **317**, 713–720 (1998).

47. Davis, B. R. *et al.* Effect of antihypertensive therapy on weight loss. *Hypertension* **19**, 393–399 (1992).

48. Cranston, W. I., Semmence, A. M., Richardson, D. W. & Barnett, C. F. Effect of triamterene on elevated arterial pressure. *Am. Heart J.* **70**, 455–460 (1965).

49. Rossner, S., Taylor, C. L., Byington, R. P. & Furberg, C. D. Long term propranolol treatment and changes in body weight after myocardial infarction. *Br. Med. J.* **300**, 902–903 (1990).

50. Macmahon, S. W., Bernstein, L., Macdonald, G. J., Andrews, G. & Blacket, R. B. Comparison of Weight Reduction With Metoprolol in Treatment of Hypertension in Young Overweight Patients. *Lancet* **325**, 1233–1236 (1985).

51. Messerli, F. H. *et al.* Body Weight Changes with β-Blocker Use: Results from GEMINI. *Am. J. Med.* **120**, 610–615 (2007).

52. Longo, M. *et al.* Adipose tissue dysfunction as determinant of obesity-associated metabolic complications. *Int. J. Mol. Sci.* **20**, (2019).

53. Kahn, C. R., Wang, G. & Lee, K. Y. Altered adipose tissue and adipocyte function in the pathogenesis of metabolic syndrome. *J. Clin. Invest.* **129**, 3990–4000 (2019).

54. Rondini, E. A. & Granneman, J. G. Single cell approaches to address adipose tissue stromal cell heterogeneity. *Biochem. J.* **477**, 583–600 (2020).

55. Shao, M. *et al.* De novo adipocyte differentiation from Pdgfrβ+ preadipocytes protects against pathologic visceral adipose expansion in obesity. *Nat. Commun.* **9**, 1–16 (2018).

56. Sun, K. *et al.* Adipose tissue remodeling and obesity. **121**, 2094–2101 (2011).

57. Tang, W. *et al.* White fat progenitor cells reside in the adipose vasculature. *Science (80-.).* **322**, 583–586 (2008).

58. Jeffery, E., Church, C. D., Holtrup, B., Colman, L. & Rodeheffer, M. S. Rapid depot-specific activation of adipocyte precursor cells at the onset of obesity. *Nat. Cell Biol.* **17**, 376–385 (2015).

59. Engin, A. Fat Cell and Fatty Acid Turnover in Obesity. *Adv. Exp. Med. Biol.* **960**, 135–160 (2017).

60. Okuno, M. *et al.* Perilla oil prevents the excessive growth of visceral adipose tissue in rats by down-regulating adipocyte differentiation. *J. Nutr.* **127**, 1752–1757 (1997).

61. Srebp, A. D. D., Kim, J. B., Lowell, B. B. & Spiegelman, B. M. Nutritional and insulin regulation of fatty acid synthetase and leptin gene expression through ADD1/SREBP1. **101**, 1–9 (1998).

62. Piegelman, B. R. M. S. ADD1/SREBP1 activates PPARγ through the production of endogenous ligand. **95**, 4333–4337 (1998).

63. Huang, X. & Dubiel, W. The COP9 signalosome controls adipocyte differentiation by regulating CHOP protein stability. *Engineering* (2012) doi:10.4236/eng.2012.410b050.

64. Hammarstedt, A., Gogg, S., Hedjazifar, S., Nerstedt, A. & Smith, U. Impaired adipogenesis and dysfunctional adipose tissue in human hypertrophic obesity. *Physiol. Rev.* **98**, 1911–1941 (2018).

65. Shepherd, P. R. *et al.* Adipose cell hyperplasia and enhanced glucose disposal in transgenic mice overexpressing GLUT4 selectively in adipose tissue. *J. Biol. Chem.* **268**,

22243–22246 (1993).

66. Goldberg, I. J., Eckel, R. H. & Abumrad, N. A. Regulation of fatty acid uptake into tissues: Lipoprotein lipase- And CD36-mediated pathways. *Journal of Lipid Research* (2009) doi:10.1194/jlr.R800085-JLR200.

67. Baillie, A. G. S., Coburn, C. T. & Abumrad, N. A. Reversible binding of long-chain patty acids to purified FAT, the adipose CD36 homolog. *J. Membr. Biol.* (1996) doi:10.1007/s002329900111.

68. Wang, H. & Eckel, R. H. Lipoprotein lipase: From gene to obesity. *Am. J. Physiol. - Endocrinol. Metab.* **297**, (2009).

69. Hajri, T., Han, X. X., Bonen, A. & Abumrad, N. A. Defective fatty acid uptake modulates insulin responsiveness and metabolic responses to diet in CD36-null mice. *J. Clin. Invest.* (2002) doi:10.1172/JCI0214596.

70. Pajed, L. *et al.* Advanced lipodystrophy reverses fatty liver in mice lacking adipocyte hormone-sensitive lipase. *Commun. Biol.* **4**, 1–13 (2021).

71. Zimmermann, R. *et al.* Fat Mobilization in Adipose Tissue Is Promoted by Adipose Triglyceride Lipase. *Sci. New Ser.* **306**, 1383–1386 (2016).

72. Jenkins, C. M. *et al.* Identification, cloning, expression, and purification of three novel human calcium-independent phospholipase A2 family members possessing triacylglycerol lipase and acylglycerol transacylase activities. *J. Biol. Chem.* **279**, 48968–48975 (2004).

73. Villena, J. A., Roy, S., Sarkadi-Nagy, E., Kim, K. H. & Hei, S. S. Desnutrin, an adipocyte gene encoding a novel patatin domain-containing protein, is induced by fasting and glucocorticoids: Ectopic expression of desnutrin increases triglyceride hydrolysis. *J. Biol.*

Chem. **279**, 47066–47075 (2004).

74. Rydén, M. *et al.* Comparative studies of the role of hormone-sensitive lipase and adipose triglyceride lipase in human fat cell lipolysis. *American Journal of Physiology - Endocrinology and Metabolism* vol. 292 (2007).

75. Osuga, J. I. *et al.* Targeted disruption of hormone-sensitive lipase results in male sterility and adipocyte hypertrophy, but not in obesity. *Proc. Natl. Acad. Sci. U. S. A.* **97**, 787–792 (2000).

76. Wang, S. P. *et al.* The adipose tissue phenotype of hormone-sensitive lipase deficiency in mice. *Obes. Res.* **9**, 119–128 (2001).

77. Kim, B. S., Pallua, N., Bernhagen, J. & Bucala, R. The macrophage migration inhibitory factor protein superfamily in obesity and wound repair. *Exp. Mol. Med.* **47**, (2015).

78. Skurk, T., Alberti-Huber, C., Herder, C. & Hauner, H. Relationship between adipocyte size and adipokine expression and secretion. *J. Clin. Endocrinol. Metab.* **92**, 1023–1033 (2007).

79. Sakaue, S. *et al.* Regulation of macrophage migration inhibitory factor (MIF) expression by glucose and insulin in adipocytes in vitro. *Mol. Med.* **5**, 361–371 (1999).

80. Hotamisligil, G. S., Shargill, N. S. & Spiegelman, B. M. Adipose expression of tumor necrosis factor-α: Direct role in obesity-linked insulin resistance. *Science (80-.).* **259**, 87–91 (1993).

81. Pradhan, A. D., Manson, J. E., Rifai, N., Buring, J. E. & Ridker, P. M. C-reactive protein, interleukin 6, and risk of developing type 2 diabetes mellitus. *J. Am. Med. Assoc.* **286**, 327–334 (2001).

82. Panee, J. Monocyte chemoattractant protein 1 (MCP-1) in obesity and diabetes. *Cytokine* **60**, 1–12 (2012).

83. Depreester, E. *et al.* Influence of adipocyte size and adipose depot on the number of adipose tissue macrophages and the expression of adipokines in dairy cows at the end of pregnancy. *J. Dairy Sci.* **101**, 6542–6555 (2018).

84. Lee, M. J., Wu, Y. & Fried, S. K. Adipose tissue heterogeneity: Implication of depot differences in adipose tissue for obesity complications. *Mol. Aspects Med.* **34**, 1–11 (2013).

85. Kim, J. Y. *et al.* Obesity-associated improvements in metabolic profile through expansion of adipose tissue. *J. Clin. Invest.* **117**, 2621–2637 (2007).

86. Stern, J. H., Rutkowski, J. M. & Scherer, P. E. Adiponectin, Leptin, and Fatty Acids in the Maintenance of Metabolic Homeostasis through adipose tissue crosstalk. *Cell Metab.* **23**, 770–784 (2016).

87. Münzberg, H. & Morrison, C. D. Structure, production and signaling of leptin. *Metabolism.* **64**, 13–23 (2015).

88. Palhinha, L. *et al.* Leptin induces proadipogenic and proinflammatory signaling in adipocytes. *Front. Endocrinol. (Lausanne).* **10**, (2019).

89. Zhang Y *et al.* Positional cloning of the mouse obese gene and its human homologue. *Nature* **372**, 425–432 (1994).

90. Coleman, D. L. Obese and diabetes: Two mutant genes causing diabetes-obesity syndromes in mice. *Diabetologia* **14**, 141–148 (1978).

91. Nishina, P. M., Lowe, S., Wang, J. & Paigen, B. Characterization of plasma lipids in

genetically obese mice: The mutants obese, diabetes, fat, tubby, and lethal yellow. *Metabolism* **43**, 549–553 (1994).

92. Haluzik, M. *et al.* Genetic background (C57BL/6J Versus FVB/N) strongly influences the severity of diabetes and insulin resistance in ob/ob mice. *Endocrinology* **145**, 3258–3264 (2004).

93. Grisouard, J. *et al.* Both inflammatory and classical lipolytic pathways are involved in lipopolysaccharide-induced lipolysis in human adipocytes. *Innate Immun.* **18**, 25–34 (2012).

94. Uysal, K. T., Wiesbrock, S. M., Marino, M. W. & Hotamisligil, G. S. Protection from obesity-induced insulin resistance in mice lacking TNF- α function. *Nature* (1997) doi:10.1038/39335.

95. Shoelson, S. E., Herrero, L. & Naaz, A. Obesity, inflammation, and insulin resistance. *Gastroenterology* **132**, 2169–2180 (2007).

96. Ouchi, N., Parker, J. L., Lugus, J. J. & Walsh, K. Adipokines in inflammation and metabolic disease. *Nat. Rev. Immunol.* **11**, 85–97 (2011).

97. Lingvay, I., Sumithran, P., Cohen, R. V & le Roux, C. W. Obesity management as a primary treatment goal for type 2 diabetes: time to reframe the conversation. *Lancet* **6736**, (2021).

98. Magkos, F. *et al.* Effects of moderate and subsequent progressive weight loss on metabolic function and adipose tissue biology in humans with obesity. *Cell Metab.* **23**, 591–601 (2016).

99. Byrne, Christopher D. Wild, S. H. *The Metabolic Syndrome*. (2011).

100. Daskalopoulou, S. S., Mikhailidis, D. P. & Elisaf, M. Prevention and treatment of the metabolic syndrome. *Angiology* **55**, 589–612 (2004).

101. Moore, M. C. *et al.* Sources of carbon for hepatic glycogen synthesis in the conscious dog. *J. Clin. Invest.* **88**, 578–587 (1991).

102. Petersen, M. C. & Shulman, G. I. Mechanisms of insulin action and insulin resistance. *Physiological Reviews* vol. 98 2133–2223 (2018).

103. Tong, Y., Xu, S., Huang, L. & Chen, C. Obesity and insulin resistance: Pathophysiology and treatment. *Drug Discov. Today* **27**, 822–830 (2022).

104. Zhang, N. *et al.* Berberine decreases insulin resistance in a PCOS rats by improving GLUT4: Dual regulation of the PI3K/AKT and MAPK pathways. *Regul. Toxicol. Pharmacol.* **110**, 104544 (2020).

105. Ye, J. Mechanisms of insulin resistance in obesity. *Front. Med. China* **7**, 14–24 (2013).

106. Galicia-Garcia, U. *et al.* Pathophysiology of type 2 diabetes mellitus. *Int. J. Mol. Sci.* **21**, 1–34 (2020).

107. Hirosumi, J. *et al.* A central role for JNK in obesity and insulin resistance. *Nature* **420**, 333–336 (2002).

108. Gregor, M. F. & Hotamisligil, G. S. Inflammatory Mechanisms in Obesity. *Annu. Rev. Immunol.* **29**, 415–445 (2011).

109. Boura-Halfon, S. & Zick, Y. Phosphorylation of IRS proteins, insulin action, and insulin resistance. *Am. J. Physiol. - Endocrinol. Metab.* **296**, (2009).

110. Perseghin, G., Petersen, K. & Shulman, G. I. Cellular mechanism of insulin resistance:

Potential links with inflammation. *Int. J. Obes.* **27**, S6–S11 (2003).

111. Saponaro, C., Gaggini, M., Carli, F. & Gastaldelli, A. The subtle balance between lipolysis and lipogenesis: A critical point in metabolic homeostasis. *Nutrients* **7**, 9453–9474 (2015).

112. Paul Angulo, M. D. Nonalcoholic Fatty Liver Disease. *N. Engl. J. Med.* **346**, 1221–1231 (2002).

113. Younossi, Z. *et al.* Global burden of NAFLD and NASH: Trends, predictions, risk factors and prevention. *Nat. Rev. Gastroenterol. Hepatol.* **15**, 11–20 (2018).

114. Cassidy, S. & Syed, B. A. Nonalcoholic steatohepatitis (NASH) drugs market. *Nat. Rev. Drug Discov.* **15**, 745–746 (2016).

115. Anushiravani, A., Haddadi, N., Pourfarmanbar, M. & Mohammadkarimi, V. Treatment options for nonalcoholic fatty liver disease: A double-blinded randomized placebo-controlled trial. *Eur. J. Gastroenterol. Hepatol.* **31**, 613–617 (2019).

116. Ali, E. S. *et al.* The glucagon-like peptide-1 analogue exendin-4 reverses impaired intracellular Ca2 + signalling in steatotic hepatocytes. *Biochim. Biophys. Acta - Mol. Cell Res.* **1863**, 2135–2146 (2016).

117. Akbar, S. M. F. *et al.* Macrophage migration inhibitory factor in hepatocellular carcinoma and liver cirrhosis; relevance to pathogenesis. *Cancer Lett.* (2001) doi:10.1016/S0304-3835(01)00606-1.

118. Saltiel, A. R. & Olefsky, J. M. Inflammatory mechanisms linking obesity and metabolic disease. *J. Clin. Invest.* **127**, 1–4 (2017).

119. Wikipedia contributors. Hepatic stellate cell. *Wikipedia, The Free Encyclopedia.*

1050211958 http://www.ncbi.nlm.nih.gov/pubmed/8550043 (2021).

120. Koyama, Y. & Brenner, D. A. Liver inflammation and fibrosis. *J. Clin. Invest.* **127**, 55–64 (2017).

121. Apovian, C. M. *et al.* Pharmacological management of obesity: An endocrine society clinical practice guideline. *J. Clin. Endocrinol. Metab.* **100**, 342–362 (2015).

122. Lau, D. & Padwal, R. In adults with overweight or obesity, continued weekly semaglutide after a 20-wk run-in improved weight loss. *Ann. Intern. Med.* **174**, JC88 (2021).

123. Wadden, T. A. *et al.* Effect of subcutaneous Semaglutide vs placebo as an adjunct to intensive behavioral therapy on body weight in adults with overweight or obesity: The Step 3 randomized clinical trial. *JAMA - J. Am. Med. Assoc.* **325**, 1403–1413 (2021).

124. Marso, S. P. *et al.* Semaglutide and Cardiovascular Outcomes in Patients with Type 2 Diabetes. *N. Engl. J. Med.* **375**, 1834–1844 (2016).

125. Van Gaal, L. & Dirinck, E. Pharmacological approaches in the treatment and maintenance of weight loss. *Diabetes Care* **39**, S260–S267 (2016).

126. Knudsen, L. B. & Lau, J. The discovery and development of liraglutide and semaglutide. *Front. Endocrinol. (Lausanne).* **10**, (2019).

127. Approaches, N., Approaches, N., Loss, T. O. W. & Loss, T. O. W. Nonpharmacologic approaches to weight loss. *English J.* **346**, 591–602 (2002).

128. Heck, A. M., Yanovski, J. A. & Calis, K. A. Orlistat, a new lipase inhibitor for the management of obesity. *Pharmacotherapy* **20**, 270–279 (2000).

129. Secher, A. *et al.* The arcuate nucleus mediates GLP-1 receptor agonist liraglutide-

dependent weight loss. *J. Clin. Invest.* **124**, 4473–4488 (2014).

130. Dias, S., Paredes, S. & Ribeiro, L. Drugs involved in dyslipidemia and obesity treatment: Focus on axdipose tissue. *Int. J. Endocrinol.* **2018**, (2018).

131. Beiroa, D. *et al.* GLP-1 agonism stimulates brown adipose tissue thermogenesis and browning through hypothalamic AMPK. *Diabetes* **63**, 3346–3358 (2014).

132. Wadden, T. A. *et al.* Weight maintenance and additional weight loss with liraglutide after low-calorie-diet-induced weight loss: The SCALE maintenance randomized study. *Int. J. Obes.* **37**, 1443–1451 (2013).

133. Doggrell, S. A. Sgemaglutide in type 2 diabetes–is it the best glucagon-like peptide 1 receptor agonist (GLP-1R agonist)? *Expert Opin. Drug Metab. Toxicol.* **14**, 371–377 (2018).

134. Davies, M. *et al.* Effect of oral semaglutide compared with placebo and subcutaneous semaglutide on glycemic control in patients with type 2 diabetes a randomized clinical trial. *JAMA - J. Am. Med. Assoc.* **318**, 1460–1470 (2017).

135. Wilding, J. P. H. *et al.* Once-Weekly Semaglutide in adults with overweight or obesity. *N. Engl. J. Med.* **384**, 989–1002 (2021).

136. FDA NEWS RELEASE. FDA NEWS RELEASE FDA approves first oral GLP-1 treatment for type 2 diabetes Inquiries. *FDA* https://www.fda.gov/news-events/press-announcements/fda-approves-first-oral-glp-1-treatment-type-2-diabetes (2019).

137. Ward, N. C., Watts, G. F. & Eckel, R. H. Statin Toxicity: Mechanistic Insights and Clinical Implications. *Circ. Res.* **124**, 328–350 (2019).

138. Derosa, G., Sahebkar, A. & Maffioli, P. The role of various peroxisome proliferator-

activated receptors and their ligands in clinical practice. *J. Cell. Physiol.* **233**, 153–161 (2018).

139. Aguirre, L. *et al.* Several statins increase body and liver fat accumulation in a model of metabolic syndrome. *J. Physiol. Pharmacol.* **64**, 281–288 (2013).

140. Garg, A. *et al.* Role of niacin in current clinical practice: A systematic review. *Am. J. Med.* **130**, 173–187 (2017).

141. Calder, P. C. n-3 Fatty acids and cardiovascular disease: Evidence explained and mechanisms explored. *Clin. Sci.* **107**, 1–11 (2004).

142. Shattat, G. F. A review article on hyperlipidemia: Types, treatments and new drug targets. *Biomed. Pharmacol. J.* **7**, 399–409 (2014).

143. Stefanović, A. *et al.* Dyslipidemia in type 2 diabetes mellitus. *Arh. Farm. (Belgr).* **69**, 338–348 (2019).

144. Mollazadeh, H. *et al.* Effects of statins on mitochondrial pathways. *J. Cachexia. Sarcopenia Muscle* **12**, 237–251 (2021).

145. Fuchs, C. D. *et al.* Colesevelam attenuates cholestatic liver and bile duct injury in Mdr2-/- mice by modulating composition, signalling and excretion of faecal bile acids. *Gut* **67**, 1683–1691 (2018).

146. Poynten, A. M. *et al.* Nicotinic acid-induced insulin resistance is related to increased circulating fatty acids and fat oxidation but not muscle lipid content. *Metabolism.* **52**, 699–704 (2003).

147. Kashyap, M. L., Ganji, S., Nakra, N. K. & Kamanna, V. S. Niacin for treatment of nonalcoholic fatty liver disease (NAFLD): novel use for an old drug? *J. Clin. Lipidol.* **13**,

873–879 (2019).

148. Ganji, S. H., Kashyap, M. L. & Kamanna, V. S. Niacin inhibits fat accumulation, oxidative stress, and inflammatory cytokine IL-8 in cultured hepatocytes: Impact on non-alcoholic fatty liver disease. *Metabolism.* **64**, 982–990 (2015).

149. István, R. Effect of ezetimibe on glucose metabolism and inflammatory markers in adipose tissue. *Lege Artis Med.* **31**, 123–126 (2021).

150. Kim, S. H. *et al.* Ezetimibe ameliorates steatohepatitis via AMP activated protein kinase-TFEB-mediated activation of autophagy and NLRP3 inflammasome inhibition. *Autophagy* **13**, 1767–1781 (2017).

151. Michos, E. D., McEvoy, J. W. & Blumenthal, R. S. Lipid management for the prevention of atherosclerotic cardiovascular disease. *N. Engl. J. Med.* **381**, 1557–1567 (2019).

152. Demers, A. *et al.* PCSK9 induces CD36 degradation and affects long-chain fatty acid uptake and triglyceride metabolism in adipocytes and in mouse liver. *Arterioscler. Thromb. Vasc. Biol.* **35**, 2517–2525 (2015).

153. Filippatos, T. D., Kei, A., Rizos, C. V. & Elisaf, M. S. Effects of PCSK9 inhibitors on other than low-density lipoprotein cholesterol lipid variables. *J. Cardiovasc. Pharmacol. Ther.* **23**, 3–12 (2018).

154. Bargut, T. C. L., Frantz, E. D. C., Mandarim-De-Lacerda, C. A. & Aguila, M. B. Effects of a diet rich in n-3 polyunsaturated fatty acids on hepatic lipogenesis and beta-oxidation in mice. *Lipids* **49**, 431–444 (2014).

155. Cipolletta, D. *et al.* PPAR-γ is a major driver of the accumulation and phenotype of adipose tissue T reg cells. *Nature* **486**, 549–553 (2012).

156. Kalyani, R. R. Glucose-Lowering Drugs to Reduce Cardiovascular Risk in Type 2 Diabetes. *N. Engl. J. Med.* **384**, 1248–1260 (2021).

157. Stensel, D. *Obesity and diabetes*. *Exercise Physiology in Special Populations* (2020). doi:10.1016/B978-0-443-10343-8.00002-0.

158. DeFronzo, R. A. *et al.* Type 2 diabetes mellitus. *Nat. Rev. Dis. Prim.* **1**, 1–23 (2015).

159. Mottalib, A. *et al.* Weight Management in Patients with Type 1 Diabetes and Obesity. *Curr. Diab. Rep.* **17**, (2017).

160. Qiao, Y. C. *et al.* Efficacy and safety of pramlintide injection adjunct to insulin therapy in patients with type 1 diabetes mellitus: A systematic review and meta-analysis. *Oncotarget* **8**, 66504–66515 (2017).

161. Mori, R. C. T., Hirabara, S. M., Hirata, A. E., Okamoto, M. M. & Machado, U. F. Glimepiride as insulin sensitizer: Increased liver and muscle responses to insulin. *Diabetes, Obes. Metab.* **10**, 596–600 (2008).

162. Schork, A. *et al.* Effect of SGLT2 inhibitors on body composition, fluid status and renin-angiotensin-aldosterone system in type 2 diabetes: a prospective study using bioimpedance spectroscopy. *Cardiovasc. Diabetol.* **18**, 1–12 (2019).

163. Calandra, T. & Roger, T. Macrophage migration inhibitory factor: A regulator of innate immunity. *Nat. Rev. Immunol.* **3**, 791–800 (2003).

164. Bloom, B. R. & Bennett, B. Mechanism of a reaction in vitro associated with delayed-type hypersensitivity. *Science (80-.).* **153**, 80–82 (1966).

165. David, J. R. Delayed hypersensitivity in vitro: its mediation by cell-free substances formed by lymphoid cell-antigen interaction. *Proc. Natl. Acad. Sci. U. S. A.* **56**, 72–77

(1966).

166. Bacher, M. *et al.* Migration inhibitory factor expression in experimentally induced endotoxemia. *Am. J. Pathol.* **150**, 235–246 (1997).

167. Hirokawa, J. *et al.* Identification of macrophage migration inhibitory factor in adipose tissue and its induction by tumor necrosis factor-α. *Biochem. Biophys. Res. Commun.* **235**, 94–98 (1997).

168. Vujicic, M. *et al.* The critical role of macrophage migration inhibitory factor in insulin activity. *Cytokine* **69**, 39–46 (2014).

169. Potolicchio, I., Santambrogio, L. & Strominger, J. L. Molecular interaction and enzymatic activity of macrophage migration inhibitory factor with immunorelevant peptides. *J. Biol. Chem.* (2003) doi:10.1074/jbc.M302854200.

170. Bacher, M. *et al.* MIF expression in the rat brain: Implications for neuronal function. *Mol. Med.* **4**, 217–230 (1998).

171. Moon, H. Y. *et al.* Macrophage migration inhibitory factor mediates the antidepressant actions of voluntary exercise. *Proc. Natl. Acad. Sci. U. S. A.* **109**, 13094–13099 (2012).

172. Song, S., Xiao, Z., Dekker, F. J., Poelarends, G. J. & Melgert, B. N. Macrophage migration inhibitory factor family proteins are multitasking cytokines in tissue injury. *Cell. Mol. Life Sci.* **79**, 1–19 (2022).

173. Leng, L. & Bucala, R. Cross-Kingdom analysis of diversity, evolutionary history, and site selection within the eukaryotic macrophage migration inhibitory factor superfamily claire. *Crit. Care Med.* **33**, (2005).

174. Amanda Sparkesa, b, Patrick De Baetseliera, b, Kim Roelantsc, Carl De Treza, d, Stefan

Mageza, d, e, Jo A. Van Ginderachtera, b, Geert Raesa, b, Richard Bucalaf, and Benoît Stijlemansa, b. The non-mammalian MIF superfamily.pdf. 473–482 (2017).

175. Merk, M., Mitchell, R. A., Endres, S. & Bucala, R. D-dopachrome tautomerase (D-DT or MIF-2): Doubling the MIF cytokine family. *Cytokine* **59**, 10–17 (2012).

176. Heller, J. *et al.* NMR characterization of structure, backbone dynamics, and glutathione binding of the human macrophage migration inhibitory factor (MIF). 1655–1661 (1996).

177. Donnelly, S. C. & Bucala, R. Macrophage migration inhibitory factor: A regulator of glucocorticoid activity with a critical role in inflammatory disease. *Mol. Med. Today* **3**, 502–507 (1997).

178. Sun, H. W., Bernhagen, J., Bucala, R. & Lolis, E. Crystal structure at 2.6-Å resolution of human macrophage migration inhibitory factor. *Proc. Natl. Acad. Sci. U. S. A.* **93**, 5191–5196 (1996).

179. Pantouris, G. *et al.* Regulation of mif enzymatic activity by an allosteric site at the central solvent channel. *Cell Chem. Biol.* **27**, 740-750.e5 (2020).

180. Schindler, L., Dickerhof, N., Hampton, M. B. & Bernhagen, J. Post-translational regulation of macrophage migration inhibitory factor: Basis for functional fine-tuning. *Redox Biol.* **15**, 135–142 (2018).

181. Bozza, M. *et al.* Targeted disruption of migration inhibitory factor gene reveals its critical role in sepsis. *J. Exp. Med.* **189**, 341–346 (1999).

182. Toh, M.-L. *et al.* Regulation of il-1 and tnf receptor expression and function by endogenous macrophage migration inhibitory factor. *J. Immunol.* **177**, 4818–4825 (2006).

183. Flaster, H., Bernhagen, J., Calandra, T. & Bucala, R. The macrophage migration

inhibitory factor-glucocorticoid dyad: Regulation of inflammation and immunity. *Molecular Endocrinology* (2007) doi:10.1210/me.2007-0065.

184. Leng, L. *et al.* MIF signal transduction initiated by binding to CD74. *J. Exp. Med.* **197**, 1467–1476 (2003).

185. Mitchell, R. A., Metz, C. N., Peng, T. & Bucala, R. Sustained mitogen-activated protein kinase (MAPK) and cytoplasmic phospholipase A2 activation by macrophage migration inhibitory factor (MIF): Regulatory role in cell proliferation and glucocorticoid action. *J. Biol. Chem.* **274**, 18100–18106 (1999).

186. Heinrichs, D. *et al.* Macrophage migration inhibitory factor (MIF) exerts antifibrotic effects in experimental liver fibrosis via CD74. *Proc. Natl. Acad. Sci. U. S. A.* **108**, 17444–17449 (2011).

187. Miller, E. J. *et al.* Macrophage migration inhibitory factor stimulates AMP-activated protein kinase in the ischaemic heart. *Nature* **451**, 578–582 (2008).

188. Cheng, W. L. *et al.* Macrophage migration inhibitory factor increases atrial arrhythmogenesis through CD74 signaling. *Transl. Res.* **216**, 43–56 (2020).

189. Shi, X. *et al.* CD44 is the signaling component of the macrophage migration inhibitory factor-cd74 receptor complex. *Immunity* **25**, 595–606 (2006).

190. Gore, Y. *et al.* Macrophage migration inhibitory factor induces B cell survival by activation of a CD74-CD44 receptor complex. *J. Biol. Chem.* **283**, 2784–2792 (2008).

191. Gil-Yarom, N. *et al.* CD74 is a novel transcription regulator. *Proc. Natl. Acad. Sci. U. S. A.* **114**, 562–567 (2017).

192. Bernhagen, J. *et al.* MIF is a noncognate ligand of CXC chemokine receptors in

inflammatory and atherogenic cell recruitment. *Nat. Med.* **13**, 587–596 (2007).

193. Kamir, D. *et al.* A Leishmania Ortholog of Macrophage Migration Inhibitory Factor Modulates Host Macrophage Responses . *J. Immunol.* **180**, 8250–8261 (2008).

194. Schwartz, V. *et al.* A functional heteromeric MIF receptor formed by CD74 and CXCR4. *FEBS Lett.* **583**, 2749–2757 (2009).

195. Chatterjee, M. *et al.* Macrophage migration inhibitory factor limits activation-induced apoptosis of platelets via CXCR7-dependent Akt signaling. *Circ. Res.* **115**, 939–949 (2014).

196. Klasen, C. *et al.* MIF Promotes B Cell Chemotaxis through the Receptors CXCR4 and CD74 and ZAP-70 Signaling. *J. Immunol.* **192**, 5273–5284 (2014).

197. Alampour-Rajabi, S. *et al.* MIF interacts with CXCR7 to promote receptor internalization, ERK1/2 and ZAP-70 signaling, and lymphocyte chemotaxis. *FASEB J.* **29**, 4497–4511 (2015).

198. Schwartz, V. *et al.* Role for CD74 and CXCR4 in clathrin-dependent endocytosis of the cytokine MIF. *Eur. J. Cell Biol.* **91**, 435–449 (2012).

199. Kleemann, R. *et al.* Intracellular action of the cytokine MIF to modulate AP-1 activity and the cell cycle through Jab1. *Nature* **408**, 211–216 (2000).

200. Burger-Kentischer, A. *et al.* Binding of JAB1/CSN5 to MIF is mediated by the MPN domain but is independent of the JAMM motif. *FEBS Lett.* **579**, 1693–1701 (2005).

201. Lue, H. *et al.* Rapid and transient activation of the ERK MAPK signalling pathway by macrophage migration inhibitory factor (MIF) and dependence on JAB1/CSN5 and Src kinase activity. *Cell. Signal.* **18**, 688–703 (2006).

202. Lue, H. *et al.* Macrophage migration inhibitory factor (MIF) promotes cell survival by activation of the Akt pathway and role for CSN5/JAB1 in the control of autocrine MIF activity. *Oncogene* **26**, 5046–5059 (2007).

203. Clarke, A. R. *et al.* Thymocyte apoptosis induced by p53-dependent and independent pathways. *Nature* (1993) doi:10.1038/362849a0.

204. Lowe, S. W., Schmitt, E. M., Smith, S. W., Osborne, B. A. & Jacks, T. P53 is required for radiation-induced apoptosis in mouse thymocytes. *Nature* (1993) doi:10.1038/362847a0.

205. Schulz, R. *et al.* Inhibiting the HSP90 chaperone destabilizes macrophage migration inhibitory factor and thereby inhibits breast tumor progression. *J. Exp. Med.* **209**, 275–289 (2012).

206. Klemke, L. *et al.* Hsp90-stabilized MIF supports tumor progression via macrophage recruitment and angiogenesis in colorectal cancer. *Cell Death Dis.* **12**, (2021).

207. Israelson, A. *et al.* Macrophage migration inhibitory factor as a chaperone inhibiting accumulation of misfolded SOD1. *Neuron* **86**, 218–232 (2015).

208. Leyton-Jaimes, M. F. *et al.* Endogenous macrophage migration inhibitory factor reduces the accumulation and toxicity of misfolded SOD1 in a mouse model of ALS. *Proc. Natl. Acad. Sci. U. S. A.* **113**, 10198–10203 (2016).

209. Kim, H. R. *et al.* Elevated levels of macrophage migration inhibitory factor in women with metabolic syndrome. *Horm. Metab. Res.* **43**, 642–645 (2011).

210. Dandona, P. *et al.* Increased plasma concentration of macrophage Migration Inhibitory Factor (MIF) and MIF mRNA in mononuclear cells in the obese and the suppressive action of metformin. *Journal of Clinical Endocrinology and Metabolism* vol. 89 5043–

5047 (2004).

211. González-Muniesa, P., Marrades, M. P., Martínez, J. A. & Moreno-Aliaga, M. J. Differential proinflammatory and oxidative stress response and vulnerability to metabolic syndrome in habitual high-fat young male consumers putatively predisposed by their genetic background. *Int. J. Mol. Sci.* **14**, 17238–17255 (2013).

212. Noriyuki Yabunake, Jun Nishihira, Yuka Mizue, Mitsuru Kumagai, Yoshinori Ohtsuka, Masahiro Imamura, M. A. Elevated serum content of macrophage migration inhibitory factor in patients with type 2 diabetes. *Diabetes Care* **23**, 253–261 (2000).

213. Herder, C. *et al.* Association of systemic concentrations of macrophage migration inhibitory factor with impaired glucose tolerance and type 2 diabetes: results from the cooperative health research in the region of augsburg, survey 4 (kora s4). *Diabetes Care* vol. 29 368–371 (2006).

214. Baugh, J. A. *et al.* A functional promoter polymorphism in the macrophage migration inhibitory factor (MIF) gene associated with disease severity in rheumatoid arthritis. *Genes Immun.* **3**, 170–176 (2002).

215. Radstake, T. R. D. J. *et al.* Correlation of rheumatoid arthritis severity with the genetic functional variants and circulating levels of macrophage migration inhibitory factor. *Arthritis Rheum.* **52**, 3020–3029 (2005).

216. Donn, R. *et al.* Mutation screening of the macrophage migration inhibitory factor gene: Positive association of a functional polymorphism of macrophage migration inhibitory factor with juvenile idiopathic arthritis. *Arthritis Rheum.* **46**, 2402–2409 (2002).

217. Sakaue, S. *et al.* Promoter polymorphism in the macrophage migration inhibitory factor

gene is associated with obesity. *Int. J. Obes.* **30**, 238–242 (2006).

218. Tilstam, P. V., Qi, D., Leng, L., Young, L. & Bucala, R. MIF family cytokines in cardiovascular diseases and prospects for precision-based therapeutics. *Expert Opin. Ther. Targets* **21**, 671–683 (2017).

219. Coban, N., Onat, A., Yildirim, O., Can, G. & Erginel-Unaltuna, N. Oxidative stress-mediated (sex-specific) loss of protection against type-2 diabetes by macrophage migration inhibitory factor (MIF)-173G/C polymorphism. *Clin. Chim. Acta* **438**, 1–6 (2015).

220. Hotamisligil, G. S. & Spiegelman, B. M. Tumor necrosis factor α: A key component of the obesity-diabetes link. *Diabetes* **43**, 1271–1278 (1994).

221. Alzamil, H. Elevated serum tnf- α is related to obesity in type 2 diabetes mellitus and is associated with glycemic control and insulin resistance. *J. Obes.* **2020**, 5–9 (2020).

222. Fontes-Cal, T. C. M. *et al.* Crosstalk between plasma cytokines, inflammation, and liver damage as a new strategy to monitoring nafld progression. *Front. Immunol.* **12**, 1–10 (2021).

223. Wascher, T. C. *et al.* Chronic TNF-α neutralization does not improve insulin resistance or endothelial function in 'healthy' men with metabolic syndrome. *Mol. Med.* **17**, 189–193 (2011).

224. Morrison, M. C. & Kleemann, R. Role of macrophage migration inhibitory factor in obesity, insulin resistance, type 2 diabetes, and associated hepatic co-morbidities: A comprehensive review of human and rodent studies. *Frontiers in Immunology* vol. 6 (2015).

225. Koska, J. *et al.* mRNA concentrations of MIF in subcutaneous abdominal adipose cells are associated with adipocyte size and insulin action. *Int. J. Obes.* **33**, 842–850 (2009).

226. Ikeda, D. *et al.* Knockdown of macrophage migration inhibitory factor disrupts adipogenesis in 3T3-L1 cells. *Endocrinology* **149**, 6037–6042 (2008).

227. Atsumi, T. *et al.* The proinflammatory cytokine macrophage migration inhibitory factor regulates glucose metabolism during systemic inflammation. *J. Immunol.* **179**, 5399–5406 (2007).

228. Lee, J. *et al.* Ultraviolet A Regulates Adipogenic Differentiation of Human Adipose Tissue-derived Mesenchymal Stem Cells via Up-regulation of Kruppel-like Factor 2. *J. Biol. Chem.* **285**, 32647–32656 (2010).

229. Neuschwander-Tetri, B. A. Non-alcoholic fatty liver disease. *BMC Med.* **15**, 1–6 (2017).

230. Barnes, M. A. *et al.* Macrophage migration inhibitory factor contributes to ethanol-induced liver injury by mediating cell injury, steatohepatitis, and steatosis. *Hepatology* **57**, 1980–1991 (2013).

231. Heinrichs, D. *et al.* Unexpected pro-fibrotic effect of mif in non-alcoholic steatohepatitis is linked to a shift in nkt cell populations. *Cells* **10**, 1–17 (2021).

232. Heinrichs, D. *et al.* Protective role of macrophage migration inhibitory factor in nonalcoholic steatohepatitis. *FASEB J.* **28**, 5136–5147 (2014).

233. Heinrichs, D. *et al.* Macrophage migration inhibitory factor (MIF) exerts antifibrotic effects in experimental liver fibrosis via CD74. *Proceedings of the National Academy of Sciences of the United States of America* vol. 108 17444–17449 (2011).

234. Bernhagen, J. *et al.* Purification, bioactivity, and secondary structure analysis of mouse

and human macrophage migration inhibitory factor (mif). *Biochemistry* **33**, 14144–14155 (1994).

235. Fingerle-Rowson, G. *et al.* The p53-dependent effects of macrophage migration inhibitory factor revealed by gene targeting. *Proc. Natl. Acad. Sci. U. S. A.* **100**, 9354–9359 (2003).

236. Sreih, A. G. *et al.* Role of macrophage migration inhibitory factor in granulomatosis with polyangiitis. *Arthritis Rheumatol.* **70**, 2077–2086 (2018).

237. Zebisch, K., Voigt, V., Wabitsch, M. & Brandsch, M. Protocol for effective differentiation of 3T3-L1 cells to adipocytes. *Anal. Biochem.* **425**, 88–90 (2012).

238. Atcc, C. D. O. F. & Reagents, c. *Chemically-induced differentiation of atcc® cl-173tm (3t3-l1) using single-component commercially-available reagents*. (2020).

239. Hare, A. A. *et al.* Optimization of N-benzyl-benzoxazol-2-ones as receptor antagonists of macrophage migration inhibitory factor (MIF). *Bioorganic Med. Chem. Lett.* **20**, 5811–5814 (2010).

240. Leng, L. *et al.* A Small-Molecule Macrophage Migration Inhibitory Factor Antagonist Protects against Glomerulonephritis in Lupus-Prone NZB/NZW F1 and MRL/ lpr Mice . *J. Immunol.* **186**, 527–538 (2011).

241. Cui, A., Hu, Z., Han, Y., Yang, Y. & Li, Y. Optimized analysis of in Vivo and in vitro hepatic steatosis. *J. Vis. Exp.* **2017**, 1–6 (2017).

242. Fogarty, L. C. *et al.* Mcl-1 and Bcl-xL are essential for survival of the developing nervous system. *Cell Death Differ.* **26**, 1501–1515 (2019).

243. Mehlem, A., Hagberg, C. E., Muhl, L., Eriksson, U. & Falkevall, A. Imaging of neutral lipids by oil red O for analyzing the metabolic status in health and disease. *Nat. Protoc.* **8**,

1149–1154 (2013).

244. Cardiff, R. D., Miller, C. H. & Munn, R. J. Manual hematoxylin and eosin staining of mouse tissue sections. *Cold Spring Harb. Protoc.* **2014**, 655–658 (2014).

245. Suvik and Effendy. the Use of Modified Masson ' S Trichrome Staining in Collagen Evaluation in Wound Healing Study. *Malaysian J. Vet. Res.* **3**, 39–47 (2012).

246. Ranjit, S. *et al.* Regulation of fat specific protein 27 by isoproterenol and TNF-α to control lipolysis in murine adipocytes. *J. Lipid Res.* **52**, 221–236 (2011).

247. Long, Y. *et al.* ROS-induced NLRP3 inflammasome priming and activation mediate PCB 118- induced pyroptosis in endothelial cells. *Ecotoxicol. Environ. Saf.* **189**, 109937 (2020).

248. Kopelman, P. G. Obesity as a medical problem. **404**, 635–643 (2000).

249. Kraemer, F. B. & Shen, W. J. Hormone-sensitive lipase: Control of intracellular tri-(di-)acylglycerol and cholesteryl ester hydrolysis. *Journal of Lipid Research* (2002) doi:10.1194/jlr.R200009-JLR200.

250. Jocken, J. W. E. *et al.* Adipose triglyceride lipase and hormone-sensitive lipase protein expression is decreased in the obese insulin-resistant state. *J. Clin. Endocrinol. Metab.* **92**, 2292–2299 (2007).

251. Langin, D. *et al.* Adipocyte lipases and defect of lipolysis in human obesity. *Diabetes* **54**, 3190–3197 (2005).

252. Rittig, N. *et al.* Regulation of lipolysis and adipose tissue signaling during acute endotoxin-induced inflammation: A human randomized crossover trial. *PLoS One* **11**, 1–13 (2016).

253. Church, T. S. *et al.* Obesity, macrophage migration inhibitory factor, and weight loss. *Int. J. Obes.* **29**, 675–681 (2005).

254. Lee, W. J. *et al.* AMPK activation increases fatty acid oxidation in skeletal muscle by activating PPARα and PGC-1. *Biochem. Biophys. Res. Commun.* **340**, 291–295 (2006).

255. Foretz, M., Even, P. C. & Viollet, B. AMPK activation reduces hepatic lipid content by increasing fat oxidation in vivo. *Int. J. Mol. Sci.* **19**, (2018).

256. Kim, S.-J. *et al.* AMPK phosphorylates desnutrin/atgl and hormone-sensitive lipase to regulate lipolysis and fatty acid oxidation within adipose tissue. *Mol. Cell. Biol.* **36**, 1961–1976 (2016).

257. Hoehn, K. L. *et al.* IRS1-independent defects define major nodes of insulin resistance. *Cell Metab.* **7**, 421–433 (2008).

258. Choi, S. M. *et al.* Insulin regulates adipocyte lipolysis via an akt-independent signaling pathway. *Mol. Cell. Biol.* **30**, 5009–5020 (2010).

259. Saksida, T., Stosic-Grujicic, S., Timotijevic, G., Sandler, S. & Stojanovic, I. Macrophage migration inhibitory factor deficiency protects pancreatic islets from palmitic acid-induced apoptosis. *Immunol. Cell Biol.* **90**, 688–698 (2012).

260. Nakamura, A. *et al.* Macrophage migration inhibitory factor drives pathology in a mouse model of spondyloarthritis and is associated with human disease. *Sci. Transl. Med.* **13**, 1–17 (2021).

261. Yoo, S. A. *et al.* MIF allele-dependent regulation of the MIF coreceptor CD44 and role in rheumatoid arthritis. *Proc. Natl. Acad. Sci. U. S. A.* **113**, E7917–E7926 (2016).

262. Calandra, B. T., Bernhagen, J., Mitchell, R. a & Bucala, R. The macrophage is an

important and previously unrecognized source of macrophage migration inhibitory factor. *J. Exp. Med. Rockefeller Univ. Press* **179**, 1895–1902 (1994).

263. Filbey, K. J. *et al.* Macrophage migration inhibitory factor (MIF) is essential for type 2 effector cell immunity to an intestinal helminth parasite. *Front. Immunol.* **10**, 1–18 (2019).

264. Berndt, J. *et al.* Adipose triglyceride lipase gene expression in human visceral obesity. *Exp. Clin. Endocrinol. Diabetes* **116**, 203–210 (2008).

265. Kang, I. & Bucala, R. The immunobiology of MIF: function, genetics and prospects for precision medicine. *Nat. Rev. Rheumatol.* **15**, 427–437 (2019).

266. Qi, D. *et al.* Cardiac macrophage migration inhibitory factor inhibits JNK pathway activation and injury during ischemia/reperfusion. *J. Clin. Invest.* **119**, 3807–3816 (2009).

267. Lue, H., Dewor, M., Leng, L., Bucala, R. & Bernhagen, J. Activation of the JNK signalling pathway by macrophage migration inhibitory factor (MIF) and dependence on CXCR4 and CD74. *Cell. Signal.* **23**, 135–144 (2011).

268. Haemmerle, G. *et al.* Hormone-sensitive lipase deficiency in mice causes diglyceride accumulation in adipose tissue, muscle, and testis. *J. Biol. Chem.* **277**, 4806–4815 (2002).

269. Albert, J. S. *et al.* Null mutation in hormone-sensitive lipase gene and risk of type 2 diabetes. *N. Engl. J. Med.* **370**, 2307–2315 (2014).

270. Harada, K. *et al.* Resistance to high-fat diet-induced obesity and altered expression of adipose-specific genes in HSL-deficient mice. *Am. J. Physiol. - Endocrinol. Metab.* **285**, 1182–1195 (2003).

271. Finucane, O. M. *et al.* Macrophage migration inhibitory factor deficiency ameliorates high-fat diet induced insulin resistance in mice with reduced adipose inflammation and

hepatic steatosis. *PLoS One* **9**, 1–14 (2014).

272. Huang, Y. *et al.* A pref-1-controlled non-inflammatory mechanism of insulin resistance. *iScience* **26**, 106923 (2023).

273. Qi, D. & Rodrigues, B. Glucocorticoids produce whole body insulin resistance with changes in cardiac metabolism. *Am. J. Physiol. - Endocrinol. Metab.* **292**, (2007).

274. Pavone, L. M. & Norris, R. A. Distinct signaling pathways activated by 'extracellular' and 'intracellular' serotonin in heart valve development and disease. *Cell Biochem. Biophys.* **67**, 819–828 (2013).

275. Bao, Y. L. *et al.* Animal and Organoid Models of Liver Fibrosis. *Front. Physiol.* **12**, (2021).

276. Cai, J., Zhang, X. J. & Li, H. The role of innate immune cells in nonalcoholic steatohepatitis. *Hepatology* **70**, 1026–1037 (2019).

277. Borghese, F. & Clanchy, F. Il. CD74: An emerging opportunity as a therapeutic target in cancer and autoimmune disease. *Expert Opinion on Therapeutic Targets* (2011) doi:10.1517/14728222.2011.550879.

278. Sanchez-Niño, M. D. *et al.* MIF, CD74 and other partners in kidney disease: Tales of a promiscuous couple. *Cytokine Growth Factor Rev.* **24**, 23–40 (2013).

279. Kayagaki, N. *et al.* Caspase-11 cleaves gasdermin D for non-canonical inflammasome signalling. *Nature* **526**, 666–671 (2015).

280. Shi, J. *et al.* Inflammatory caspases are innate immune receptors for intracellular LPS. *Nature* **514**, 187–192 (2014).

281. Kajiwara, Y. *et al.* A Critical Role for Human Caspase-4 in Endotoxin Sensitivity. *J. Immunol.* **193**, 335–343 (2014).

282. Huang, D., Deyu, T. C., Chua, R. Y. R., Kemeny, D. M. & Siew, H. W. Nitric-oxide synthase 2 interacts with CD74 and inhibits its cleavage by caspase during dendritic cell development. *J. Biol. Chem.* **283**, 1713–1722 (2008).

283. Carpino, G. *et al.* Alpha-SMA expression in hepatic stellate cells and quantitative analysis of hepatic fibrosis in cirrhosis and in recurrent chronic hepatitis after liver transplantation. *Dig. Liver Dis.* **37**, 349–356 (2005).

284. Streba, L. A. M., Vere, C. C., Rogoveanu, I. & Streba, C. T. Nonalcoholic fatty liver disease, metabolic risk factors, and hepatocellular carcinoma: An open question. *World J. Gastroenterol.* **21**, 4103–4110 (2015).

285. Tamura, S. & Shimomura, I. Contribution of adipose tissue and de novo lipogenesis to nonalcoholic fatty liver disease. *J. Clin. Invest.* **115**, 1139–1142 (2005).

286. Irimia, J. M. *et al.* Lack of liver glycogen causes hepatic insulin resistance and steatosis in mice. *J. Biol. Chem.* **292**, 10455–10464 (2017).

287. Bessone, F., Razori, M. V. & Roma, M. G. Molecular pathways of nonalcoholic fatty liver disease development and progression. *Cell. Mol. Life Sci.* **76**, 99–128 (2019).

288. Alvehus, M., Burén, J., Sjöström, M., Goedecke, J. & Olsson, T. The human visceral fat depot has a unique inflammatory profile. *Obesity* **18**, 879–883 (2010).

289. de Sant'Ana, L. P. *et al.* Absence of the Caspases 1/11 Modulates Liver Global Lipid Profile and Gut Microbiota in High-Fat-Diet-Induced Obese Mice. *Front. Immunol.* **10**, 1–13 (2020).

290. Weisberg, S. P. *et al.* Obesity is associated with macrophage accumulation in adipose tissue. *J Clin Invest.* **112**, 1796–1808 (2003).

291. Al-Abed, Y. *et al.* ISO-1 binding to the tautomerase active site of MIF inhibits its pro-inflammatory activity and increases survival in severe sepsis. *J. Biol. Chem.* **280**, 36541–36544 (2005).

292. Morand, E. F., Leech, M. & Bernhagen, J. MIF: A new cytokine link between rheumatoid arthritis and atherosclerosis. *Nat. Rev. Drug Discov.* **5**, 399–411 (2006).

293. Benigni, F. *et al.* The proinflammatory mediator macrophage migration inhibitory factor induces glucose catabolism in muscle. *J. Clin. Invest.* **106**, 1291–1300 (2000).

294. Kim, S. *et al.* AMPK phosphorylates desnutrin/atgl and hormone-sensitive lipase to regulate lipolysis and fatty acid oxidation within adipose tissue. *Mol. Cell. Biol.* **36**, 1961–1976 (2016).

295. Djouder, N. *et al.* PKA phosphorylates and inactivates AMPKα to promote efficient lipolysis. *EMBO J.* (2010) doi:10.1038/emboj.2009.339.

296. Morigny, P. *et al.* Interaction between hormone-sensitive lipase and ChREBP in fat cells controls insulin sensitivity. *Nat. Metab.* **1**, 133–146 (2019).

297. Xia, B. *et al.* Adipose tissue deficiency of hormone-sensitive lipase causes fatty liver in mice. *PLoS Genet.* **13**, 1–17 (2017).

298. Girousse, A. *et al.* Partial inhibition of adipose tissue lipolysis improves glucose metabolism and insulin sensitivity without alteration of fat mass. *PLoS Biol.* **11**, (2013).

299. Riese, R. J., Brö mme, D. & Natkin, L. R. Essential role for cathepsin s in mhc class ii–associated invariant chain processing and peptide loading. *Immunity* **4**, 357–366 (1996).

300. Driessen, C. *et al.* Cathepsin S controls the trafficking and maturation of MHC class II molecules in dendritic cells. *J. Cell Biol.* **147**, 775–790 (1999).

301. Schneppenheim, J. *et al.* Signal-peptide-peptidase-like 2a is required for CD74 intramembrane proteolysis in human B cells. *Biochem. Biophys. Res. Commun.* **451**, 48–53 (2014).

302. van Kempen, T. S. *et al.* Impaired proteolysis by SPPL2a causes CD74 fragment accumulation that can be recognized by anti-CD74 autoantibodies in human ankylosing spondylitis. *Eur. J. Immunol.* **50**, 1209–1219 (2020).

303. Starlets, D. *et al.* Cell-surface CD74 initiates a signaling cascade leading to cell proliferation and survival. *Blood* **107**, 4807–4816 (2006).

304. Rye, R. The structure of an intermediate in class II MHC maturation: CLIP bound to HLA-DR3. *Nature* **378**, 603–605 (1995).

305. Freisewinkel, I. M., Schenck, K. & Koch, N. The segment of invariant chain that is critical for association with major histocompatibility complex class II molecules contains the sequence of a peptide eluted from class II polypeptides. *Proc. Natl. Acad. Sci. U. S. A.* **90**, 9703–9706 (1993).

306. Leng, L. *et al.* MIF signal transduction initiated by binding to CD74. *J. Exp. Med.* **197**, 1467–1476 (2003).

307. Lebeaupin, C. *et al.* ER stress induces NLRP3 inflammasome activation and hepatocyte death. *Cell Death Dis.* **6**, 1–12 (2015).

308. Al Mamun, A. *et al.* Role of pyroptosis in liver diseases. *Int. Immunopharmacol.* **84**, (2020).

309. Hurley, R. L. *et al.* Regulation of AMP-activated protein kinase by multisite phosphorylation in response to agents that elevate cellular cAMP. *J. Biol. Chem.* (2006) doi:10.1074/jbc.M606676200.

310. Ahmadian, M., Wang, Y. & Sul, H. S. Lipolysis in adipocytes. *International Journal of Biochemistry and Cell Biology* vol. 42 555–559 (2010).

311. Loomba, R., Friedman, S. L. & Shulman, G. I. Mechanisms and disease consequences of nonalcoholic fatty liver disease. *Cell* **184**, 2537–2564 (2021).

312. Sreih, A. *et al.* Dual effect of the macrophage migration inhibitory factor gene on the development and severity of human systemic lupus erythematosus. *Arthritis and Rheumatism* vol. 63 3942–3951 (2011).